

Water Quality

BIGHT'08



Southern California Bight
2008 Regional Monitoring
Program
Vol. VII

SOUTHERN CALIFORNIA BIGHT 2008 REGIONAL MONITORING PROGRAM: VII. Water Quality

December 2012

Meredith D.A.Howard¹, George Robertson², Martha Sutula¹, Burton H. Jones³, Nikolay P. Nezlin¹, Yi Chao³, Hartmut Frenzel⁴, Michael J. Mengel², David A. Caron³, Bridget Seegers³, Ashmita Sengupta¹, Erica Seubert³, Dario W. Diehl¹ and Stephen B. Weisberg¹

¹Southern California Coastal Water Research Project

²Orange County Sanitation District

³University of Southern California

⁴Remote Sensing Solutions, Inc. West Coast Office

⁵University of California, Los Angeles

Southern California Coastal Water Research Project

3535 Harbor Blvd, Suite 110

Costa Mesa, CA 92626

Phone: (714) 755-3500

Bight '08 Offshore Water Quality Technical Committee Members

Member	Affiliation
Chair:	
George Robertson	Orange County Sanitation District
Co-Chair:	
Meredith Howard	Southern California Coastal Water Research Project
David Caron	University of Southern California
Yi Chao	University of California, Los Angeles
Chris Crompton	Orange County Resources and Development Management Dept.
Wanda Cross	Santa Ana Regional Water Quality Control Board
Dario Diehl	Southern California Coastal Water Research Project
Paul DiGiacomo	National Oceanic and Atmospheric Administration
Hartmut Frenzel	University of California, Los Angeles
Dominic Gregorio	State Water Resources Control Board
Scott Johnson	City of Oxnard/Aquatic Bioassay and Consulting Laboratories, Inc.
Burt Jones	University of Southern California
Mike Kelly	City of San Diego
Michael Lyons	Los Angeles Regional Water Quality Control Board
Karen McLaughlin	Southern California Coastal Water Research Project
Mike Mengel	Orange County Sanitation District
Marilyn Yuen Murphy	National Oceanic and Atmospheric Administration
Nick Nezin	Southern California Coastal Water Research Project
Jim Rounds	City of Los Angeles
Alex Steele	Los Angeles County Sanitation Districts
Fred Stern	Los Angeles County Sanitation Districts
Astrid Schnetzer	University of Southern California
Bridget Seegers	University of Southern California
Erica Seubert	University of Southern California
Martha Sutula	Southern California Coastal Water Research Project
Ted von Bitner	Orange County Resources and Development Management Dept.
Steve Weisberg	Southern California Coastal Water Research Project

Foreword

The Southern California Bight 2008 Regional Monitoring Program (Bight '08) is part of an effort to provide an integrated assessment of environmental condition through cooperative regional-scale monitoring. The Bight '08 program is a continuation of regional surveys conducted in 1994, 1998 and 2003, and represents the joint efforts of more than 90 participating organizations. The Bight '08 program consists of several elements including: Sediment Toxicity, Sediment Chemistry, Areas of Special Biological Significance (ASBS), Demersal Fishes and Megabenthic Invertebrates, Benthic Macrofauna, Offshore Water Quality, Rocky Reefs, Shoreline Microbiology, Bioaccumulation, and most recently, Estuarine Eutrophication. Bight'08 workplans, quality assurance plans, as well as the data described in this report and assessment reports for other elements are available at www.sccwrp.org.

The proper citation for this report is: Howard, M.D.A., G. Robertson, M. Sutula, B. Jones, N. Nezlin, Y. Chao, H. Frenzel, M. Mengel, D.A. Caron, B. Seegers, A. Sengupta, E. Seubert, D. Diehl and S.B. Weisberg. 2012. Southern California Bight 2008 Regional Monitoring Program: Volume VII. Water Quality. Technical Report 710. Southern California Coastal Water Research Project. Costa Mesa, CA.

ACKNOWLEDGEMENTS

This report is a product of the dedication and hard work of many individuals who share a common goal of improving our understanding of the environmental quality of the Southern California Bight coastal waters. The authors wish to thank the members of the Bight'08 Water Quality Technical Committee for their assistance with study design, sample analysis, data analysis and report review. This study would not have been possible without the hard work, dedication and exceptional skill of the field sampling teams from the following organizations: City of San Diego, Orange County Sanitation District, Los Angeles County Sanitation District, City of Los Angeles, Southern California Coastal Water Research Project, Aquatic Bioassay and Consulting Laboratories, Weston Solutions and the Counties of San Diego, Orange, Los Angeles, and Ventura. The authors also wish to express their gratitude to Becky Schaffner (SCCWRP) for assistance with map preparation and Karlene Miller (SCCWRP) for document production.

Table of Contents

List of Figures	vii
List of Tables	xi
Executive Summary	xiii
I. Introduction	1
Background and Context.....	2
Goal and Objectives of the Offshore Water Quality Study	4
Approach.....	5
Historical Analysis of Remotely Sensed Algal Blooms	5
Comparison of Anthropogenic and Natural Nutrient Inputs	5
Algal Bloom Characterization	6
Nutrient Source Tracking	6
Audience and Organization of This Report	6
References	6
II. Phytoplankton Blooms Detected by SeaWiFS along the Central and Southern California Coast	10
Introduction	10
Methods.....	11
Study Area: Central and Southern California Coast.....	11
Offshore Extension of Remotely-Sensed Chlorophyll (CHL) as a Measure of Phytoplankton Blooms in the SCB	13
SST Anomalies as a Measure of Upwelling Events and Residence Time	16
Precipitation and Stormwater Runoff.....	17
Results.....	18
Seasonal and Spatial Patterns	18
Interannual Variations	21
Factors Affecting Blooms: Upwelling, Stormwater Runoff and Local Circulation	23
Discussion	26
Offshore CHL Extension as a Bloom Indicators	26
Factors Associated with Offshore CHL Extension: Upwelling.....	27
Other Factors Associated with Offshore CHL Extension	28
Acknowledgments	30

References	31
III. Comparison Of Natural And Anthropogenic Nutrient Sources In The Southern California Bight	39
Introduction	39
Methods.....	40
Study Area	40
Study Approach: Estimation and Comparison of Nutrient Sources.....	42
Estimation of Upwelling.....	44
Wastewater Effluent Discharge.....	49
Riverine Loads	51
Atmospheric Deposition	54
Data Integration	55
Error Analysis in TN and TP Loads	55
Results.....	55
Bightwide Regional Nitrogen and Phosphorus Loads.....	55
Sub-regional Nitrogen and Phosphorus Fluxes	57
Timing of Loads.....	60
Estimates of Contribution of Anthropogenic Activities to SCB Nutrient Loads	61
Discussion	64
Importance of Anthropogenic Nutrients in Upwelling-Dominated Ecosystems	64
Importance of Temporal and Spatial Scale of Nutrient Load Delivery	64
Uncertainty Associated with Nutrient Source Estimates.....	65
The Importance of Nutrient Ratios and Forms.....	69
Conclusions	70
Future Studies and Recommendations.....	70
References	71
IV. Characterization Of Algal Blooms and monitoring coastal ocean dynamics Within The Southern California Bight	77
Introduction	77
Methods.....	78
Field Study Components	78
Ship Surveys	79
Additional Types of Ocean Sampling	81

Data Analysis	83
Results.....	84
Regional Comparison of Upwelling.....	84
Regional and Sub-regional Comparison of Chlorophyll	85
Subregion Results of Observational Measurements	89
Discussion	110
New View of Upwelling in Supporting Algal Bloom Development.....	110
Subsurface Algal Bloom or Deep Chlorophyll Maximum Feature	110
Regional Comparison of SCB	113
HAB Species, <i>Pseudo-nitzschia</i> and Domoic Acid	113
Lessons Learned and Implications for Monitoring Algal Blooms and HAB Events	115
Future Studies and Recommendations.....	115
References	116
APPENDIX A - BIGHT '08 PARTICIPANTS	1
APPENDIX B - QUALITY ASSURANCE AND QUALITY CONTROL PROCEDURES.....	1
APPENDIX C - ADDITIONAL NUTRIENT SOURCE DATA SUMMARIZED	1
APPENDIX D - SHIP SURVEY DATA SUMMARIZED	1
APPENDIX E - RELATED MANUSCRIPTS	1

LIST OF FIGURES

Figure I-1 Study area.....	1
Figure I-2 The number of samples of domoic acid (top panel) and saxitoxin (bottom panel) levels in mussel samples that were above the regulatory limits of $20 \mu\text{g g}^{-1}$ (20 ppm) and $80 \mu\text{g } 100 \text{ g}^{-1}$ tissue (0.4 ppm) respectively.....	3
Figure II-1 Transects along the central and southern California coastline where offshore CHL extension was assessed. Dotted lines indicate circulation in the Southern California Bight (SCB)	12
Figure II-2 (a) – SeaWiFS CHL image (March 24, 2002; 19:56 UTC) with offshore transects in the bloom zone (dashed line) and away from the bloom (solid line); (b) – CHL along these two offshore transects (solid and dashed lines in panels (a) and (b) correspond); (c) - schematic sketch illustrating the method of assessment of offshore CHL extension.....	14
Figure II-3 Seasonal variability along the central and southern California coast: (a) PFEL upwelling index at 33°N ($\text{m}^3 \text{ s}^{-1}$ per 100 m of coastline); (b) SST; (c) frequency of upwelling events ($\% \text{ day}^{-1}$); (d) the zone of high CHL ($>5 \text{ mg m}^{-3}$) offshore extension (km); (e) CHL concentration averaged over 5-km inshore parts of the transects.	20
Figure II-4 Interannual variability along the central and southern California coast: (a) PFEL upwelling index ($\text{m}^3 \text{ s}^{-1}$ per 100 m of coastline) at 36°N (solid line) and 33°N (dashed line); (b) NPGO index; red dashed line is NPGO smoothed with 1-year (13-month) window; (c) frequency of upwelling events ($\% \text{ day}^{-1}$); (d) the zone of high CHL ($>5 \text{ mg m}^{-3}$) offshore extension (km); (e) CHL extension offshore positive trend (black bars–Sen’s slope; km year^{-1} ; grey bars–5% lower confidence intervals); (f) Stormwater runoff ($10^3 \text{ m}^3 \text{ day}^{-1}$	22
Figure II-5 The zone of high CHL ($>5 \text{ mg m}^{-3}$) offshore extension (km) along the central and southern California coast (a) after major rainstorms and (b) after major upwelling events.....	23
Figure II-6. Correlations (coefficients of determination R^2) between (a, b) short-term SST seasonal anomalies and (c, d) offshore CHL extension along the central and southern California coast. (a, c)—correlations between adjacent regions/transects; (b, d)—correlations between all regions/transects. Horizontal axes in (b) and (d) are roughly proportional to the distance between the regions. In particular, location R in (d) indicates the correlation between Point Arguello (PA) and San Diego (SD).	25
Figure III-1 The circulation patterns in the SCB (adapted from Hickey, 1992).....	41
Figure III-2 Regional and sub-regional SCB boundaries used to calculate fluxes of each of the four major sources.	43
Figure III-3 Conceptualization of a 3-dimensional box illustrating how the net upwelling flux was estimated from the sum of positive and negative vertical and lateral upwelling fluxes for each sub-regional area.	45

Figure III-4 Relationship between potential density (sigma-theta) and nitrate (top) and ammonium (bottom) in the Southern California Bight. Nitrate and ammonium data (black dots) are derived from the World Ocean Atlas (2005) and ROMS tests run with climatological boundary conditions, respectively	48
Figure III-5 Annual total nitrogen loads (in MT N Year ⁻¹) by source, with total nitrogen components separated into nitrate plus nitrite, organic nitrogen, and ammonia.	56
Figure III-6 Annual phosphorus load for each source, with total phosphorus components separated as phosphate and other phosphorus.	57
Figure III-7 Annual nitrogen flux for upwelling, effluent, riverine runoff, and atmospheric deposition by sub-region.	58
Figure III-8 Annual phosphorus flux (MT P Km ⁻² Year ⁻¹) for upwelling, effluent, riverine runoff, and atmospheric deposition.	59
Figure III-9 Nitrogen loads as wet- and dry-weather organic (ON) and dissolved inorganic nitrogen (DIN) for rivers. The height of the bar is the total magnitude of the load.	61
Figure III-10 Net change from 'pre-urbanization' (bars on the left) and post-urbanization (bars on the right) riverine runoff loads of nitrogen and phosphorus on a Bightwide and sub-regional scale for TN (top panel) and TP (bottom panel).	63
Figure III-11 Total nitrogen and total phosphorus loads for the 13-year model analysis for riverine runoff.	67
Figure III-12 Ecosystem indices 2005 to 2012 for the Pacific Decadal Oscillation (PDO) Index, the El Niño/Southern Oscillation (ENSO) Index, and the PFEL Upwelling Anomaly Index (from the Orange County Sanitation District Annual Report, 2011).	68
Figure III-13 El Nino index (NINO3.4 is sea surface temperature anomaly in the equatorial Pacific region 5°N–5°S:170–120°W) (A) during 1990–2011 and (B) in January–June 2010.	69
Figure IV-1 Sampling locations for the ocean field components collected as part of this study. Pier Stations were monitored as part of the SCCOOS program; ESP sites indicate MBARI Environmental Sample Processors.	79
Figure IV-2 Regional Comparison of upwelling in SCB in 2010 from automated sensors on the SCCOOS Piers (top) and NDBC Buoys (bottom). SIO stands for Scripps Institute of Oceanography.	85
Figure IV-3 Remotely-sensed chlorophyll concentration averaged over open SCB from January through June 2010 (red bars) and monthly climatologies (blue dashed line).	86
Figure IV-4 Remotely-sensed chlorophyll concentration (mg m ⁻³) for each sub-region from January through June 2010 (red bars) and monthly climatologies (blue dashed line).	87
Figure IV-5 Calibrated chlorophyll fluorescence data from the ship surveys averaged for each survey in each subregion for all depths from surface to 50m.	88
Figure IV-6 Calibrated chlorophyll fluorescence data from the ship surveys averaged for each survey in each subregion for different depths. The top left panel is the surface to 15m averages, the	

top right panel is the 15-30m chlorophyll- <i>a</i> averages, the lower left panel is the 30-45m chlorophyll- <i>a</i> averages and the lower right panel is the >45m chlorophyll- <i>a</i> averages.	89
Figure IV-7 Temperature observations from the NDBC buoy and the Newport Pier in 2010.	91
Figure IV-8 SCCOOS Newport Pier data summarized for the spring of 2010. The top graph shows cell counts), and the bottom graph summarizes the HAB species cell counts and nitrate concentrations.	92
Figure IV-9 Glider Observations in late April and early May. The glider moved in a zig-zag pattern up the coast with LA harbor to the north (but not shown) and Newport to the east (shown). Temperature is shown in the top panel and chlorophyll fluorescence data is shown in the bottom panel.	93
Figure IV-10 Temperature (top panel) and chlorophyll fluorescence (bottom panel) from ship surveys in April and May. Images on the left reflect data collected from the April 20, 2010 survey, middle images reflect data collected from the April 27, 2010 survey, and images on the right reflect data collected from the May 4, 2010 survey.	94
Figure IV-11 Offshore and nearshore Environmental Sample Processor (ESP) data collected in April 2010.	96
Figure IV-12 Temperature observations from the NDBC buoy and at the Scripps Institute of Oceanography (SIO) Pier.	97
Figure IV-13 Ship-based observations for . temperature (0-18°C; top panel) and chlorophyll (scale range from 0-4 $\mu\text{g L}^{-1}$; bottom panel). Images on the left reflect observations from the March 1-2, 2010 survey, and images on the right reflect observations from the March 12, 2010 survey.	98
Figure IV-14 SCCOOS Scripps Institute of Oceanography (SIO) Pier data summarized for the spring of 2010. The top image shows respective assemblage cell counts and nitrate concentrations; the bottom panel shows HAB species cell counts and nitrate concentrations.	100
Figure IV-15 Temperature observations from the NDBC buoy and at the Santa Monica Pier.	101
Figure IV-16 SCCOOS Santa Monica Bay Pier data summarized for the spring of 2010, including HAB species cell counts and nitrate concentrations.	102
Figure IV-17 The temperature (top panel) and calibrated chlorophyll fluorescence (bottom panel) from the ship surveys in March before the observed upwelling event. Images on the left reflect observations from the March 5, 2010 survey, and images on the right reflect observations from the March 8, 2010 survey.	103
Figure IV-18 Temperature (top panel) and calibrated chlorophyll fluorescence (bottom panel) from the ship surveys in March after the observed upwelling event. Images on the left reflect observations from the March 12, 2010 survey, and images on the right reflect observations from the March 15, 2010 survey.	105
Figure IV-19 Temperature observations from the NDBC buoy in Ventura.	106
Figure IV-20 Temperature and chlorophyll fluorescence from the ship surveys in Ventura in March. ...	107

Figure IV-21 Temperature and chlorophyll fluorescence from the ship surveys in Ventura in May	108
Figure IV-22 The SCCOOS Stern's Wharf Pier data, HAB species cell counts and nitrate concentrations, summarized for the spring of 2010.....	109
Figure IV-23 SCCOOS glider transects in the SCB.	111
Figure IV-24 The SCCOOS Glider Data.	112

LIST OF TABLES

Table III-1 List of N and P form analyzed for each nutrient source and analytical reference.....	42
Table III-2 Area of Each Sub-region.	43
Table III-3 List of polynomial parameters for the biogeochemical boundary conditions in ascending order, e.g. $\text{NO}_3(\sigma_\theta > 26.8) = -20258 + 1484.7 * \sigma_\theta + -27.1422 * \sigma^2$	47
Table III-4 Location and relative size of POTWs used for effluent discharge load estimates by sub-region. S= Small; L = Large.....	49
Table III-5 Targeted analytes and analytical methods by participating agency for wastewater effluents.	50
Table III-6 Number of wet- and dry-weather watershed sites and respective monitored events by County/Subregion.....	51
Table III-7 Targeted analytes and analytical methods by participating agency for riverine loads.....	52
Table III-8 Runoff coefficients (C) for stormwater discharge and average concentrations of ammonium, nitrate, phosphate, TP, and TN in runoff by land-use. Values from Ackerman and Schiff (2003) unless otherwise noted.....	53
Table III-9 Annual loads of TN and TP and component forms (as percent of total) for each nutrient source (in MT Year^{-1}) and the nitrogen constituents as the percentage of total nitrogen. NA = not analyzed for this source.	56
Table III-10 Summary of the standard error calculated for nitrogen and phosphorus components of riverine runoff and effluent. Absolute and standard error reported in Kg Year^{-1}	57
Table III-11 Annual TN flux ($\text{MT N Km}^{-2} \text{Year}^{-1}$) by source for each sub-region.....	59
Table III-12 Annual phosphorus flux ($\text{MT P Km}^{-2} \text{Year}^{-1}$) for each sub-region. ND = No data.	60
Table III-13 The total nitrogen flux ($\text{MT N Km}^{-2} \text{Year}^{-1}$) for natural nutrient sources (upwelling and atmospheric deposition) and for natural and anthropogenic sources (all sources; data from Table III-11) to the SCB	62
Table IV-1 Data products discussed and participants in weekly trigger meetings.....	80
Table IV-2 Parameters collected during the ship based surveys.	81
Table IV-3 SCCOOS Pier sampling locations and responsible participants.	81
Table IV-4 Continuously sampled SCCOOS Pier-based indicators and discrete water sample analytes collected weekly discrete water.	82
Table IV-5 The nutrient ratios and average concentrations summarized for the March surveys pre-upwelling (March 2 & 3, 2010) and post-upwelling (March 23 & 24, 2010) for OCS and LACSD ship surveys. The Redfield Ratios are listed in parenthesis.....	90
Table IV-6 Average nutrient ratios, nutrient concentrations, and discrete chlorophyll- <i>a</i> concentrations summarized for the pre-upwelling (April 20, 2010), post-upwelling (April 27, 2010), and	

relaxation (May 4, 2010) events during the Orange County surveys. The Redfield ratios are listed in parenthesis.	95
Table IV-7 Nutrient ratios and average concentrations summarized for the March surveys pre-upwelling (March 1 and 2, 2010) and post-upwelling (March 12, 2010). The Redfield Ratios are listed in parenthesis.	99
Table IV-8 Nutrient ratios and concentrations summarized for the March surveys pre-upwelling (March 5 and 8, 2010) and post-upwelling (March 12 and 15, 2010)..	104
Table IV-9 The average nutrient ratios and concentrations summarized for the March surveys pre-upwelling (March 1, 2, 2010) and post-upwelling (March 23 and 24, 2010)..	109

EXECUTIVE SUMMARY

Introduction

Algal blooms occur in coastal waters in response to a variety of environmental conditions (temperature, light availability, currents etc.). Nutrients, in particular, are critical to the development and/or maintenance of algal blooms. Most algal blooms are harmless, necessary, and beneficial to the function of aquatic ecosystems. However, some blooms can have negative impacts to the environment, human health, and the economy and are thus referred to as “harmful algal blooms” (HABs). Globally, HAB events are increasing in frequency and intensity in coastal waters. Nutrient pollution from anthropogenic activities has been shown to be the most significant environmental factors contributing to the global expansion of HABs. Nutrient inputs associated with anthropogenic activities such as agricultural land use, contaminated groundwater, and discharge of treated and untreated wastewater provide significant sources of nitrogen (the primary limiting macronutrient for algae in coastal waters) that have been linked to increased HAB events.

In the coastal waters of the Southern California Bight (SCB), there is a generally held perception that algal blooms and HAB events appear to have been increasing in recent years. The SCB is subject to input from one of the most populated U.S. metropolitan areas via both point (municipal effluent) and non-point (urban runoff and atmospheric deposition) discharge sources. The SCB also receives large amounts of natural nutrients, primarily from upwelling (the process by which nutrient-rich oceanic deep water is brought to the surface). There is a generally held perception that the quantity of anthropogenic nutrients is negligible relative to natural nutrient sources. However, no previous regional scale studies have been conducted to quantify the relative magnitude of natural and anthropogenic nutrient sources to the SCB, nor have any studies documented the increase in algal blooms to test the accuracy of these commonly held perceptions.

Key Questions

The Bight 2008 Offshore Water Quality study provided an opportunity to conduct the first large scale characterization of algal bloom patterns and estimation of the relative magnitude of anthropogenic versus natural nutrient sources to the SCB. Environmental managers and scientists from 76 organizations, including sanitation and stormwater agencies, municipalities, State and Federal regulatory agencies, and universities collaborated to answer three questions:

1. Are algal blooms increasing in frequency and are there areas where chronic blooms ('hotspots') are evident in the SCB?
2. What are the relative nutrient contributions of natural and anthropogenic sources to the SCB on bightwide and local spatial scales?
3. What are the mechanisms behind how algal blooms develop? Do blooms develop offshore or inshore, in the subsurface or surface depths?

Study Approach

The water quality study design for Bight'08 was divided into three main components: 1) Historical Analysis of Remotely Sensed Algal Blooms, 2) Comparison of Anthropogenic and Natural Nutrient Inputs, and 3) Algal Bloom Characterization. A special study was also conducted to determine whether nutrient sources (atmospheric deposition, wastewater, stormwater, and upwelling) could be identified from their stable isotope signatures in a common form of nitrogen (nitrate) in coastal waters.

1) Historical Analysis of Remotely Sensed Algal Blooms. Historic patterns in algal bloom occurrence and spatial extent were assessed using remote sensing to determine how frequently algal blooms occur and if this frequency has increased over the last decade. An analysis of surface algal blooms was conducted using remotely-sensed surface chlorophyll concentration and sea surface temperature from 1997-2007.

2) Comparison of Anthropogenic and Natural Nutrient Inputs. The relative magnitude of major nitrogen (N) and phosphorus (P) sources to the SCB (upwelling, wastewater discharge, riverine runoff and atmospheric deposition) were quantified using a combination of modeling and field studies over a one-year period. Estimates of upwelling include the novel use of the Regional Ocean Model System (ROMS) hydrodynamic model coupled with a biogeochemical model to provide a spatially- and a temporally-integrated estimate of this important nutrient source. As part of the nutrient source comparison, a special study was conducted to determine whether nutrient sources could be identified from their stable isotope signatures. The special study involved two parts: 1) determination of nutrient specific isotope ratios in nutrient sources such as wastewater effluent, river discharge and upwelled water; and 2) field measurements of seawater to determine if source signatures were maintained in the SCB or if they were over-written by biological transformations. The intent was to determine if isotopic signatures could be used to provide an additional line of evidence to identify nutrient sources that support algal blooms.

3) Algal Bloom Characterization. The purpose of this component was to characterize the spatial and temporal patterns of a spring algal bloom and determine the origin of bloom development. The physical, chemical, and biological oceanographic features of the development, evolution and dissipation of a spring algal bloom were characterized. This aspect of the study utilized remote sensing and gliders in combination with pier-based and ship-based sampling between February and May 2010 to provide a multi-disciplinary dataset capable of covering a wide range of temporal and spatial scales.

Study Findings

Question 1: Are algal blooms increasing and are there areas in which chronic blooms ('hotspots') are evident in the SCB? The results of the historical analysis using satellite imagery (1997-2007) showed that the extent of algal blooms have increased significantly over the past 10 years in the SCB. Seasonally, blooms occurred consistently during the spring and early summer during upwelling periods. However, chronic algal bloom 'hotspots,' regions with year round high chlorophyll signatures, were identified in several areas in the SCB including the Santa Barbara Channel, the San Pedro Shelf, Santa Monica Bay, South San Diego, and the Ensenada coast. These algal bloom hotspots were co-located with

anthropogenic nutrient inputs such as wastewater discharge outfalls and major river mouths, as well as with geographic areas that had longer residence times of coastal waters.

Question 2: What are the relative nutrient contributions of natural and anthropogenic sources to the SCB on bightwide and local spatial scales? At a regional, bightwide scale, the Bight '08 Water Quality study found that natural sources dominate anthropogenic sources of nutrients by 1 order of magnitude for nitrogen and 2 orders of magnitude for phosphorus. At smaller sub-regional scales, that are ecologically relevant to understanding algal blooms, the anthropogenic sources of nitrogen were comparable in magnitude to natural sources in Santa Barbara, Ventura, Santa Monica Bay, San Pedro Bay, and San Diego nearshore regions. While this study provided estimates of nutrient sources within an order of magnitude, the results suggest that anthropogenic nutrients are important at spatial scales relevant to algal blooms. Because algal productivity in SCB coastal waters is limited by the amount of nitrogen, anthropogenic inputs have doubled the amount of nitrogen available to support algal blooms. Among anthropogenic sources, POTW effluent typically exceeded riverine loads and atmospheric deposition by 1-2 orders of magnitude.

Recent studies have shown that the form of nitrogen, not just the quantity, is important for HABs and algal blooms. The sources of nitrogen to the SCB are comprised of different forms of nitrogen, mainly nitrate (plus nitrite), ammonia, and organic nitrogen (including urea). Dissolved inorganic nitrogen (DIN), the most biologically available form, was the dominant form in most natural and anthropogenic sources. As expected, upwelling was mostly comprised of nitrate, effluent was mostly comprised of ammonia and riverine runoff was dominated by nitrate and organic nitrogen forms. Despite the large ammonia component of effluent, this source contributed a significant nitrate (plus nitrite) load to the SCB, larger than the entire nitrogen contribution from riverine runoff.

Findings of Special Study. As part of the investigation into the relative contributions of natural and anthropogenic sources, a pilot study was employed to determine if isotopes could be used to identify different sources of nutrients in seawater samples taken in proximity to bloom events. The special study documented that the nitrogen and oxygen isotopic signatures of nitrate in the different sources (wastewater effluent, riverine discharge and upwelled water) had distinct isotopic signatures, or fingerprints. The isotopic signatures from SCB nearshore samples were somewhat unique, but not enough to trace different nutrient sources in the SCB. Although nutrient input from atmospheric deposition was found to be less significant than input from other sources, the signature of atmospheric deposition sources was clearly identified in some surface samples in nearshore waters. However, it is possible that atmospheric deposition at the ocean surface may be more significant, but when integrated over increased water depth, it diminishes in importance relative to other nutrient sources.

Question 3: What are the mechanisms behind how algal blooms develop? Do blooms develop offshore, inshore, in the subsurface, or at surface depths? This study component provided new insights into algal bloom development and evolution in the SCB. Prior to this study, upwelling was perceived to support algal bloom development by providing nutrients to surface waters for existing surface algal populations. The Bight'08 Water Quality findings showed that algal bloom development was observed in

both the surface and subsurface depths and in both the offshore and inshore locations within the SCB. The subsurface algal bloom was observed in most regions but was not detectable via remote sensing. This study documented that upwelling can be a physical mechanism that transports existing subsurface algal blooms into surface waters, provides direct connectivity between the two populations, and results in bloom intensification in surface waters due to higher light and nutrient conditions.

Recommended Next Steps

Evaluate if there is a trend of increased frequency of algal blooms and refine the temporal and spatial trends and patterns of algal blooms in the SCB. The results of the remote sensing study determined that the spatial extent of algal blooms has increased over the last decade in the SCB. However, this is a relatively short time scale in which to evaluate an oceanographic trend. Additionally, the presence of a subsurface algal feature was consistently identified which is not visible via remote sensing. Two types of research are recommended:

- (1) Utilize existing longer-term water quality datasets that capture the subsurface component to investigate this trend over longer timescales. Two existing datasets are appropriate for this analysis. The first dataset consists the California Cooperative Oceanic Fisheries Investigations (CalCOFI, www.calcofi.org) time-series of oceanographic data, which spans a 60 year period and provides a much larger spatial scope of data than was provided by the Bight'08 study. The second dataset consists of survey data from the Central Bight Water Quality group and City of San Diego NPDES permit monitoring programs, which has chlorophyll *a* data for 15 years.
- (2) Utilize sediment cores to investigate trends in phytoplankton productivity and HAB prevalence on decade to century timescales. Similar studies have been conducted in the past to deconstruct the relative influence of climate and oceanographic variability from anthropogenic influence.

Refine and validate models to assess various anthropogenic and natural nutrient source scenarios and provide a multi-year nutrient source analysis. Models are needed to evaluate the effect of anthropogenic nutrients on phytoplankton productivity and related effects such as coastal hypoxia. Models can determine the net change in these parameters on different temporal and spatial scales under different management scenarios. The types of models used in this study, with additional calibration and validation, can be used to simulate scenarios of altered magnitude and forms of nutrients to coastal waters. The modeled nutrient loads reported in this study were limited to annual time scales because of uncertainties in upwelling predictions on shorter (daily-seasonal) time scales. However, effects of nutrient delivery to the coastal ocean are more ecologically relevant for primary productivity and algal bloom development if considered on these shorter time scales. The timing of nutrient sources may be as important as their magnitude because some sources are chronic, (daily wastewater effluent discharge into oceans and into rivers), whereas other sources are seasonal (riverine runoff and upwelling). Therefore, the relative importance of different nutrient sources on the development and maintenance of algal blooms may vary seasonally. To capture these higher-frequency timescales, existing models need to be refined and validated for smaller spatial scales and shorter (daily to weekly), timescales. In addition, these models can be used to conduct a multi-year comparative source analysis to determine interannual variability for each source. There is existing data that would

allow for a multi-year analysis of effluent and riverine sources. The upwelling component could be estimated by hindcasting the models over several years.

Investigate subsurface algal blooms. Subsurface algal blooms and high chlorophyll were observed in most regions in this study. While these results provided a new view of algal bloom development, they also raised several questions. Future Bight studies need to:

1. Identify the nutrient source(s) associated with these subsurface algal blooms
2. Determine how often and in what seasons subsurface algal blooms develop
3. Determine the pervasiveness of the subsurface algal blooms
4. Investigate how far offshore subsurface algal blooms are located using the existing datasets discussed above
5. Determine the light levels and algal community composition associated with these features

I. INTRODUCTION

The Southern California Bight (SCB; Figure I-1) is an open embayment between Point Conception and Cape Colnett (south of Ensenada), Baja California. Complex bathymetry and currents contribute to a diversity of habitats and marine organisms, including more than 500 species of fish and several thousand species of invertebrates. The SCB is a major migration route for marine bird and mammal populations and ranks among the most diverse ecosystems in north temperate waters. Beyond its ecological value, the SCB coastal zone is a substantial economic resource. In addition to being home to more than 20 million people (NRC 1990), southern California receives more than 100 million visitors to its beaches and coastal areas annually. The combination of resident and transient populations has resulted in a highly developed urban environment that has greatly altered the natural landscape. The conversion of open land to impervious surfaces has included dredging and filling over 75% of the region's historic bays and estuaries (Horn and Allen 1985) and extensive alternations of coastal streams and rivers (Brownlie and Taylor 1981, NRC 1990). This "hardening of the coast" has changed both the timing and rate of runoff releases to coastal waters and can affect water quality through the addition of sediment, toxic chemicals, pathogens, and nutrients. In addition to input of urban runoff via storm drains and channelized rivers and streams, numerous municipal wastewater treatment facilities, power-generating stations, industrial treatment facilities, and oil platforms discharge effluents to the SCB.

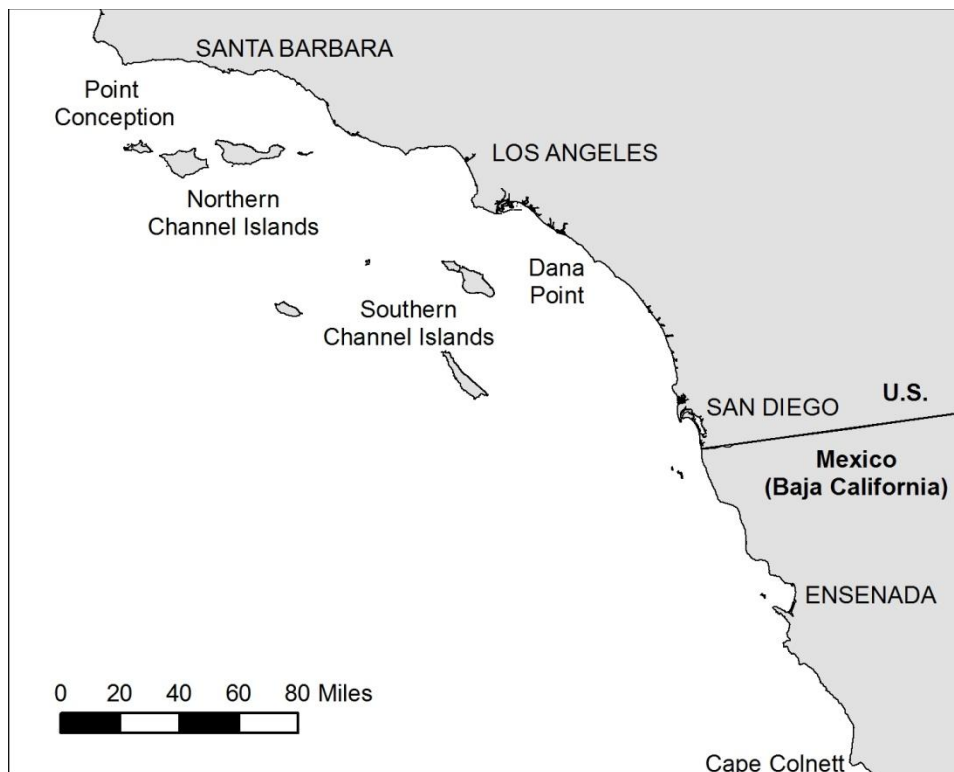


Figure I-1 Study area.

Although the effects of anthropogenic stressors to the SCB are not well understood, a Bightwide perspective is needed to coordinate, contextualize and manage these effects. The Southern California Bight Regional Monitoring Program is an integrated, multi-disciplinary, collaborative study that provides a unique platform for collecting data for Bightwide perspectives. The Bight Regional Monitoring Program is now a partnership of more than 60 organizations (Appendix A) collaborating to address management questions of regional importance to the Bight's offshore, nearshore, and estuarine habitats. The program's surveys provide a mechanism for developing standardized methods, quality assurance protocols, and data transfer standards. This ensures that all survey data can be integrated and provides the foundation for enhanced coordination among the various southern California monitoring programs. Offshore Water Quality has been a long-standing component of the Bight Regional Monitoring Program. During the 2008 study cycle, the Bight Offshore Water Quality Committee chose to focus its efforts to better characterize algal blooms in the SCB and the relative nutrient contribution from four major sources to the SCB.

This document provides a summary of the findings, conclusions, and recommendations from the Offshore Water Quality component of the Southern California Bight 2008 Regional Monitoring Program (Bight'08).

Background and Context

Algal blooms occur along the coast in response to a variety of environmental conditions (temperature, light availability, currents). Nutrients, in particular, are considered critical to the development and/or maintenance of algal blooms. Most blooms are harmless and beneficial to marine and freshwater ecosystem functions. However, some blooms can have negative impacts on the environment, human health, and the economy; such blooms are referred to as "harmful algal blooms" (HABs). Mechanism categories used to classify a bloom as harmful include mechanical (gill irritation), physical (viscosity and gelatinous barriers and mucoid layer reduction which lead to gill clogging and death), biochemical (anoxia, production of toxins or allelopathic deterrents to grazers), and communal (ambush predation) (Smayda 1997).

In coastal waters, HABs are increasing globally in both frequency and intensity (Smayda 1990; Hallegraeff 1993, 2004; Anderson et al. 2002; Glibert et al. 2005a; Anderson et al. 2008, see summary <http://www.whoi.edu/redtide/page.do?pid=14898>). In the SCB, there is a perception that HAB events are increasing. Toxic outbreaks of *Pseudo-nitzschia*, an algal diatom that produces the toxin domoic acid, were considered rare prior to 2000 (Lange et al. 1994); however, in recent years frequent occurrences and high concentrations of this toxin in southern California coastal waters have been documented (Trainer et al. 2000, Busse et al. 2006, Schnetzer et al. 2007, Caron et al. 2010, Caron, unpublished data; see Figure I-2). Domoic acid is considered to be the toxin of highest frequency in recent years in the SCB and therefore of the most concern for research, monitoring and management (Figure I-2). There has been so much attention paid to these events, that in 2008, the Southern California Coastal Ocean Observing System (SCCOOS) established an ongoing HAB Program to collect weekly HAB species and toxin information from five pier locations (<http://www.sccoos.org/data/habs/index.php>). Due to the public health implications associated with marine toxins, the California Department of Public Health

(CDPH) monitors toxin levels in shellfish and will close both commercial and recreational harvesting when alert levels are exceeded in order to minimize the potential for shellfish poisoning through human consumption.

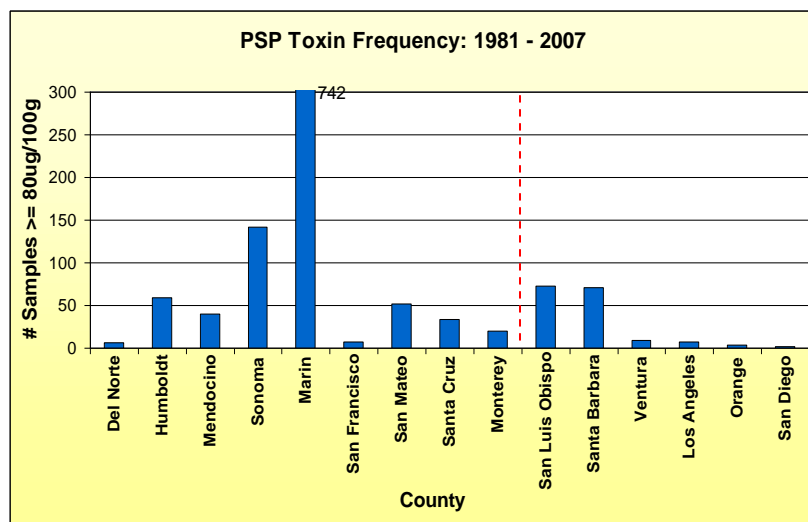
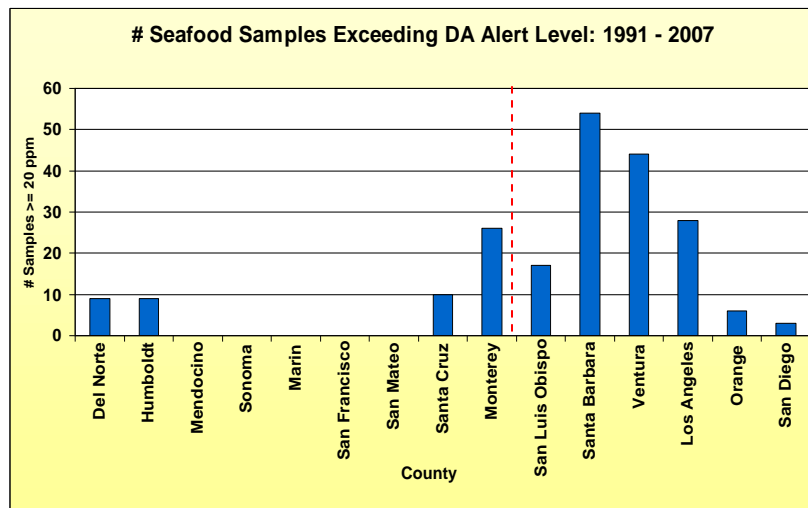


Figure I-2 The number of samples of domoic acid (top panel) and saxitoxin (bottom panel) levels in mussel samples that were above the regulatory limits of $20 \mu\text{g g}^{-1}$ (20 ppm) and $80 \mu\text{g } 100 \text{ g}^{-1}$ tissue (0.4 ppm) respectively. The counties to the right of the red dashed lines represent the Bight'08 study area. (Gregg Langlois, California Department of Public Health, www.cdph.ca.gov).

Globally, nutrient pollution from anthropogenic activities has been shown to be the most significant factor contributing to the expansion of HABs. Many factors contribute to the increase in anthropogenic nutrient inputs to marine coastal waters, including: human population growth (which leads to increases sewage discharges), coastal watershed development, agricultural and aquaculture runoff into the

coastal oceans, and fossil fuel emissions (Anderson et al. 2002, Howarth 2008). Agricultural runoff, wastewater and sewage discharge, and groundwater discharge have all been shown to provide significant sources of nitrogen that have been linked to increased HAB events and/or primary production (Lapointe 1997, 2004, 2005a,b; Anderson et al. 2002, 2008; Glibert et al. 2005a, 2006; Heisler et al. 2008). While many previous studies have focused on agricultural runoff, wastewater has also been found to promote HABs, increase primary productivity, and to be more important than upwelling as a nitrogen source in some regions (Chisholm et al. 1997; Lapointe 1997, 2004, 2005b; Jaubert et al. 2003; Thompson and Waite 2003). Nitrogen has been the focus of most coastal eutrophication studies because it has been shown to be the primary limiting macronutrient for algae in coastal waters as well as in California (Dugdale 1967; Ryther and Dunstan 1971, Eppley et al. 1979; Nixon 1986, 1995; Kudela and Dugdale 2000). However, recent studies have shown that the form of nitrogen, not just the quantity, is important for HABs and algal blooms (Glibert et al. 2006, Howard et al. 2007, Switzer 2008, Kudela et al. 2008, Cochlan et al. 2008).

Despite the demonstrated linkages between anthropogenic nutrient inputs and HABs, there is a general perception that in upwelling systems, such as California, the quantity of anthropogenic nutrient inputs is small relative to upwelling, and therefore has little effect on the productivity of coastal waters. The role of anthropogenic nutrients in upwelling systems, such as California, is controversial, as there are two opposing views on whether these nutrients have any significant effect on primary productivity in coastal waters. One view holds that the quantity of anthropogenic inputs is small relative to upwelling, and therefore anthropogenic nutrients have little effect. The alternate view holds that there are such a large number of anthropogenic sources, there must be some effect on coastal ocean ecosystems. However, there have been no studies that have quantified the natural and anthropogenic sources on regional or local scales to determine which perception is accurate. However, a growing number of studies have suggested a linkage between anthropogenic nitrogen sources and HABs in California, and many have focused on anthropogenically-influenced riverine runoff (Kudela and Cochlan 2000, Kudela and Chavez 2004, Beman et al. 2005, Kudela et al. 2008).

Controversy aside, there have been no previous regional scale studies in the SCB to determine if the frequency or intensity of algal blooms and/or HABs are actually increasing; nor have there been any studies to determine if anthropogenic nutrients influence algal blooms in this region. Furthermore, there have been no regional or local scale studies to quantify the relative magnitude of natural and anthropogenic inputs. Still, physiological studies have shown that several common California HAB species are capable of utilizing anthropogenic nitrogen forms, such as urea (Herndon and Cochlan 2007, Cochlan et al. 2008, Kudela et al. 2008) for growth. Toxin production can be increased under these conditions (Howard et al. 2007); therefore, it is important to investigate not only the sources of nutrients but also the nutrient forms.

Goal and Objectives of the Offshore Water Quality Study

The overall goal of the Bight '08 Offshore Water Quality study was to determine if anthropogenic nutrient sources are influencing algal blooms in the SCB. The specific study objectives designed to address this goal were:

- 1) Determine the frequency of algal blooms and identify chronic algal bloom hotspots in the SCB.
- 2) Establish the relative nutrient contributions of four major sources to the SCB (upwelling, wastewater effluent, terrestrial runoff, atmospheric deposition).
- 3) Characterize the spatial and temporal patterns of algal blooms, with an emphasis on the most common HAB in the SCB, *Pseudo-nitzschia*, which produces the toxin, domoic acid (DA).
- 4) Special Study: Track different nutrient sources in seawater using isotopes to identify specific source signatures.

The first objective was to determine how frequently algal blooms occur and if this frequency has increased over the last decade. The second objective was to establish the relative annual nutrient (nitrogen, phosphorus) contributions from both natural and anthropogenic sources to the SCB (upwelling, wastewater effluent, terrestrial runoff and atmospheric deposition). The third objective was to characterize the spatial and temporal patterns of algal blooms, with an emphasis on the occurrence of *Pseudo-nitzschia* and the toxin domoic acid. The fourth objective was a special study on methods to determine if nutrient sources had different isotopic signatures and could be tracked from environmental ocean samples.

Approach

The Bight'08 Offshore Water Quality study design was divided into four main components:

1. Historical Analysis of Remotely Sensed Algal Blooms
2. Comparison of Anthropogenic and Natural Nutrient Inputs
3. Algal Bloom Characterization
4. Special Study on Nutrient Source Tracking

Historical Analysis of Remotely Sensed Algal Blooms

Historic patterns in algal bloom frequency and spatial extent were assessed using remote sensing. An analysis of surface algal blooms was conducted using remotely-sensed surface chlorophyll concentration (SeaWiFS ocean color) and sea surface temperature (derived from AVHRR infrared measurements) from 1997-2007.

Comparison of Anthropogenic and Natural Nutrient Inputs

The major sources of nutrients to the SCB (upwelling, wastewater discharge, terrestrial runoff, and atmospheric deposition) were quantified to an order of magnitude for nitrogen and phosphorus. Upwelling was estimated by coupling 1) the physical circulation model (ROMS which is currently used by both SCCOOS and Central and Northern California Ocean Observing System (CeNCOOS)), and 2) a biogeochemical (nutrients, phytoplankton, zooplankton – NPZ) model. Wastewater discharge loads were estimated by analyzing effluent samples quarterly for one year and using reported flow information. Terrestrial runoff was estimated using empirical samples combined with modeling to fill in the data

gaps. Atmospheric deposition was estimated using published wet deposition rates and dry deposition rates from a SCCWRP pilot study.

Algal Bloom Characterization

The physical, chemical, and biological oceanographic features were characterized, and an intensive observational study of the development, evolution and dissipation of algal blooms was conducted. The observational study combined remote sensing, gliders, and pier- and ship-based sampling during February - May 2010 to provide a multi-disciplinary dataset covering a wide range of temporal and spatial scales to characterize algal blooms. SCCOOS HAB Program information (from piers), automated instrumentation (water temperature), and ROMS model forecasts combined with satellite imagery were used to determine environmental conditions and the timing of ship surveys to capture oceanographic features

Nutrient Source Tracking

This special study had two parts: 1) determination of nutrient specific isotope ratios in nutrient sources such as wastewater effluent, river discharge and upwelled water; and 2) field measurement of seawater to determine if source signatures were maintained in the SCB or if they were over-written by biological transformations. Water was collected from the SCB on Los Angeles County Sanitation District (LACSD) and Orange County Sanitation District (OCSD) cruises along vertical and horizontal profiles from offshore discharge outfalls and along the San Gabriel and Santa Ana River transects.

Audience and Organization of This Report

The B'08 Offshore Water Quality Report presents a summary of the findings for water quality and natural resource managers. The report is organized into six sections. Sections II, III, and IV are technical sections that will be submitted independently as manuscripts to scientific journals; as such, each section contains introduction, methods, results, discussion, and conclusion sections. Appendices contain supplemental information relevant to the study, including: the Quality Assurance and Quality Control Procedures (Appendix B), additional nutrient source comparison data summarized (Appendix C), ship survey data for the entire study (Appendix D), and related manuscripts (Appendix E).

References

Anderson, D.M., Glibert, P.M., and Burkholder, J.M., 2002. Harmful algal blooms and eutrophication: Nutrient sources, composition, and consequences. *Estuaries* 25: 704-726.

Anderson, D.M., Burkholder, J.M., Cochlan, W.P., Glibert, P.M., Gobler, C.J., Heil, C.A., Kudela, R.M., Parsons, M.L., Rensel, J.E., Townsend, D.W., Trainer, V.L., Vargo, G.A., 2008. Harmful algal blooms and eutrophication: Examining linkages from selected coastal regions of the United States. *Harmful Algae* 8: 39-53.

Beman, M., Arrigo, K., Matson, P., 2005. Agricultural runoff fuels large phytoplankton blooms in vulnerable areas of the ocean. *Nature* 434: 211-214.

- Brownlie, W.R. and B.D. Taylor, 1981. Sediment management for Southern California mountains, coastal plains and shoreline; part C, coastal sediment delivery by major rivers in Southern California. Environmental Quality Laboratory Report No. 17-C. California Institute of Technology. Pasadena, CA.
- Busse, L.B., Venrick, E.L., Antrobus, R., Miller, P.E., Vigilant, V., Silver, M.W., Mengelt, C., Mydlarz, L., Prezelin, B.B., 2006. Domoic acid in phytoplankton and fish in San Diego, CA, USA. *Harmful Algae* 5(1): 91-101.
- Caron, D.A., M.E. Garneau, E. Seubert, M.D.A. Howard, L. Darjany, A. Schnetzer, I. Cetinic, G. Filteau, P. Lauri, B. Jones, and S. Trussell, 2010. Harmful algae and their potential impacts on desalination operations off southern California. *Journal of Water Research* 44: 385-416.
- Chisholm, J.R.M., Fernex, F.E., Mathieu, D., Jaubert, J.M., 1997. Wastewater discharge, seagrass decline and algal proliferation on the Cote d'Azur. *Mar. Poll. Bull.* 34: 78-84.
- Cochlan, W.P., Herndon, J., Kudela, R.M., 2008. Inorganic and organic nitrogen uptake by the toxigenic diatom *Pseudo-nitzschia australis* (Bacillariophyceae). *Harmful Algae* 8: 111-118.
- Dugdale, R. C., 1967. Nutrient limitation in the sea: Dynamics, identification and significance. *Limnology and Oceanography* 12: 685-695.
- Eppley, R., Renger, E., Harrison, W., 1979. Nitrate and phytoplankton production in California coastal waters. *Limnology and Oceanography* 24: 483-494.
- Glibert, P.M., Anderson, D.M., Gentien, P., Granéli, E., and Sellner, K.G., 2005a. The global, complex phenomena of harmful algal blooms. *Oceanography* 18: 137-147.
- Glibert, P.M., Seitzinger, S., Heil, C.A., Burkholder, J.M., Parrow, M.W., Codispoti, L.A., and Kelly, V., 2005b. The role of eutrophication in the global proliferation of harmful algal blooms. *Oceanography* 18: 198-209.
- Glibert, P.M., Harrison, J., Heil, C., and Seitzinger, S., 2006. Escalating worldwide use of urea- a global change contributing to coastal eutrophication. *Biogeochemistry* 77: 441-463.
- Hallegraeff, G.M., 1993. A review of harmful algal blooms and their apparent global increase. *Phycologia* 32: 79-99.
- Hallegraeff, G.M., 2004. Harmful algal blooms: a global overview. *In: Manual on Harmful Marine Microalgae*. Hallegraeff, G.M., Anderson, D.M., and Cembella, A.D. (Eds.), France. UNESCO Publishing 25-49.
- Heisler, J., Glibert, P., Burkholder, J., Anderson, D., Cochlan, W., Dennison, W., Gobler, C., Dortch, Q., Heil, C., Humphries, E., Lewitus, A., Magnien, R., Marshall, H., Sellner, K., Stockwell, D., Stoecker, D., Suddleson, M., 2008. Eutrophication and harmful algal blooms: a scientific consensus. *Harmful Algae* 8: 3-13.

- Herndon, J., Cochlan, W.P., 2007. Nitrogen utilization by the raphidophyte *Heterosigma akashiwo*: growth and uptake kinetics in laboratory cultures. *Harmful Algae* 6: 260–270.
- Howarth, R.W., 2008. Coastal nitrogen pollution: a review of sources and trends globally and regionally. *Harmful Algae* 8: 14–20.
- Howard, M.D.A., Cochlan, W.P., Ladizinsky, N., Kudela, R.M., 2007. Nitrogenous preference of toxigenic *Pseudo-nitzschia australis* (Bacillariophyceae) from field and laboratory experiments. *Harmful Algae* 6(2): 206–217.
- Jaubert, J.M., Chisholm, J.R.M., Minghelli-Roman, A., Marchioretti, M., Morrow, J.H., Ripley, H.T., 2003. Re-evaluation of the extent of *Caulerpa taxifolia* development in the northern Mediterranean using airborne spectrographic sensing. *Mar. Ecol. Progr. Ser.* 263: 75–82.
- Kudela, R., Dugdale, R., 2000. Nutrient regulation of phytoplankton productivity in Monterey Bay, California. *Deep-Sea Research II* 47: 1023–1053.
- Kudela, R.M., Cochlan, W.P., 2000. The kinetics of nitrogen and carbon uptake and the influence of irradiance for a natural population of *Lingulodinium polyedrum* (Pyrrophyta) off southern California. *Aquat. Microbial Ecol.* 21: 31–47.
- Kudela, R.M. and Chavez, F.P., 2004. The impact of coastal runoff on ocean color during an El Nino year in central California. *Deep Sea Research* 51(10-11): 1173–1185.
- Kudela, R.M., Lane, J.Q., Cochlan, W.P., 2008. The potential role of anthropogenically derived nitrogen in the growth of harmful algae in California, USA. *Harmful Algae* 8: 103–110.
- Lapointe, B.E., 1997. Nutrient thresholds for bottom-up control of macroalgal blooms on coral reefs in Jamaica and southeast Florida. *Limnology and Oceanography*. 42 (5, part 2): 1119–1131.
- Lapointe, B.E., Barile, P.J., Wynne, M.J., Yentsch, C.S., 2005a. Reciprocal Invasion: Mediterranean native *Caulerpa ollivieri* in the Bahamas supported by human nitrogen enrichment. *Aq. Invad.* 16(2): 2–5.
- Lapointe, B., Peter J. Barile, Mark M. Littler, Diane S. Littler., 2005b. Macroalgal blooms on southeast Florida coral reefs II. Cross-shelf discrimination of nitrogen sources indicates widespread assimilation of sewage nitrogen. *Harmful Algae* 4: 1106–1122.
- Lapointe, B.E., Barile, P.J., Matzie, W.R., 2004. Anthropogenic nutrient enrichment of seagrass and coral reef communities in the lower Florida keys: discrimination of local versus regional nitrogen sources. *J. Exp. Mar. Biol. Ecol.* 308(1): 23–58.
- National Research Council (NRC), 1990. Monitoring southern California's coastal waters. National Academy Press. Washington, DC.
- Nixon, S. W., 1986. Marine end Environmental Pollution. In *Nutrient dynamics and the productivity of marine coastal waters* (Halwagy, R., Clayton, D., and Behbehani, M., eds.). Alden Press, Oxford, UK. 97–115.

Nixon, S. W., 1995. Coastal marine eutrophication: A definition, social causes, and future concerns. *Ophelia* 41: 199–219.

Ryther, J., and Dunstan, W., 1971. Nitrogen, phosphorus and eutrophication in the coastal marine environment. *Science* 171: 1008–1112.

Schnetzer, A., Miller, P.E., Schaffner, R.A., Stauffer, B.A., Jones, B.H., Weisberg, S.B., DiGiacomo, P.M., Berelson, W.M., Caron, D.A., 2007. Blooms of *Pseudo-nitzschia* and domoic acid in the San Pedro Channel and Los Angeles harbor areas of the Southern California Bight, 2003 - 2004. *Harmful Algae* 6(3): 372-387.

Smayda, T.J., 1990. Novel and nuisance phytoplankton blooms in the sea: evidence for a global epidemic. Granéli, E., Gundström, B., Edler, L., and Anderson, D.M., eds. Elsevier, New York, New York, USA. *Toxic Marine Phytoplankton* 29-40.

Switzer, T. Urea loading from a spring storm - Knysna estuary, South Africa. *Harmful Algae* 8: 66-69.

Thompson, P., Waite, A., 2003. Phytoplankton responses to wastewater discharges at two sites in Western Australia. *Marine and Freshwater Research* 54: 721-735.

Trainer, V.L., Adams, N.G., Bill, B.D., Stehr, C.M., Wekell, J.C., Moeller, P., Busman, M., Woodruff, D., 2000. Domoic acid production near California coastal upwelling zones, June 1998. *Limnology and Oceanography* 45(8): 1818-1833.

Smayda, T.J., 1997. Harmful algal blooms: Their ecophysiology and general relevance to phytoplankton blooms in the sea. *Limnology and Oceanography* 42: 1137-1153.
Hallegraeff, 2004.

II. PHYTOPLANKTON BLOOMS DETECTED BY SEAWIFS ALONG THE CENTRAL AND SOUTHERN CALIFORNIA COAST

Introduction

Increases in the frequency and magnitude of phytoplankton blooms have been documented in many coastal ocean zones throughout the world (e.g., Gregg et al. 2005, Kahru and Mitchell 2008, Boyce et al. 2010). This trend has been viewed as a serious environmental concern, because phytoplankton blooms can result in hypoxia, shading of submerged aquatic vegetation, and toxin-producing harmful algal blooms (HABs) (Anderson et al. 2002, Glibert et al. 2005). An apparent increase of phytoplankton blooms in general, and HABs in particular, throughout the world's oceans is attributed to both climatic and anthropogenic factors, including the response of certain phytoplankton groups to global warming and increased nutrient loading (Glibert et al. 2006, Anderson et al. 2008, Heisler et al. 2008, Paerl and Huisman 2008).

The relative importance of drivers to the increased frequency and duration of phytoplankton blooms in different coastal ocean regions is still unclear (e.g., Kahru et al. 2009). Drivers are thought to include: climate change associated with intensification of natural upwelling (Bakun et al. 2010); increased anthropogenic nutrient loading via terrestrial and groundwater runoff (Nixon 1995, Paerl 1997); wastewater discharge (National Research Council 2000); and atmospheric deposition (Paerl 1997). In eastern boundary current systems, such as those found in coastal California, vertical wind-driven nutrient flux (upwelling) is known to be a dominant factor in controlling primary productivity (Barber and Smith 1981). Also, it is widely held among coastal resource managers that terrestrial nutrient sources are a relatively minor factor in comparison with upwelling, even when those sources are elevated from anthropogenic inputs in highly urbanized coastal areas such as the Southern California Bight (SCB), a region that contains 25% of the US coastal population (Culliton et al. 1990). Better understanding of the relative importance of the magnitude and timing of various nutrient sources, as well as knowledge of how ecological factors, including: oceanic circulation, frequency and duration of upwelling events, water residence time, and depth, might control biological responses to nutrient sources are necessary for improved management of environmentally important coastal areas like California.

Satellite remote sensing of ocean color is a powerful method for analyzing seasonal cycles and interannual trends in phytoplankton biomass (e.g., Banse and English 1994, Longhurst 1995, McClain 2009). Its use has been problematic in coastal waters, where traditional methods may be subject to significant inaccuracies and lead to inaccurate conclusions (e.g., Gregg and Casey 2004). In particular, the standard algorithms of ocean color data processing (O'Reilly et al. 1998) was developed for clean open ocean waters and usually overestimates chlorophyll in shallow near-shore zones because of the presence of colored dissolved organic matter and suspended matter (e.g., Muller-Karger et al. 2005). Another important factor leading to inaccurate assessment of chlorophyll in shallow waters is bottom reflectance, which depends on bathymetric depth and water transparency (e.g., Maritorena et al. 1994, Cannizzaro and Carder 2006). In narrow coastal zones, remotely-sensed signals may be contaminated by

landmass reflection (“adjacency effect” of atmospheric diffuse transmittance, Santer and Schmechtig 2000) and terrigenous absorbing aerosols (Moulin et al. 2001, Claustre et al. 2002, Ransibrahmanakul and Stumpf 2006). Consequently, the use of remotely sensed ocean color to understand spatial and temporal patterns in phytoplankton blooms requires alternative methods that circumvent terrestrial interferences.

In this study, the offshore extension of the zones of high remotely-sensed chlorophyll concentration (CHL) were used to study spatial and temporal patterns in phytoplankton blooms in narrow coastal areas along the central and southern California coastline. The objectives of this study were to: 1) demonstrate the offshore extension of the zone of high remotely-sensed chlorophyll concentration as a measure of phytoplankton blooms in the regions characterized by narrow continental shelf and low terrestrial discharge; 2) characterize the magnitude, extent, seasonal, and interannual variability of phytoplankton blooms in central and southern California; and 3) compare the effect of different environmental factors (upwelling, stormwater discharge, and oceanic residence time) on offshore extensions of these blooms.

Methods

Study Area: Central and Southern California Coast

The SCB is typically defined as the coastal and shelf region from Point Conception (34.45°N) to the Mexican border (32.53°N). To compare phytoplankton variations in the SCB to areas to the north and south, the study region was defined as 31°N–36°N (Figure II-1), including the southern part of the central California coast (from Lopez Point to Point Conception) and northern Baja California to Cabo Colnett (the southern boundary of the upwelling zone; Schwing and Mendelssohn 1997).

Coastal circulation in the SCB is part of a large-scale circulation pattern that is dominated by the cold equatorward California Current (CC) flowing from the north (Figure II-1). This meandering current divides the CC ecosystem into a productive nearshore region and an oligotrophic offshore region (Hayward and Venrick 1998, Kim et al. 2009). To the north of Point Conception, the coastline is directed from the north to the south, and stable equatorward winds generate coastal upwelling. To the south of Point Conception, the coastline turns eastward forming the SCB basin. The bottom topography of the SCB consists of ranges of submarine mountains and valleys and is neither classical continental shelf nor continental slope (Emery 1960). The basins between ridges are rather deep (>500 m), and the SCB is bordered by a narrow shelf 3- to 6-km wide. Within the SCB, the CC stream turns to south–southeast (Figure II-1) and passes along the continental slope. At about 32°N, a branch of the CC turns eastward and splits as it approaches the coast (Haury et al. 1993, Chereskin and Niiler 1994). The main core continues equatorward along the Baja California coast, while the rest recirculates poleward along the SCB coast (Harms and Winant 1998, Bray et al. 1999) and forms a large gyre known as the Southern California Eddy. The near-shore poleward branch of this eddy is called the Southern California Countercurrent (SCC Sverdrup and Fleming 1941).

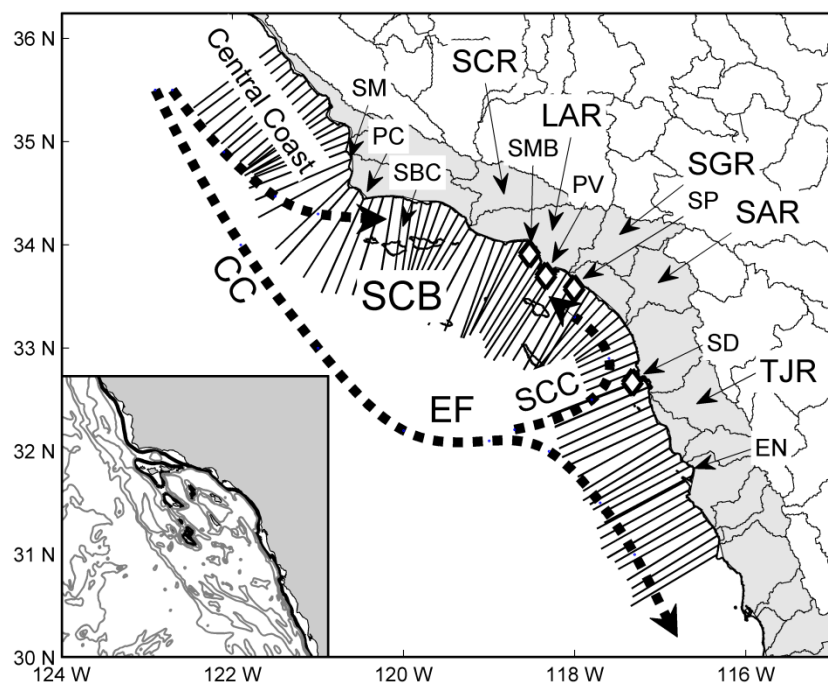


Figure II-1 Transects along the central and southern California coastline where offshore CHL extension was assessed. Dotted lines indicate circulation in the Southern California Bight (SCB): California Current (CC), Ensenada Front (EF), Southern California Countercurrent (SCC). SM—Santa Maria; PC—Point Conception; SBC—Santa Barbara Channel; SMB—Santa Monica Bay; PV—Palos Verdes Peninsula; SP—San Pedro Shelf; SD—San Diego; EN—Ensenada. Watersheds draining to the ocean are shadowed. Major watersheds: SCR—Santa Clara River (includes also Calleguas Creek); LAR—Los Angeles River; SGR—San Gabriel River; SAR—Santa Ana River (includes also San Diego Creek); TJR—Tijuana River. Major POTW outfalls (diamonds) are located in SMB, PV, SP and SD. Inset shows SCB bathymetry; thick black line is the 200m isobath.

Seasonal variations of oceanic conditions in the study region are characterized by dramatic changes in the spring. These changes are referred to as the “spring transition” and include the sudden (during approximately one-week period in March–April) onset of the spring/summer upwelling regime in the coastal ocean (Strub et al. 1987a, b; Bograd et al. 2009). In the spring, atmospheric conditions over the eastern north Pacific abruptly change, forming a high-pressure system centered at 45°N:140°W and a low-pressure cell over the southwest continental United States that results in consistently intensive equatorward winds alongshore (Strub and James 1988). According to traditional views, the intensity of the equatorward CC increases, compared to the poleward SCC, in the spring, and its jet migrates onshore while its eastward branches penetrate into the SCB (Hickey 1979, Bray et al. 1999). Later in summer, the CC jet migrates offshore, where it remains until winter (Reid and Mantyla 1976, Bray et al. 1999, Haney et al. 2001), while the warm SCC penetrates further to the north and west within the SCB. However, a more recent study (Lynn et al. 2003) did not observe onshore migration of the CC during the spring transition. Instead, a coastal upwelling jet was observed to develop independently of the CC; later this jet evolved offshore and regenerated the CC core. Seasonal intensification of coastal upwelling

enriches the upper euphotic layer with nutrients and substantially increases its primary production (Barber and Smith 1981). Earlier studies have documented intensive upwelling along the Central Coast from April through September (e.g., Bakun and Nelson 1991) and weak all-season upwelling in the SCB (Winant and Dorman 1997). According to Lynn and Simpson (1987), regular spring coastal upwelling in the SCB is limited to a small region around Pt. Conception and the northern portion of the SCB; on this basis Mantyla et al. (2008) conclude that phytoplankton growth in southern California's coastal waters must be supported by nutrient input other than coastal upwelling or advection.

Another potential source of nutrients for phytoplankton growth in the SCB coastal zone is stormwater discharge resulting from episodic storm events that typically occur between late fall and early spring. The study region has a Mediterranean climate, with an average annual rainfall of 10–100 cm (e.g., Nezlin and Stein 2005), falling primarily during winter months (December through March), and approximately 20 annual storm events (Ackerman and Weisberg 2003). Winter runoff to the SCB contributes more than 95% of the total annual runoff volume (Schiff et al. 2000, Ackerman and Weisberg 2003). The coastal watersheds that drain to the SCB are comprised of approximately 14,000 km² (Figure II-1) with both urban and agricultural land uses (Ackerman and Schiff 2003). Previous studies (Warrick et al. 2005) have documented low contributions from stormwater nutrient discharge relative to the total nutrient budget of SCB coastal waters, even during wet years (e.g., 1998) when stormwater discharge was assessed to have been two orders of magnitude higher than other years. However, the influence of freshwater discharge on phytoplankton growth is uncertain and needs further clarification to more fully understand how stormwater runoff affects physical stratification and circulation, suspended sediments, and the concentration and spatial distribution of nutrients, especially in the vicinity of river mouths.

In addition to nutrient loading attributed to winter runoff, Publicly Owned Treatment Works (POTW) discharge is another potential nutrient source (Eppley et al. 1972); the nutrient contribution of total POTW effluent to the SCB is comparable with stormwater runoff (total discharge in 2000 >45,000 mt, Lyon and Stein 2009). In contrast to highly seasonal stormwater discharge, POTW flow is constant all-year round. In this study, the locations of anthropogenic nutrient sources (major river mouths and four major POTWs) were factored into data interpretation.

Offshore Extension of Remotely-Sensed Chlorophyll (CHL) as a Measure of Phytoplankton Blooms in the SCB

Because this study is focused on the narrow near-shore coastal ocean zone, the approach used is based on the assumption that the influence of land interferences on the ocean color signal (measured by satellite sensor) dramatically decreases within a short (few kilometers) distance offshore. Thus, when the offshore CHL extension increases (i.e., during bloom events), there is an increased likelihood that phytoplankton pigments are responsible for the ocean color signal (as compared with suspended sediments, colored dissolved organic matter (CDOM), land and bottom reflection, etc.). Averaging CHL in this narrow near-shore zone may include the pixels located at the ocean-land edge where ocean color signal is most corrupted. This approach is illustrated in Figure II-2ab, where two offshore transects represent high (dashed line) vs. low phytoplankton biomass (solid line). Even in the absence of bloom activity, the absolute value of CHL in the narrow near-shore zone exceeds CHL extension in the bloom

zone. This high CHL value may be attributed to the effect of land proximity (land and bottom reflection, suspended sediments, CDOM, etc.), rather than high phytoplankton biomass close to shore. At the same time, the offshore extension of the zone of high CHL concentration ($>5 \text{ mg m}^{-3}$) in the bloom zone is significantly larger than in the near-shore zone ($\sim 23 \text{ km}$ vs. $\sim 3 \text{ km}$; Figure II-2b).

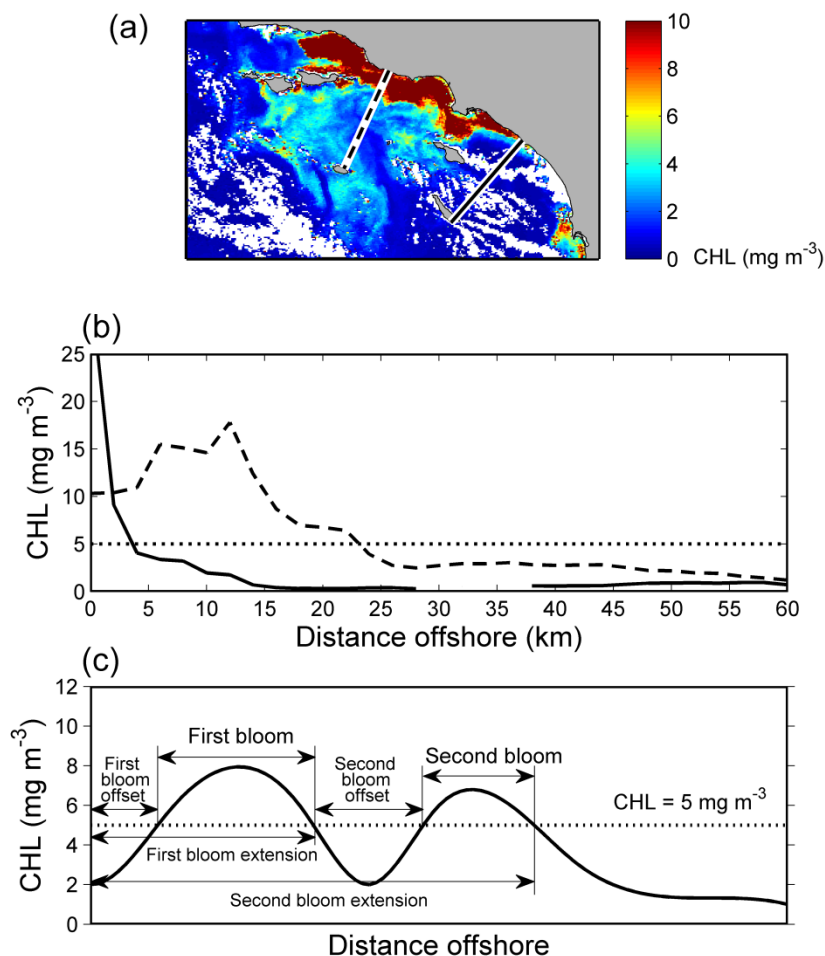


Figure II-2 (a) – SeaWiFS CHL image (March 24, 2002; 19:56 UTC) with offshore transects in the bloom zone (dashed line) and away from the bloom (solid line); (b) – CHL along these two offshore transects (solid and dashed lines in panels (a) and (b) correspond); (c) - schematic sketch illustrating the method of assessment of offshore CHL extension.

This method of characterizing offshore CHL extension in the SCB was used to analyze ocean color data collected by the Sea-viewing Wide-Field-of-view Sensor (SeaWiFS) onboard OrbView-2 satellite from November 7, 1997 to October 31, 2007. All satellite overpasses along the US West Coast were processed for CHL using the OC4 algorithm (O'Reilly et al. 1998) and standard atmospheric correction methods (Gordon and Wang 1994). The standard method of ocean color data processing was preferred because it adequately describes CHL over most of the SCB (characterized by narrow shelf and low terrestrial

discharge) excluding the pixels at the ocean/land edge. An alternative approach, i.e., processing ocean color data using specific methods developed for optically shallow waters, may have improved CHL assessment in the narrow near-shore zone but decreased CHL accuracy in the rest of the study area.

The Level 2 CHL images (i.e., the data in sensor coordinates) were transformed into Level 3 maps (i.e., regular grids of 29°N–39°N :130°W–115°W with 1-km resolution in pseudo-sinusoidal projection for a total 6003 files).

To estimate the zone of offshore CHL extension, CHL data were averaged (as medians) in circular regions with 5-km radii located at 2-km intervals along 100-km offshore transects (Figure II-1). By using 5-km radii, CHL along each offshore transect was averaged within a 10-km zone and smoothed by a 10-km filtering window. In total, 85 transects were located 10 km apart along the coast, from 31°N to 36°N. The direction (azimuth) of each transect was normal to the direction of the 100-km part of the coastline centered at the transect/coast intersection. Medians were used because CHL distribution in the ocean is asymmetric (Banse and English 1994, Campbell 1995). In the near-shore zone CHL contains inaccurate measurements that can be treated as outliers, and, as such, medians are expected to be closer to modal values than arithmetic or geometric means.

In this study, a CHL “bloom” zone was defined as an area with CHL concentration $>5 \text{ mg m}^{-3}$ (note that the method of calculation implies that CHL along offshore transects was smoothed by 10-km window). The CHL threshold of 5 mg m^{-3} was selected on the basis of its total statistical distribution; this threshold was approximately the 85th percentile of the entire 10-year CHL dataset within the 5-km near-shore area. In SCB, the location of 5 mg m^{-3} is close to (and may be treated as) a CHL frontal boundary, because similar analysis done with other thresholds (e.g. 4 or 3 mg m^{-3}) resulted in different absolute values but almost identical temporal and spatial patterns. For each transect, the offshore extension of the CHL “bloom” zone (measured in km) was calculated. Because phytoplankton blooms can be spatially patchy and include several areas with $\text{CHL} > 5 \text{ mg m}^{-3}$, the bloom zone nearest to the coastline was defined as “coastal” and included in the analysis when its offshore offset (i.e., the distance between the coast and the bloom) did not exceed 5 km. The extent of additional bloom patches was added to the extent of the first bloom zone when the offset between the first and the second bloom zones did not exceed 10 km (Figure II-2c). Note that in this study the offshore CHL extension was used as a quantitative measure of phytoplankton blooms rather than a metric for classifying data into “bloom” vs. “not bloom” periods (cf. Kim et al. 2009).

To analyze bloom seasonality, daily CHL extensions offshore in each region were averaged for each day (1–365), and the seasonal cycles were smoothed using a one-month (31-day) cosine filter. Here and below, the size of the smoothing filter windows were selected by trial-and-error and based on the criteria of the best interpretation of the results.

Interannual variability was analyzed after smoothing daily offshore CHL extensions using a one-year (365-day) cosine filter. To test for trends in offshore CHL extension, Sen's Nonparametric Estimator of Slope (Sen 1968) was used. This robust estimator allows missing data, makes no assumptions on data distribution, and is not affected by gross data errors and outliers. Trends were computed from

decimated (set to 10-day intervals) smoothed data. Statistical significance of the trends was tested by calculating the ranks for the upper and lower confidence intervals using the Mann-Kendall statistic and the normal Z-statistic. The median slope was defined as statistically different from zero (for the selected 95% confidence interval) if the zero did not lie between the upper and lower confidence limits.

SST Anomalies as a Measure of Upwelling Events and Residence Time

Upwelling events along the California coast were analyzed on the basis of daily sea surface temperature (SST) infrared data collected by Advanced Very High Resolution Radiometers (AVHRR) in 1997–2007 and processed by Pathfinder (Version 5) project (Kilpatrick et al. 2001). The dataset was obtained from the Physical Oceanography Distributed Active Archive Center (PO.DAAC) Ocean Earth Science Information Partners Program (ESIP) Tool (POET) website as regular grids of 4.5-km spatial resolution in equidistant cylindrical projection. Daytime and nighttime SST data were merged using an averaging method (see Gregg 2007). Mean SST were estimated for each day for 85 regions with 10-km radii located at intersections between the offshore CHL transects and the coastline.

Upwelling events were defined as the periods of abrupt SST decrease. For this, SST variations in each coastal region were split among three types of variation in frequency range: 1) seasonal variability (climatology over a 1-year period); 2) low-frequency “background” variability; and 3) high-frequency variability, assumed to be associated with upwelling events. Seasonal SST climatology was estimated by averaging SST for each day (1–365) during 1997–2007 and smoothing the resulting time-series with a 1-month (31-day) cosine-filter. After subtraction of climatology, the resulting time series (seasonal anomalies) for each region were linearly interpolated for daily intervals (to fill missing data) and split between low-frequency “background” SST variations (SST seasonal anomalies smoothed using a 365-day cosine filter) and the remaining high-frequency SST variations. The days when the high-frequency SST component was $< 1.5^{\circ}\text{C}$ (total 2.75% of observations) were classified as “upwelling events”. This method appeared to be more accurate during seasonal SST increases and less accurate during the second half of the year when abrupt temperature drops were thought to be associated with factors other than upwelling (see results). Seasonal patterns of “upwelling frequency” were calculated for each day and smoothed using a 2-month (61-day) cosine-filter. Interannual variability was analyzed after smoothing the data with a 365-day cosine-filter.

Offshore CHL extension and high-frequency SST variations were used for a coarse evaluation of residence time along the SCB coast. The coefficients of correlation (R^2) between short-term SST seasonal anomalies and offshore CHL extensions in the 85 analyzed regions/transects were calculated on the basis of the entire period of observations (1997–2007). To assess significance of R^2 , each time series was adjusted for autocorrelation and the “critical” R^2 at 0.95 confidence level was calculated for each pair of adjacent series using Chelton’s method (see Pyper and Peterman 1998). It was hypothesized that correlations in SST and CHL indicated an interchange between these regions: high correlations are associated with intensive circulation and short residence time, while low correlations were associated with sluggish circulation and long residence time within natural boundaries. Using the term “residence time” the difference between our assessment and quantitative estimation of water residence time in coastal waters and estuaries were considered (e.g., Ketchum 1951).

The frequency of upwelling events was compared to the upwelling index (UI) in central and southern California calculated at the Pacific Fisheries Environmental Laboratory (PFEL) from the intensity of upwelling-favorable wind. The methodology of PFEL UI assessment is based upon Ekman's theory of mass transport due to wind stress. The intensity of offshore water transport was calculated every six hours from a global field of atmospheric pressure at sea level of 1° spatial resolution. Monthly UI and UI anomalies ($\text{m}^3 \text{s}^{-1}$ per 100 m of coastline) at 33°N, 119°W and 36°N, 122°W were obtained from PFEL website (<http://www.pfeg.noaa.gov/>).

The intensity of upwelling events and phytoplankton blooms were compared to the North Pacific Gyre Oscillation (NPGO) climatic index (Di Lorenzo et al. 2008), which measures changes in the North Pacific gyres circulation; its maxima are associated with upwelling-favorable and minima with upwelling-unfavorable conditions to the south of 38°N. The data were obtained from the NPGO website (<http://www.o3d.org/npgo/>).

Twenty-eight major upwelling events were selected for analysis of their effect on phytoplankton blooms. Upwelling events were estimated from a continuous (at 1-h intervals) record of ocean surface temperature obtained by the national Data Buoy Center (NDBC) mooring 46025 in the Santa Monica Bay (33.749°N:119.053°W; depth 905.3 m; 33 Km offshore). The time series was analyzed in a way similar to AVHRR SST (i.e., split into seasonal, long-term, and short-term variations). The days when at least 50% of temperature measurements were 1.5°C lower than background (i.e., seasonal plus long-term components) were classified as “upwelling events”. Offshore CHL extensions were averaged for the days referenced to the beginning of an upwelling event.

Precipitation and Stormwater Runoff

Continuous flow data only exists for a small percentage of all rivers that discharge into the SCB. Therefore, daily stormwater runoff Q ($\text{m}^3 \text{day}^{-1}$) was modeled using the Rational Method (O'Loughlin et al. 1996), a spreadsheet model that is based on optimized runoff coefficients in conjunction with the watershed land-use pattern and the estimated averaged rainfall.

The Rational Method is similar to the EPA's Simple Method, though events with no runoff are excluded from the Rational model, which estimates runoff as a function of drainage area (A , km^2), mean rainfall intensity (I , mm day^{-1}), and the runoff coefficient (C):

$$Q = A \cdot I \cdot C. \tag{1}$$

The drainage area A was defined using the hydraulic unit code (HUC). The model domain includes all southern California coastal watersheds in San Diego, Orange, Riverside, Los Angeles, San Bernardino, Ventura and Santa Barbara counties with an initial total watershed area of 27,380 km^2 (Figure 1). Watershed areas larger than 52 km^2 upstream of dams were excluded in the model domain, in order to mimic the retention of water by dams (Ackerman and Schiff 2003). Extensive land-use information available was sorted into six categories: agriculture, commercial, industrial, open, residential, and other urban. The sorted land-use data was used to characterize the drainage area.

Daily precipitation in central and southern California from January 1997 through December 2007 was calculated on basis of the data obtained from the National Oceanic and Atmospheric Administration (NOAA) National Environmental Satellite, Data and Information Service (NESDIS) National Climatic Data Center (NCDC) Climate Data Online (CDO) database (<http://www7.ncdc.noaa.gov/CDO/cdo>). Daily measurements collected by ~200 rain gauge stations were downloaded and transformed to mean precipitation (cm day^{-1}) over 98 southern California watersheds from Pt. Conception to the Mexican border. For this, all available precipitation data were interpolated within each watershed on a regular grid using a Biharmonic Spline Interpolation method (Sandwell 1987). The watersheds were divided in grids with a minimum 5 rows/columns (grid resolution ≤ 0.02 degrees); for the larger watersheds, where 5 rows/column grids resulted in a coarser resolution, larger grids were used, keeping the grid resolution constant at 0.02 degrees.

The runoff coefficient (C) was assigned to watersheds varied with topography, land-use, vegetal cover, soil type, and soil moisture content. A bounded iterative optimization was used to determine runoff coefficients from measured local runoff. The goal of this optimization was to produce a set of runoff coefficients for each land-use type within the SCB (Ackerman and Schiff 2003). In cases for which land-use varied within a watershed, segments of the watershed with different land-use were estimated individually. Resulting interannual variations were smoothed using a 183-day square filter.

To compare the effect of stormwater runoff and upwelling events on phytoplankton blooms, 23 major storms were selected and analyzed in conjunction with 28 major upwelling events (see above). For each storm event, accumulated precipitation exceeded 2.5 cm. The offshore CHL extensions were averaged for the days referenced to the beginning of rainstorm.

Results

Seasonal and Spatial Patterns

In the SCB, the zones of $\text{CHL} > 5 \text{ mg m}^{-3}$ were observed mostly nearshore. Only in the Santa Barbara Channel did the “first” bloom offset regularly exceed 5 km, which could be attributed to the zones of high CHL around the Channel Islands (not shown). Correspondingly, the near-shore bloom events were regularly observed along the entire SCB coastline. The “second” (offshore) bloom zones (see Figure II-2C) were scarce and observed mostly around the Channel Islands. Nearshore bloom “hotspots” (the regions where CHL extension offshore was measurable throughout most of the year) included areas near Santa Maria (Central Coast), the Santa Barbara Channel, the Palos Verdes Shelf, San Pedro Bay, southern San Diego, and Ensenada (Figure II-3D).

Along the Central Coast, blooms began roughly in April and lasted until November, especially near Santa Maria. Blooms in this region tended to be large ($> 6 \text{ km}$ offshore), particularly in the spring. Initiation of blooms in the spring coincided with seasonal intensification of coastal upwelling-generating winds (Figure II-3A). Spring intensification of coastal upwelling along the Central Coast was evident from seasonal SST minima (Figure II-3B), which to the north of Pt. Conception occurred approximately two months later than in the SCB (April vs. February). Along the Central Coast, the frequency of short-term upwelling events was low all year round (Figure II-3C). In contrast to the SCB, this indicated steady

oceanographic conditions. During the summer, a steady upwelling regime along the Central Coast was evident from the SST (Figure II-3B), which was significantly lower than in the SCB, coinciding with high intensity of upwelling-favorable winds (cf. Figure II-3A).

South of Point Conception, blooms generally started in the spring and lasted 2–3 months throughout most of the SCB, extending as far as 6 km offshore during the bloom peak (typically in April). Blooms were most pronounced in the Santa Barbara Channel, Santa Monica and San Pedro Bays, and along the northern Baja California coast (Figure II-3D). Initiation of blooms in the spring was associated with the spring transition, when upwelling-favorable winds strengthened (Figure II-3A) and upwelling events started in the northern and central parts of the SCB (Figure II-3C). The frequency of upwelling events in this area was high from February to October. In the southern part of the SCB, upwelling was frequent from June to August. The SCB demonstrated more intensive upwelling in fall as compared with spring (Figure II-3C), which appears to be counterintuitive and attributable to inaccurate removal of seasonal variability in the data set. During the period of temperature increase (February–July), temperature drops were associated mostly with upwelling events, while during the period of temperature decrease (August–February) short-term SST decreases may have resulted from short periods of seasonal cooling that were more intensive than the smoothed seasonal SST cycles used in this study.

The averaged CHL within the 5-km near-shore regions (Figure II-3E) demonstrated seasonal patterns that were similar to, but less obvious than, those of corresponding offshore CHL extensions (Figure II-3D). In particular, CHL zones proximal to major river mouths showed a summer minima and winter maxima that coincided with the timing of seasonal stormwater runoff maxima.

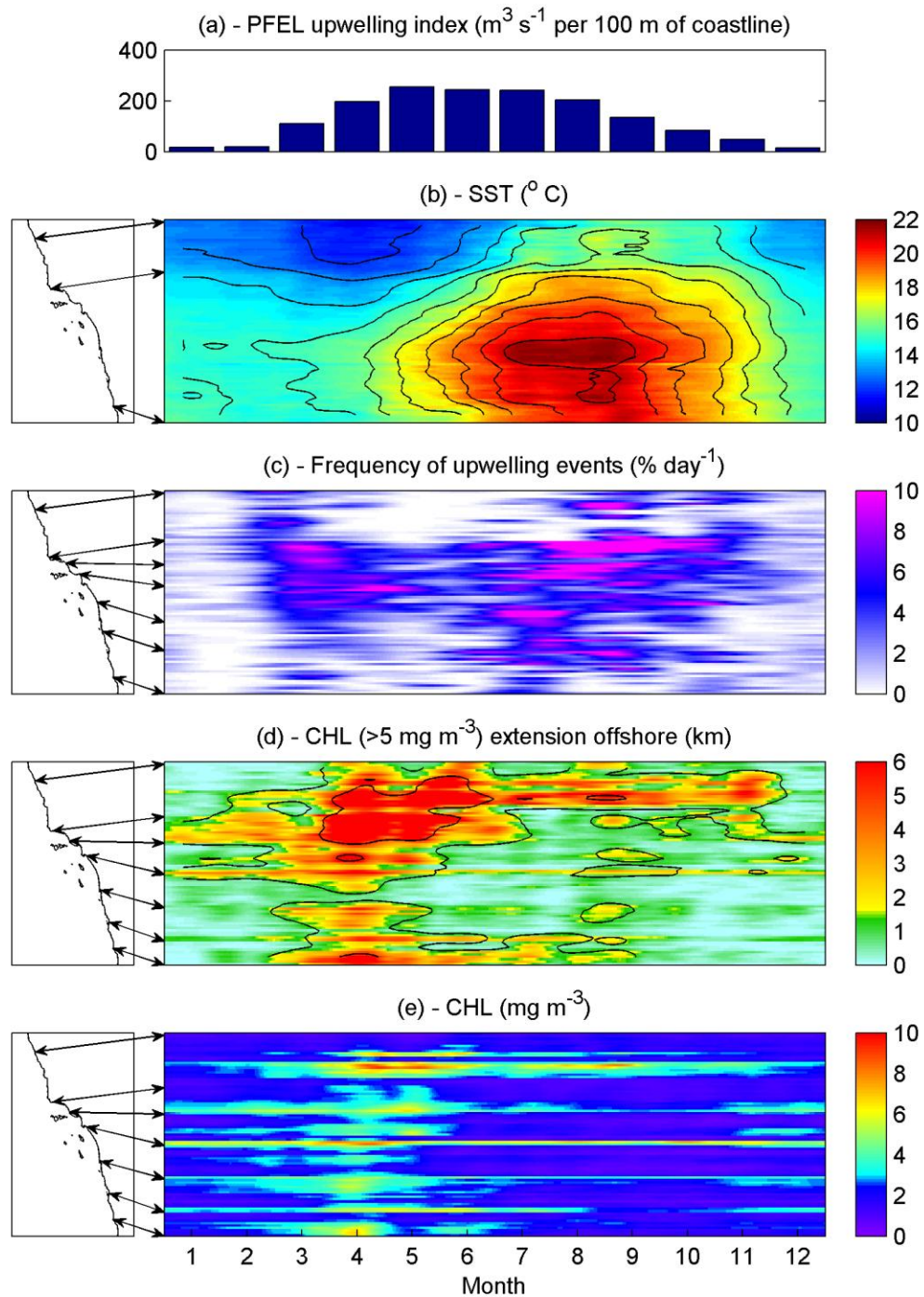


Figure II-3 Seasonal variability along the central and southern California coast: (a) PFEL upwelling index at 33°N ($\text{m}^3 \text{s}^{-1}$ per 100 m of coastline); (b) SST; (c) frequency of upwelling events ($\% \text{ day}^{-1}$); (d) the zone of high CHL ($>5 \text{ mg m}^{-3}$) offshore extension (km); (e) CHL concentration averaged over 5-km inshore parts of the transects.

Interannual Variations

An increasing trend of offshore CHL extension was observed during 1997–2007 for both the Central Coast and the SCB (Figure II-4D, E). The most evident growth of the zone of high CHL was observed in the southern part of the Central Coast, the Santa Barbara Channel, Santa Monica Bay, and San Diego ($0.2\text{--}0.4\text{ km year}^{-1}$). Almost all trend assessments (excluding Pt. Conception) were statistically significant with a 95% confidence level, which could be attributed to the large number of observations (371).

Similar analysis performed on averaged CHL in the 5-km near-shore regions also demonstrated a significant positive trend (not shown). In contrast to offshore CHL extensions, these trends were most pronounced near the river mouths, where remotely-sensed CHL concentration was likely to be measured most inaccurately. Surprisingly, these positive trends could not be attributed to stormwater runoff variations, as stormwater runoff demonstrated small ($100\text{--}3000\text{ m}^3\text{ year}^{-1}$), but significant negative trends over the entire study area (not shown).

At a large spatial scale (i.e., within the entire study area), the most intensive upwelling events and phytoplankton blooms were observed simultaneously. Compared to other years, larger offshore CHL extensions were observed in summer 2000–2001 along the Central Coast, in summer 2004 along the Central Coast and in the Santa Barbara Channel, and in summer 2005–2006 throughout the entire study region. Most of these periods (2000–2001 and 2005–2006) were characterized by high frequency of upwelling events in the SCB. Only in 2004 were the higher than normal phytoplankton blooms not coinciding with the higher than normal upwelling intensity observed in the northern part of the study area (Figure II-4A, C). Notably, the periods with the greatest frequency of upwelling events in the SCB coincided with the extremes in the smoothed NPGO cycle, both positive in 2000–2001 and negative in 2005 (Figure II-4B).

The effect of the interannual variability in stormwater runoff on the intensity of coastal phytoplankton blooms bightwide was less evident compared to upwelling. Runoff was higher than normal during the winter/spring of 1997–1998 and 2004–2005 (Figure II-4F). Stormwater runoff during 2004–2005 coincided with the beginning of intensive upwelling and very intensive phytoplankton blooms both along the Central Coast and in the SCB. However, torrential rains in 1997–1998 (El Niño year) and the resulting intensive runoff did not correspond to an increase in the offshore CHL extension. During the rest of the observed period, stormwater runoff appeared to coincide with an increased offshore extension of blooms in those areas proximal to the mouths of major rivers. The latter, however, could be partly attributed to the confounding effect of stormwater plumes on ocean color rather than phytoplankton blooms.

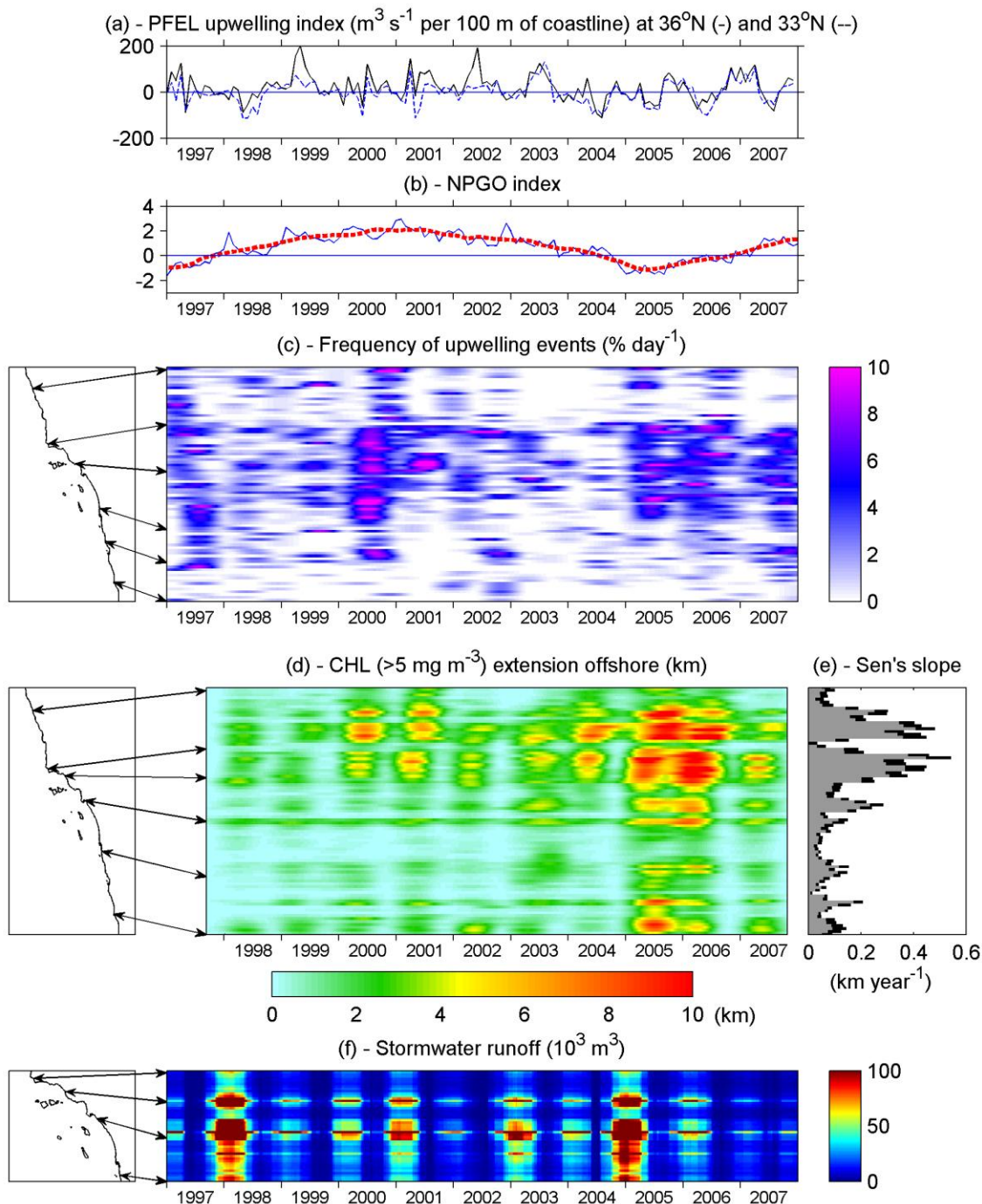


Figure II-4 Interannual variability along the central and southern California coast: (a) PFEL upwelling index ($\text{m}^3 \text{s}^{-1}$ per 100 m of coastline) at 36°N (solid line) and 33°N (dashed line); (b) NPGO index; red dashed line is NPGO smoothed with 1-year (13-month) window; (c) frequency of upwelling events ($\% \text{ day}^{-1}$); (d) the zone of high CHL ($>5 \text{ mg m}^{-3}$) offshore extension (km); (e) CHL extension offshore positive trend (black bars—Sen's slope; km year^{-1} ; grey bars—5% lower confidence intervals); (f) Stormwater runoff ($10^3 \text{ m}^3 \text{ day}^{-1}$).

Factors Affecting Blooms: Upwelling, Stormwater Runoff and Local Circulation

Analysis of 23 major storm events and 38 upwelling events supports the hypothesis that upwelling was the dominant factor affecting phytoplankton blooms in the SCB and along the Central Coast. Our analysis suggested that the role of stormwater runoff in promoting phytoplankton blooms was more likely limited to areas proximal to river mouths.

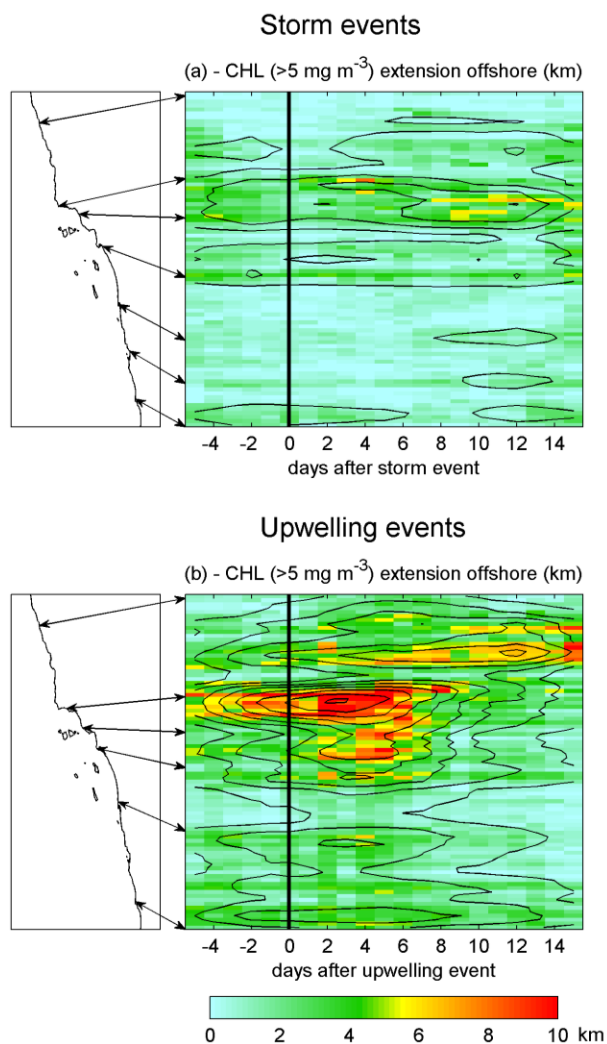


Figure II-5 The zone of high CHL ($>5 \text{ mg m}^{-3}$) offshore extension (km) along the central and southern California coast (a) after major rainstorms and (b) after major upwelling events.

After major upwelling events, zones of high CHL extended by 10 km offshore (Figure II-5B) for 5–8 days in the SCB and for at least 15 days along the Central Coast. In the Santa Barbara Channel, phytoplankton blooms started to appear 4 days before the date designated as an “upwelling event” (i.e., an abrupt decrease of the surface water temperature in the Santa Monica Bay) in this study. This time lag characterizes the spatial pattern of upwelling and resulting bloom development throughout the SCB from the north to the south.

After storm events, only a slight increase (by 2 km) in the offshore CHL extension was observed for 8–14 days in “hotspot” areas close to river mouths (Santa Clara/Calleguas, Los Angeles/San Gabriel, Santa Ana/San Diego Creek and Tijuana Rivers; Figure II-5A). Similarly, offshore CHL extensions increased by 5 km 5–15 days after storms in the Santa Barbara Channel.

Upwelling events affected the entire study region, including the SCB and the Central Coast, rather than its parts. The correlation (R^2) among short-scale SST seasonal anomalies in different parts of the study area (Figure II-6B) substantially exceeded the correlation among offshore CHL extensions (Figure II-6D). All R^2 coefficients were significant even after adjustment for autocorrelation (the number of degrees of freedom decreased from >4000 to 175 for SST and 196 for CHL making $R^2 \approx 0.04$ significant at a 0.95 confidence level). Also, correlations among SST in adjacent regions were not always high; for these locations, low correlation was attributed to low intensity of horizontal mixing. Such “natural boundaries” were observed near Pt. Conception, Santa Monica Bay, Palos Verdes Peninsula and San Diego (Figure II-6A). A similar pattern in variability was observed in the offshore CHL extension (Figure II-6C); low correlation was observed near Pt. Conception, San Diego, and Ensenada. In most of these regions, the frequency of CHL blooms was higher than in other parts of the SCB (Figures 3D and 4D).

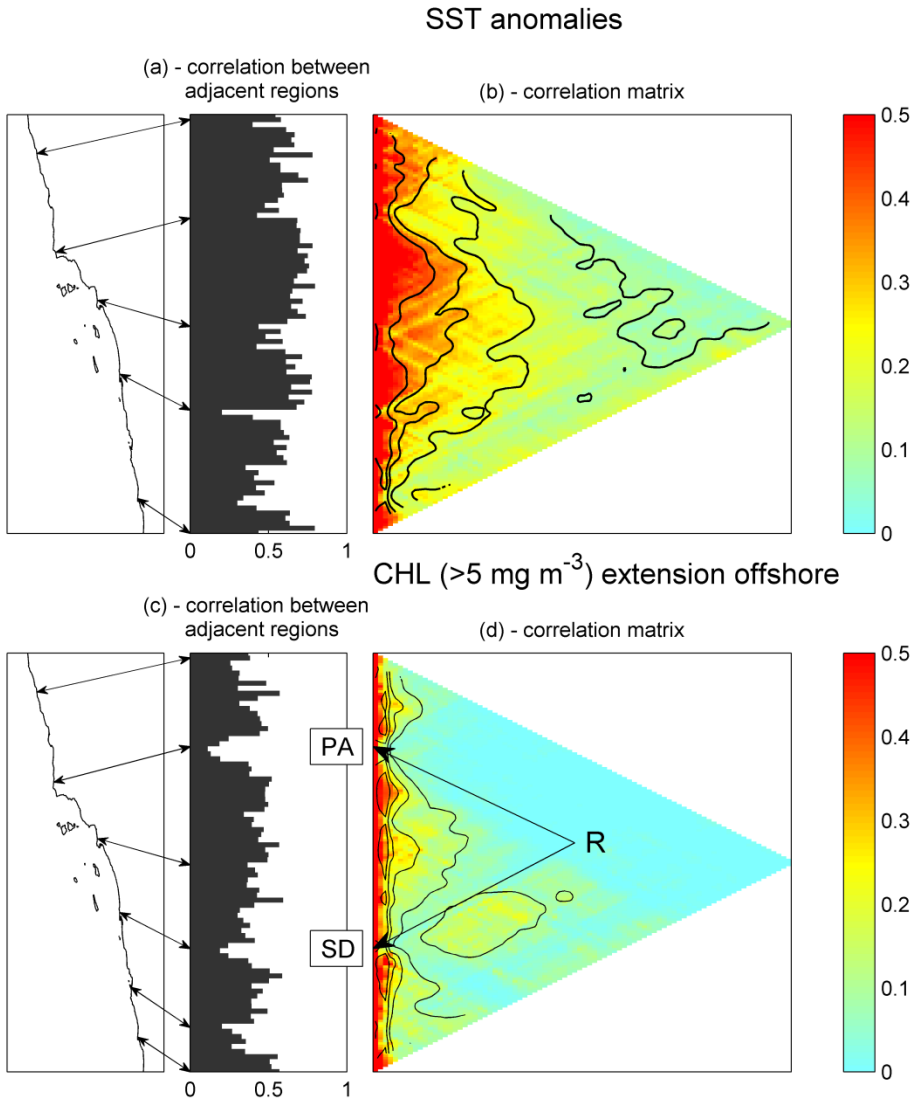


Figure II-6. Correlations (coefficients of determination R^2) between (a, b) short-term SST seasonal anomalies and (c, d) offshore CHL extension along the central and southern California coast. (a, c)—correlations between adjacent regions/transects; (b, d)—correlations between all regions/transects. Horizontal axes in (b) and (d) are roughly proportional to the distance between the regions. In particular, location R in (d) indicates the correlation between Point Arguello (PA) and San Diego (SD).

Discussion

Offshore CHL Extension as a Bloom Indicators

Climatological patterns of phytoplankton biomass are often examined on the basis of averaged remotely sensed CHL concentrations (e.g., Banse and English 1994, Longhurst 1995, McClain 2009). The results, however, are influenced by the accuracy of the estimated chlorophyll concentration of every pixel, which results in an inaccurate assessment (typically overestimation) of phytoplankton biomass in the near-shore ocean zone, where the ocean color signal can be biased by sediment loads in river plumes, unusual amounts of CDOM, bottom and landmass reflection, etc. Quantification of these effects to correct remotely-sensed CHL concentration (e.g. Dall'Olmo et al. 2005, Cannizzaro and Carder 2006, Ransibrahmanakul and Stumpf 2006) is labor consuming and the accuracy of these methods is questionable.

Use of the offshore CHL extension method avoids erroneous conclusions associated with traditional approaches based on the absolute value of remotely sensed CHL. In particular, CHL near SCB river mouths demonstrated a seasonal cycle with a summer minimum and winter maximum corresponding to the seasonal magnitude of stormwater runoff, which was attributed to contamination of ocean color signal by suspended sediments and CDOM near river mouths (e.g. Nezlin et al. 2008) rather than phytoplankton productivity. In the analysis of interannual trends, CHL concentrations demonstrated a high positive trend only near river mouths. Conversely, removal of this effect through use of offshore CHL extension revealed a positive interannual trend over most of the study region. On a bightwide scale, seasonal patterns illustrated by the offshore CHL extension were similar to those documented by Hayward and Venrick (1998) in a 12-year time series of chlorophyll measurements conducted by the CalCOFI program in the far offshore zone.

While the offshore CHL extension is a promising method, it is important to note that it does have some limitations. First, its use in the assessment of phytoplankton blooms is valid only in coastal regions like the SCB, with a narrow shelf and low freshwater discharge (i.e., in the areas where land contamination of ocean color dramatically decreases offshore). Second, it is important to note that use of Level 3 satellite imagery of approximately 1-km resolution appears appropriate for analysis of the bloom zone, which has an order of magnitude of 5–10 km during bloom events and 0–2 km otherwise. Imagery of this resolution is not available now from most ocean color satellite data sources and standard MODIS-Aqua and SeaWiFS Level 3 data (4.5 and 9 km, respectively) are too coarse for this purpose. Third, satellite imagery only detects the surface CHL and is unable to capture any subsurface CHL, which has been shown to be an important aspect of the development of surface phytoplankton blooms (Section IV).

Finally, the method of calculating the offshore CHL extension depends on coastline configuration. The method may indicate “hotspots” in areas with a “concave” coastline (bays) where “land effects” have a greater impact on analysis due to larger shelf zones and the positioning of transect lines. These areas in the SCB often coincide with zones of sluggish circulation, making it difficult to distinguish the effects of these factors on the offshore CHL extension as a bloom indicator.

Factors Associated with Offshore CHL Extension: Upwelling

In the SCB and along the Central Coast, this study found that upwelling is a dominant factor associated with the frequency and magnitude of phytoplankton blooms.

Upwelling in the northeastern Pacific is a large-scale phenomenon affecting the entire SCB, the Central Coast, and other areas. At a local scale, however, upwelling events and phytoplankton blooms were not always observed in parallel. In this study, during 2000–2001 upwelling events were detected in the SCB, while phytoplankton blooms were most evident along the Central Coast. This is possible because local surface measurements (including SST and ocean color) do not always indicate upwelling and bloom events when they happen. Upwelling does not always manifest itself as a decrease in SST, because cold upwelled water that enriches the upper euphotic layer with nutrients does not necessarily affect the surface layer if the water column is stratified. Once upwelling-favorable winds are dominant, it takes several days for cold water to reach the surface. This time lag depends on the depth and stratification of the mixed layer and, as such, may be seasonally and spatially variable for the same wind stress. Additionally, algal populations have been observed at subsurface depths however, the satellites are unable to detect these deep chlorophyll signatures (see Section IV, e.g., Reid et al. 1978, Cullen and Eppley 1981, Cullen et al. 1982, Cullen et al. 1983, Millan-Nunez et al. 1996). Consequently, the surface signatures of upwelling and phytoplankton blooms can be spatially separated. Anderson et al. (2008) also noted an apparent synchrony of HAB events in different California regions; they explained this synchrony with large-scale external forcing (primarily upwelling).

Along most of the SCB coast, interannual variability of the offshore CHL extension demonstrated a significant positive trend during 1997–2007. Previous studies (e.g., Gregg et al. 2005, Kahru and Mitchell 2008) have reported an increase in remotely-sensed and in situ CHL in many coastal areas worldwide, including California (Kahru et al. 2009, Kim et al. 2009). This increase may be related to climate change associated with intensification of seasonal upwelling (Bakun 1990, Bakun and Weeks 2004, Bakun et al. 2010), although its cooling effect may have been masked by a long-term increasing trend in SST (Schwing and Mendelssohn 1997). The latter was observed in this study for 1997–2007. No trends were revealed from low-frequency SST variability, and Sen's slopes were negligible in most regions (average -0.003 ± 0.026 degrees C year⁻¹). The increase in the offshore extension of phytoplankton blooms in the SCB captured over a 10-year time series is too short to understand the influence of climate change as a causal factor. Henson et al. (2010) indicated that a time series of ~40 years is needed to distinguish a global warming trend from natural variability. Surprisingly, no relationship was evident between the frequency of near-shore blooms in the SCB and the transition between the strong El Niño event in 1997–1998 and the 1998–1999 La Niña, which some authors called the most dramatic and rapid episode of climate change in modern times (Schwing et al. 2002, Peterson and Schwing 2003). In contrast, within the 100-km offshore zone the effect of the 1997–1998 El Niño on CHL was most clear throughout the observed period (Thomas et al. 2009).

Periods of high offshore CHL extension on an interannual scale coincided with both positive (in 2000–2001) and, surprisingly, negative (in 2005) extremes of smoothed NPGO climatic cycle (Di Lorenzo et al. 2008). A nonlinear relationship between NPGO and near-shore bloom activity in the SCB may be

attributed to a weak correlation between upwelling and chlorophyll resulting from its complex bottom topography (cf. Thomas et al. 2009). Positive NPGO is associated with enhanced CC circulation, resulting in early onset of upwelling, nutrient enrichment, and phytoplankton growth in the central part of the CC system (Chenillat et al. 2012). The NPGO minimum (suggesting upwelling-unfavorable conditions) was observed in 2005. Surprisingly, it was followed by the most intensive and long-lasting phytoplankton blooms in the SCB coastal zone. These blooms might have been attributed to specific features of an upwelling regime along the U.S. West Coast; the spring transition in 2005 occurred two-three months later than during other years (Schwing et al. 2006, Bograd et al. 2009). However, in the latter part of the upwelling season, coastal upwelling was stronger than normal, resulting in positive CHL anomalies in the 0–100 km offshore zone between 30°N–40°N (Thomas and Brickley 2006, Henson and Thomas 2007). A pronounced biological effect of the variations of upwelling seasonality was demonstrated earlier in the CC (Black et al. 2011).

The 5–8-day time lags between the onset of upwelling events and increases in offshore CHL extension indicate that the observed phenomena may be attributed to biological (phytoplankton growth), rather than physical (shoaling of subsurface chlorophyll maximum) processes associated with upwelling. Notably, a subsurface maximum of chlorophyll concentration is regularly observed (e.g., Millan-Nunez et al. 1996) at a depth of 20–40 m, which is invisible to satellite sensors. Upwelling-driven shoaling of this maximum can simultaneously affect SST and surface ocean color as observed from satellites. This physical effect implies a zero time lag between the decrease in SST and the increase in remotely-sensed CHL. In contrast, the biological effect of upwelling (nutrient flux to the euphotic layer fueling phytoplankton growth) implies a time lag of few days between upwelling events and phytoplankton blooms (see Henson and Thomas 2007 and the citations therein). The blooms observed in this study followed upwelling events with a 5–8-day time lag, similar to earlier observations (Nezlin and Li 2003).

No relationship was found between the frequency of upwelling events in the SCB and the PFEL upwelling index (UI), which characterizes large-scale patterns of atmospheric circulation over the west coast of North America (Bakun 1973). This lack of correspondence can be attributed to complex bottom topography in the SCB, in contrast to areas to the north and south, which are characterized by relatively straight coastlines with meridional direction coinciding with the direction of upwelling-favorable wind. The latter fits the classic scheme of Ekman upwelling, resulting in a straightforward relationship between large-scale wind patterns, upwelling intensity (UI), and phytoplankton growth. For example, in the Oregon coastal zone, UI explains ~77% of the upwelling system's interannual variability (Pierce et al. 2006). In contrast, in the SCB the results of this study indicated no relationship between UI and the frequency of upwelling events and phytoplankton blooms (cf. Kahru et al. 2009, Kim et al. 2009, Thomas et al. 2009). Previous studies also indicated that wind stress explains little of the current variability within the SCB (Lentz and Winant 1986, Noble et al. 2002, Hickey et al. 2003).

Other Factors Associated with Offshore CHL Extension

The results of this study based on 10+ years of observations demonstrated no evidence of the regional importance of stormwater discharge for phytoplankton blooms in the SCB and along the Central Coast. In both 1997–1998 and 2004–2005, when precipitation and stormwater runoff were high, the

phytoplankton response was variable. In 1997–1998 (El Niño year), phytoplankton blooms were scarce in spite of torrential rains and intensive runoff. The positive effect of stormwater nutrient discharge may have been counterbalanced by negative effect of stronger than normal nutrient limitation that resulted from an El Niño-driven deep pycnocline (e.g., Chavez et al. 1998, Chavez et al. 1999). In 2004–2005, high precipitation was followed by intensive coastal upwelling and phytoplankton blooms. As such, stormwater discharge cannot be identified as the single source of these blooms. Previous studies suggested that the contribution of river discharge to the nutrient budget in the SCB is small compared to upwelling (Warrick et al. 2005). On the other hand, nutrient contribution from terrestrial sources (including stormwater and dry weather runoff, groundwater discharge and atmospheric deposition) could be negligible at a large scale, but have a pronounced effect at a local scale, especially near river mouths and in shallow semi-enclosed basins characterized by long water residence time. In areas near river mouths and areas characterized by extended residence time, terrestrial discharge (rich in ammonia and micronutrients, e.g., iron) has been shown to enhance phytoplankton productivity and alter N:P:Si ratios that affect the taxonomic structure of phytoplankton (Paerl 1997).

When comparing the effects of storm and upwelling events on the offshore CHL extension one should keep in mind that nutrient-rich storm runoff always enters the ocean at the surface. As such, its effect would be observed by satellite sensors much better than upwelling and/or POTW discharge, which effect may or may not reach all the way to the surface. A slight increase in offshore CHL after storm events as compared with upwelling demonstrates that contamination of remotely-sensed CHL signal by CDOM and other suspended materials discharged with stormwater was not high and accentuates the effect of upwelling on phytoplankton growth in the SCB.

In this study, hot spots, areas in which the offshore CHL extension was higher than in other locations, were observed. Hot spots occurred throughout most of the year in Santa Maria (Central Coast), the Santa Barbara Channel, along the San Pedro Shelf, in the Santa Monica Bay, along the South San Diego and Ensenada coast, and in areas with long residence time co-located with large river mouths and POTW ocean outfalls (see Figure II-1 for river and POTW locations and Figure II-3 for observed CHL 'hotspots'). In the SCB, stormwater plumes extend mostly downcoast (Warrick et al. 2007) and discharged nutrients can be transported for tens of kilometers while affecting phytoplankton biomass. As such, water residence time may be an important factor regulating this process. Persistent high CHL in shallow semi-enclosed regions with long residence time has been documented in previous studies in the SCB and elsewhere. Cullen et al. (1982) suggested that the residence time of water near the coast is of great importance when determining the abundance and taxonomic characteristics of phytoplankton. In particular, coastal regions characterized by retentive circulation and stratified water column are often subject to intense dinoflagellate blooms (e.g., Ryan et al. 2008). For example, dinoflagellate blooms with chlorophyll-a concentrations as high as 500 mg m^{-3} were recorded in La Jolla Bay in May 1964–August 1966 associated with a steep shallow thermocline (Holmes et al. 1967). San Pedro Bay, a region characterized by long residence time, has recently had frequent blooms of *Pseudo-nitzschia* spp. and some of the highest concentrations of domoic acid ever recorded on the U.S. west coast (Caron 2008). In addition, Anderson et al. (2002) noted that, in areas of poor flushing, the toxic effect of HABs can be much more severe. However, the assessment of water residence time based on correlations among SST

anomalies is not sufficiently accurate to evaluate the significance of the influence of local circulation on phytoplankton growth. The mechanism of this influence could be better analyzed using mathematical modeling (cf. Mitarai et al. 2009).

In the SCB, the regions of poor flushing often coincide geographically with river mouths and POTW locations and, as such, accumulate nutrients. While the effect of stormwater discharge near major river mouths on offshore bloom extensions was limited relative to upwelling, river mouths can be a chronic, low-concentration source of nutrients through dry weather discharge; a factor not considered in this study. In the SCB's Mediterranean climate, dry weather discharge has increased as the landscape has become increasingly urbanized and supported by the import of freshwater from northern California and the Colorado River basin (Ackerman and Schiff 2003). Locally, the effect of this dry weather runoff can be substantial. Analysis of nutrient loads to the SCB demonstrated that dry-weather discharge from the Los Angeles and San Gabriel Rivers represents approximately 48% of total annual nitrogen loads to the San Pedro Bay area and 24% of total annual nitrogen loads to the entire SCB (A. Sengupta, unpublished data). Also, nutrient-rich wastewater discharge from large POTWs may be an additional continuous source of nutrients. All four large POTWs in the SCB have outfalls where “hot spots” of high offshore CHL extensions were observed, but these outfalls are also located in areas characterized by shallow depth and long residence time, or in close proximity to river mouths.

This study determined that within the SCB, upwelling is a clear driver controlling spatial and temporal patterns of remotely-sensed phytoplankton productivity. On a more refined spatial scale, terrestrial freshwater discharge and POTW discharges via ocean outfalls have the potential to affect patterns of phytoplankton productivity, particularly by increasing the duration and size of the blooms. However, a remote sensing analysis of factors associated with the spatial and temporal patterns in phytoplankton blooms in the SCB cannot effectively distinguish between the effects of wastewater, stormwater discharge, bathymetry, and water residence time. To quantify the relative influence of these nutrient sources, mathematical modeling, supported by real-time monitoring and regular surveys collecting oceanographic data, are required.

Acknowledgments

The authors would like to thank the SeaWiFS Project (Code 970.2) for the production and distribution of the SeaWiFS data. These activities are sponsored by NASA's Mission to Planet Earth Program. The authors also thank the NASA Physical Oceanography Distributed Active Archive Center at the Jet Propulsion Laboratory, California Institute of Technology for SST data and the NOAA National Data Center Climate Data Online (NNDC/CDO) for the rain gauge-measured precipitation data. We thank Doug Pirhalla (NOAA) for help in SeaWiFS data processing. Becky Shaffner helped in processing GIS watershed data. The remarks of Alex Steele, Ken Schiff, and three anonymous reviewers were extremely helpful and significantly improved the paper.

References

- Ackerman, D. and K. Schiff, 2003. Modeling storm water mass emissions to the Southern California Bight. *Journal of Environmental Engineering-ASCE* 129: 308-317, doi:310.1061/(ASCE)0733-9372(2003)1129:1064(1308).
- Ackerman, D. and S.B. Weisberg, 2003. Relationship between rainfall and beach bacterial concentrations on Santa Monica Bay beaches. *Journal of Water and Health* 1: 85-89.
- Anderson, D.M., J.M. Burkholder, W.P. Cochlan, P.M. Glibert, C.J. Gobler, C.A. Heil, R.M. Kudela, M.L. Parsons, J.E.J. Rensel, D.W. Townsend, V.L. Trainer and G.A. Vargo, 2008. Harmful algal blooms and eutrophication: Examining linkages from selected coastal regions of the United States. *Harmful Algae* 8: 39-53, doi:10.1016/j.hal.2008.1008.1017.
- Anderson, D.M., P.M. Glibert and J.M. Burkholder, 2002. Harmful algal blooms and eutrophication: Nutrient sources, composition, and consequences. *Estuaries* 25: 704-726, doi:10.1007/BF02804901.
- Bakun, A., 1973. Coastal upwelling indices, west coast of North America, 1946–1971. NOAA Tech. Rep. NMFS SSRF-671. U.S. Department of Commerce. Washington, D. C.
- Bakun, A., 1990. Global climate change and intensification of coastal ocean upwelling. *Science* 247: 198-201, doi: 10.1126/science.1247.4939.1198.
- Bakun, A., D.B. Field, A. Redondo-Rodriguez and S.J. Weeks, 2010. Greenhouse gas, upwelling-favorable winds, and the future of coastal ocean upwelling ecosystems. *Global Change Biology* 16: 1213-1228, doi: 10.1111/j.1365-2486.2009.02094.x.
- Bakun, A. and C.S. Nelson, 1991. The seasonal cycle of wind-stress curl in subtropical eastern boundary current regions. *Journal of Physical Oceanography* 21: 1815-1834, doi: 10.1175/1520-0485(1991)021<1815:TSCOWS>1812.CO;2.
- Bakun, A. and S.J. Weeks, 2004. Greenhouse gas buildup, sardines, submarine eruptions and the possibility of abrupt degradation of intense marine upwelling ecosystems. *Ecology Letters* 7: 1015-1023, doi: 10.1111/j.1461-0248.2004.00665.x.
- Banase, K. and D.C. English, 1994. Seasonality of Coastal Zone Color Scanner phytoplankton pigment in the offshore oceans. *Journal of Geophysical Research-Oceans* 99: 7323-7345, doi: 10.1029/7393JC02155.
- Barber, R.T. and R.L. Smith. 1981. Coastal upwelling ecosystems. London. in: A. R. Longhurst (Ed.), *Analysis of Marine Ecosystems*. Academic Press 31-68
- Black, B.A., I.D. Schroeder, W.J. Sydeman, S.J. Bograd, B.K. Wells and F.B. Schwing, 2011. Winter and summer upwelling modes and their biological importance in the California Current Ecosystem. *Global Change Biology* 17: 2536-2545, doi: 10.1111/j.1365-2486.2011.02422.x.

- Bograd, S.J., I.D. Schroeder, N. Sarkar, X. Qiu, W.J. Sydeman and F.B. Schwing, 2009. Phenology of coastal upwelling in the California Current. *Geophysical Research Letters* 36:L01602, doi: 10.1029/2008GL035933.
- Boyce, D.G., M.R. Lewis and B. Worm, 2010. Global phytoplankton decline over the past century. *Nature* 466: 591-596, doi: 10.1038/nature09268.
- Bray, N.A., A. Keyes and W.M.L. Morawitz, 1999. The California Current system in the Southern California Bight and the Santa Barbara Channel. *Journal of Geophysical Research-Oceans* 104: 7695-7714, doi: 10.1029/1998JC900038.
- Campbell, J.W., 1995. The lognormal-distribution as a model for biooptical variability in the sea. *Journal of Geophysical Research-Oceans* 100: 13237-13254, doi: 10.1029/13295JC00458.
- Cannizzaro, J.P. and K.L. Carder, 2006. Estimating chlorophyll a concentrations from remote-sensing reflectance in optically shallow waters. *Remote Sensing of Environment* 101: 13-24, doi: 10.1016/j.rse.2005.1012.1002.
- Caron, D.A., 2008. Collaborative HAB research and toxicity on the San Pedro Shelf. pp. B-3 in, Harmful Algal Bloom Monitoring and Alert Program (HABMAP) Working Group. The regional workshop for harmful algal blooms (HABs) in California coastal waters, Vol. Report #565. Southern California Coastal Water Research Project. Costa Mesa, CA.
- Chavez, F.P., P.G. Strutton, G.E. Friedrich, R.A. Feely, G.C. Feldman, D.G. Foley and M.J. McPhaden, 1999. Biological and chemical response of the equatorial Pacific Ocean to the 1997-98 El Niño. *Science* 286: 2126-2131, doi: 10.1126/science.2286.5447.2126.
- Chavez, F.P., P.G. Strutton and M.J. McPhaden, 1998. Biological-physical coupling in the central equatorial Pacific during the onset of the 1997-98 El Niño. *Geophysical Research Letters* 25: 3543-3546, doi: 10.1029/3598GL02729.
- Chenillat, F., P. Riviere, X. Capet, E. Di Lorenzo and B. Blanke, 2012. North Pacific Gyre Oscillation modulates seasonal timing and ecosystem functioning in the California Current upwelling system. *Geophysical Research Letters* 39.
- Chereskin, T.K. and P.P. Niiler, 1994. Circulation in the Ensenada Front - September 1988. *Deep-Sea Research Part I-Oceanographic Research Papers* 41: 1251-1287, doi: 10.1016/0967-0637(1994)90043-90044.
- Claustre, H., A. Morel, S.B. Hooker, M. Babin, D. Antoine, K. Oubelkheir, A. Bricaud, K. Leblanc, B. Queguiner and S. Maritorena, 2002. Is desert dust making oligotrophic waters greener? *Geophysical Research Letters* 29: 1469, doi: 10.1029/2001GL014056.
- Cullen, J.J. and R.W. Eppley, 1981. Chlorophyll maximum layers of the Southern California Bight and possible mechanisms of their formation and maintenance. *Oceanologica Acta* 4: 23-32.
- Cullen, J.J., F.M.H. Reid and E. Stewart, 1982. Phytoplankton in the surface and chlorophyll maximum off southern California in August, 1978. *Journal of Plankton Research* 4: 665-694.

Cullen, J.J., E. Stewart, E. Renger, R.W. Eppley and C.D. Winant, 1983. Vertical motion of the thermocline, nitracline and chlorophyll maximum layer in relation to currents on the Southern California Shelf. *Journal of Marine Research* 41: 239-262.

Culliton, T.J., M.A. Warren, T.R. Goodspeed, D.G. Remer, C.M. Blackwell and J.J. McDonough, 1990. Fifty years of population change along the nation's coasts, 1960-2010. Coastal Trends Series, Report No. 2. NOAA Strategic Assessment Branch. Rockville, MD.

Dall'Olmo, G., A.A. Gitelson, D.C. Rundquist, B. Leavitt, T. Barrow and J.C. Holz, 2005. Assessing the potential of SeaWiFS and MODIS for estimating chlorophyll concentration in turbid productive waters using red and near-infrared bands. *Remote Sensing of Environment* 96: 176-187, doi: 10.1016/j.rse.2005.1002.1007.

Di Lorenzo, E., N. Schneider, K.M. Cobb, P.J.S. Franks, K. Chhak, A.J. Miller, J.C. McWilliams, S.J. Bograd, H. Arango, E. Curchitser, T.M. Powell and P. Riviere, 2008. North Pacific Gyre Oscillation links ocean climate and ecosystem change. *Geophysical Research Letters* 35:L08607, doi: 10.1029/2007GL032838.

Emery, K.O., 1960. *The Sea off Southern California*. John Wiley and Sons, Inc. New York. 366 pp.

Eppley, R.W., A.F. Carlucci, O. Holm-Hansen, D.A. Kiefer, J.J. McCarthy and P.M. Williams. 1972. Evidence for eutrophication in the sea near southern California coastal sewage outfalls - July; 1970. *California Cooperative Oceanic Fisheries Investigations Reports* 16: 74-83.

Glibert, P.M., D.M. Anderson, P. Gentien, E. Graneli and K.G. Sellner, 2005. The global complex phenomena of Harmful Algal Blooms. *Oceanography* 18: 136-147.

Glibert, P.M., J. Harrison, C. Heil and S. Seitzinger, 2006. Escalating worldwide use of urea - a global change contributing to coastal eutrophication. *Biogeochemistry* 77: 441-463, doi: 10.1007/s10533-0005-13070-10535.

Gordon, H.R. and M. Wang, 1994. Retrieval of water-leaving radiance and aerosol optical thickness over the oceans with SeaWiFS: a preliminary algorithm. *Applied Optics* 33: 443-452, doi:10.1364/AO.1333.000443.

Gregg, W.W. (Ed.), 2007. *Ocean-Colour Data Merging*. (Vol. 6). Dartmouth, Canada: IOCCG.

Gregg, W.W. and N.W. Casey, 2004. Global and regional evaluation of the SeaWiFS chlorophyll data set. *Remote Sensing of Environment* 93: 463-479, doi: 10.1016/j.rse.2003.1012.1012.

Gregg, W.W., N.W. Casey and C.R. McClain, 2005. Recent trends in global ocean chlorophyll. *Geophysical Research Letters* 32:L03606, doi: 10.1029/2004GL021808.

Haney, R.L., R.A. Hale and D.E. Dietrich, 2001. Offshore propagation of eddy kinetic energy in the California Current. *Journal of Geophysical Research-Oceans* 106: 11709-11717, doi: 10.1029/12000JC000433.

Harms, S. and C.D. Winant, 1998. Characteristic patterns of the circulation in the Santa Barbara Channel. *Journal of Geophysical Research-Oceans* 103: 3041-3065, doi: 3010.1029/3097JC02393.

Haury, L.R., E.L. Venrick, C.L. Fey, J.A. McGowan and P.P. Niiler, 1993. The Ensenada Front: July 1985. *California Cooperative Oceanic Fisheries Investigations Reports* 34: 69-88.

Hayward, T.L. and E.L. Venrick, 1998. Nearsurface patterns in the California Current: Coupling between physical and biological structure. *Deep-Sea Research II* 45: 1617-1638, doi: 1610.1016/S0967-0645(1698)80010-80016.

Heisler, J., P.M. Glibert, J.M. Burkholder, D.M. Anderson, W.P. Cochlan, W.C. Dennison, Q. Dortch, C.J. Gobler, C.A. Heil, E. Humphries, A. Lewitus, R.E. Magnien, H.G. Marshall, K.G. Sellner, D.A. Stockwell, D.K. Stoecker and M. Suddleson, 2008. Eutrophication and harmful algal blooms: A scientific consensus. *Harmful Algae* 8: 3-13, doi:10.1016/j.hal.2008.1008.1006.

Henson, S.A., J.L. Sarmiento, J.P. Dunne, L. Bopp, I. Lima, S.C. Doney, J. John and C. Beaulieu, 2010. Detection of anthropogenic climate change in satellite records of ocean chlorophyll and productivity. *Biogeosciences* 7: 621-640, doi:610.5194/bg-5197-5621-2010.

Henson, S.A. and A.C. Thomas, 2007. Interannual variability in timing of bloom initiation in the California Current System. *Journal of Geophysical Research-Oceans* 112:C08007, doi: 08010.01029/02006JC003960.

Hickey, B.M. , 1979. The California Current system: Hypotheses and facts. *Progress in Oceanography* 8: 191-279.

Hickey, B.M., E.L. Dobbins and S.E. Allen, 2003. Local and remote forcing of currents and temperature in the central Southern California Bight. *Journal of Geophysical Research-Oceans* 108: 3081, doi:3010.1029/2000JC000313.

Holmes, R.W., P.M. Williams and R.W. Eppley, 1967. Red water in La Jolla Bay, 1964-1966. *Limnology and Oceanography* 12: 503-512.

Kahru, M., R.M. Kudela, M. Manzano-Sarabia and B.G. Mitchell, 2009. Trends in primary production in the California Current detected with satellite data. *Journal of Geophysical Research-Oceans* 114:C02004, doi: 02010.01029/02008JC004979.

Kahru, M. and B.G. Mitchell, 2008. Ocean color reveal increased blooms in various parts of the world. *EOS* 89: 170.

Ketchum, B.H., 1951. The exchanges of fresh and salt waters in tidal estuaries. *Journal of Marine Research* 10: 18-38.

Kilpatrick, K.A., G.P. Podesta and R. Evans, 2001. Overview of the NOAA/NASA advanced very high resolution radiometer Pathfinder algorithm for sea surface temperature and associated matchup database. *Journal of Geophysical Research-Oceans* 106: 9179-9197, doi: 9110.1029/1999JC000065.

- Kim, H.-J., A.J. Miller, J.A. McGowan and M.L. Carter, 2009. Coastal phytoplankton blooms in the Southern California Bight. *Progress in Oceanography* 82: 137-147, doi:10.1016/j.pocean.2009.1005.1002.
- Lentz, S.J. and C.D. Winant, 1986. Subinertial currents on the southern California shelf. *Journal of Physical Oceanography* 16: 1737-1750, doi: 10.1175/1520-0485(1986)1016<1737:SCOTSC>1732.1730.CO;1732.
- Longhurst, A.R., 1995. Seasonal cycles of pelagic production and consumption. *Progress in Oceanography* 36: 77-167, doi: 10.1016/0079-6611(1995)00015-00011.
- Lynn, R.J., S.J. Bograd, T.K. Chereskin and A. Huyer, 2003. Seasonal renewal of the California Current: The spring transition off California. *Journal of Geophysical Research-Oceans* 108: 3279, doi: 10.1029/2003JC001787.
- Lynn, R.J. and J.J. Simpson, 1987. The California Current System: The seasonal variability of its physical characteristics. *Journal of Geophysical Research-Oceans* 92: 12947-12966, doi: 10.1029/JC12092iC12912p12947.
- Lyon, G.S. and E.D. Stein, 2009. How effective has the Clean Water Act been at reducing pollutant mass emissions to the Southern California Bight over the past 35 years? *Environmental Monitoring and Assessment* 154: 413-426, doi: 10.1007/s10661-10008-10408-10661.
- Mantyla, A.W., S.J. Bograd and E.L. Venrick, 2008. Patterns and controls of chlorophyll-a and primary productivity cycles in the Southern California Bight. *Journal of Marine Systems* 73: 48-60, doi: 10.1016/j.jmarsys.2007.1008.1001.
- Maritorena, S., A.Y. Morel and B. Gentili, 1994. Diffuse reflectance of oceanic shallow waters: Influence of water depth and bottom albedo. *Limnology and Oceanography* 39: 1689-1703.
- McClain, C.R., 2009. A decade of satellite ocean color observations. *Annual Review of Marine Science* 1: 19-42, doi: 10.1146/annurev.marine.010908.163650.
- Millan-Nunez, R., S. Alvarez-Borrego and C.C. Trees, 1996. Relationship between deep chlorophyll maximum and surface chlorophyll concentration in the California Current system. *California Cooperative Oceanic Fisheries Investigations Reports* 37: 241-250.
- Mitarai, S., D.A. Siegel, J.R. Watson, C. Dong and J.C. McWilliams, 2009. Quantifying connectivity in the coastal ocean with application to the Southern California Bight. *Journal of Geophysical Research-Oceans* 114:C10026, doi: 10.1029/2008JC005166.
- Moulin, C., H.R. Gordon, R.M. Chomko, V.F. Banzon and R.H. Evans, 2001. Atmospheric correction of ocean color imagery through thick layers of Saharan dust. *Geophysical Research Letters* 28: 5-8, doi: 10.1029/2000GL011803.
- Muller-Karger, F.E., C. Hu, S. Andrefouet, R. Varela and R.C. Thunell, 2005. The color of the coastal ocean and applications in the solution of research and management problems. Springer. Dordrecht. in:

R. L. Miller , C. E. Del Castillo and B. A. McKee (Eds.), Remote Sensing of Coastal Aquatic Environments 101-127

National Research Council, 2000. Clean Coastal Waters: Understanding and Reducing the Effects of Nutrient Pollution. National Academy Press. Washington (DC). 405 pp.

Nezlin, N.P., P.M. DiGiacomo, D.W. Diehl, B.H. Jones, S.C. Johnson, M.J. Mengel, K.M. Reifel, J.A. Warrick and M. Wang, 2008. Stormwater plume detection by MODIS imagery in the southern California coastal ocean. *Estuarine, Coastal and Shelf Science* 80: 141-152, doi: 110.1016/j.ecss.2008.1007.1012.

Nezlin, N.P. and B.-L. Li, 2003. Time-series analysis of remote-sensed chlorophyll and environmental factors in the Santa Monica-San Pedro Basin off southern California. *Journal of Marine Systems* 39: 185-202, doi: 110.1016/S0924-7963(1003)00030-00037.

Nezlin, N.P. and E.D. Stein, 2005. Spatial and temporal patterns of remotely-sensed and field-measured rainfall in southern California. *Remote Sensing of Environment* 96: 228-245, doi: 110.1016/j.rse.2005.1002.1005.

Nixon, S.W., 1995. Coastal marine eutrophication: A definition, social causes, and future concerns. *Ophelia* 41: 199-219.

Noble, M.A., H.F. Ryan and P.L. Wiberg, 2002. The dynamics of subtidal poleward flows over a narrow continental shelf, Palos Verdes, CA. *Continental Shelf Research* 22: 923-944, doi: 110.1016/S0278-4343(1001)00112-00111.

O'Loughlin, G., W. Huber and B. Chocat., 1996. Rainfall-runoff processes and modelling. *Journal of Hydraulic Research* 34: 733-751.

O'Reilly, J.E., S. Maritorena, B.G. Mitchell, D.A. Siegel, K.L. Carder, S.A. Garver, M. Kahru and C. McClain, 1998. Ocean color chlorophyll algorithms for SeaWiFS. *Journal of Geophysical Research-Oceans* 103: 24937-24953, doi: 110.1029/24998JC02160.

Paerl, H.W., 1997. Coastal eutrophication and harmful algal blooms: Importance of atmospheric deposition and groundwater as "new" nitrogen and other nutrient sources. *Limnology and Oceanography* 42: 1154-1165.

Paerl, H.W. and J. Huisman, 2008. Blooms like it hot. *Science* 320: 57-58, doi: 110.1126/science.1155398.

Peterson, W.T. and F.B. Schwing, 2003. A new climate regime in northeast pacific ecosystem. *Geophysical Research Letters* 30: 1896, doi: 110.1029/2003GL017528.

Pierce, S.D., J.A. Barth, R.E. Thomas and G.W. Fleischer, 2006. Anomalously warm July 2005 in the northern California Current: Historical context and the significance of cumulative wind stress. *Geophysical Research Letters* 33:L22S04, doi: 110.1029/2006GL027149.

Pyper, B.J. and R.M. Peterman, 1998. Comparison of methods to account for autocorrelation in correlation analyses of fish data. *Canadian Journal of Fisheries and Aquatic Sciences* 55: 2127-2140.

- Ransibrahmanakul, V. and R.P. Stumpf, 2006. Correcting ocean colour reflectance for absorbing aerosols. *International Journal of Remote Sensing* 27: 1759-1774, doi: 1710.1080/01431160500380604.
- Reid, F.M.H., E. Stewart, R.W. Eppley and D. Goodman, 1978. Spatial distribution of phytoplankton species in chlorophyll maximum layers off southern California. *Limnology and Oceanography* 23: 219-226.
- Reid, J.L., Jr. and A.W. Mantyla, 1976. The effect of the geostrophic flow upon coastal sea elevations in the northern North Pacific ocean. *Journal of Geophysical Research* 81: 3100-3110.
- Ryan, J.P., J.F.R. Gower, S.A. King, W.P. Bissett, A.M. Fischer, R.M. Kudela, Z. Kolber, F. Mazzillo, E.V. Rienecker and F.P. Chavez, 2008. A coastal ocean extreme bloom incubator. *Geophysical Research Letters* 35:L12602, doi: 12610.11029/12008GL034081.
- Sandwell, D.T., 1987. Biharmonic spline interpolation of GEOS-3 and SEASAT Altimeter Data. *Geophysical Research Letters* 14: 139-142, doi: 110.1029/GL1014i1002p00139.
- Santer, R. and C. Schmechtig, 2000. Adjacency effects on water surfaces: primary scattering approximation and sensitivity study. *Applied Optics* 39: 361-375, doi: 310.1364/AO.1339.000361
- Schiff, K.C., M.J. Allen, E.Y. Zeng and S.M. Bay, 2000. Southern California. *Marine Pollution Bulletin* 41: 76-93, doi: 10.1016/S0025-1326X(1000)00103-X.
- Schwing, F.B., N.A. Bond, S.J. Bograd, T. Mitchell, M.A. Alexander and N. Mantua, 2006. Delayed coastal upwelling along the US West Coast in 2005: A historical perspective. *Geophysical Research Letters* 33:L22S01, doi: 10.1029/2006GL026911.
- Schwing, F.B. and R. Mendelssohn, 1997. Increased coastal upwelling in the California Current System. *Journal of Geophysical Research-Oceans* 102: 3421-3438, doi: 3410.1029/3496JC03591.
- Schwing, F.B., T. Murphree, L. deWitt and P.M. Green, 2002. The evolution of oceanic and atmospheric anomalies in the northeast Pacific during the El Niño and La Niña events of 1995-2001. *Progress in Oceanography* 54: 459-491, doi: 410.1016/S0079-6611(1002)00064-00062.
- Sen, P.K., 1968. Estimates of the regression coefficient based on Kendall's tau. *Journal of the American Statistical Association* 63: 1379-1389.
- Strub, P.T., J.S. Allen, A. Huyer and R.L. Smith, 1987a. Large-scale structure of the spring transition in the coastal ocean off western North America. *Journal of Geophysical Research-Oceans* 92: 1527-1544, doi: 1510.1029/JC1092iC1502p01527.
- Strub, P.T., J.S. Allen, A. Huyer, R.L. Smith and R.C. Beardsley, 1987b. Seasonal cycles of currents, temperatures, winds, and sea level over the northeast Pacific continental shelf: 35N to 48N. *Journal of Geophysical Research-Oceans* 92: 1507-1526, doi: 1510.1029/JC1092iC1502p01507.
- Strub, P.T. and C. James, 1988. Atmospheric conditions during the spring and fall transition in the coastal ocean off western United States. *Journal of Geophysical Research-Oceans* 93: 15561-15584, doi: 15510.11029/JC15093iC15512p15561.

Sverdrup, H.U. and R.H. Fleming, 1941. The waters off the coast of southern California, March to July 1937. *Bulletin of the Scripps Institution of Oceanography* 4: 261-378.

Thomas, A.C. and P. Brickley, 2006. Satellite measurements of chlorophyll distribution during spring 2005 in the California Current. *Geophysical Research Letters* 33:L22S05, doi: 10.1029/2006GL026588.

Thomas, A.C., P. Brickley and R. Weatherbee, 2009. Interannual variability in chlorophyll concentrations in the Humboldt and California Current Systems. *Progress in Oceanography* 83: 386-392, doi: 10.1016/j.pocean.2009.1007.1020.

Warrick, J.A., P.M. DiGiacomo, S.B. Weisberg, N.P. Nezlin, M.J. Mengel, B.H. Jones, J.C. Ohlmann, L. Washburn, E.J. Terrill and K.L. Farnsworth, 2007. River plume patterns and dynamics within the Southern California Bight. *Continental Shelf Research* 27: 2427-2448.

Warrick, J.A., L. Washburn, M.A. Brzezinski and D.A. Siegel, 2005. Nutrient contributions to the Santa Barbara Channel, California, from the ephemeral Santa Clara River. *Estuarine, Coastal and Shelf Science* 62: 559-574, doi: 10.1016/j.ecss.2004.1009.1033.

Winant, C.D. and C.E. Dorman, 1997. Seasonal patterns of surface wind stress and heat flux over the Southern California Bight. *Journal of Geophysical Research-Oceans* 102: 5641-5653, doi: 10.1029/5696JC02801.

III. COMPARISON OF NATURAL AND ANTHROPOGENIC NUTRIENT SOURCES IN THE SOUTHERN CALIFORNIA BIGHT

Introduction

Eutrophication of coastal waters, the accelerated accumulation of organic matter from an overabundance of algae (Nixon 1995), has greatly increased in the last several decades throughout the world, with demonstrated linkages to anthropogenic nutrient loads (see reviews Howarth et al. 2002a,b, 2008; Paerl and Piehler, 2008). Anthropogenic nutrient inputs are considered the most significant factor contributing to the global increase in the frequency and intensity of harmful algal blooms (HABs) (Smayda 1990; Anderson et al. 2002, 2008; Howarth et al. 2002; Hallegraeff 2004; Glibert et al. 2005a,b; GEOHAB 2006; Glibert et al. 2006; Heisler et al. 2008). Within the Southern California Bight (SCB), recent studies have shown that algal bloom intensity has increased over the last decade, with chronic blooms documented in areas of the SCB that have significant anthropogenic nutrient sources inputs (Nezlin et al. 2011; See Sections I and II). Prior to 2000, toxic outbreaks of *Pseudo-nitzschia* (an algal diatom that produces domoic acid) were considered rare (Lange et al. 1994); however, in recent years, frequent occurrences and high concentrations of this toxin have been documented in the SCB (Trainer et al. 2000; Busse et al. 2006; Schnetzer et al. 2007; Caron et al. 2010, unpublished data) and anthropogenic activities have been suggested as one possible cause for the increase (Barron et al., 2010). While anthropogenic nutrient loading has been shown to increase *Pseudo-nitzschia* abundances in the Gulf of Mexico (Parsons et al., 2002), this relationship has not been observed on the U.S. west coast (Lewtis et al., 2012).

Increased awareness of toxic HAB events served as the primary motivation for establishing the Southern California Coastal Ocean Observing System (SCCOOS) and, in 2008, implementing an ongoing HAB Program to collect weekly HAB species and toxin information from five pier locations (data available online, <http://www.sccoos.org/data/habs/index.php>).

Human population growth (that causes increased sewage discharges), development of coastal watersheds, agricultural and aquaculture runoff into the coastal oceans, and burning of fossil fuels are among the many factors contributing to increased eutrophication of coastal waters (Anderson et al. 2002, Howarth 2008). Anthropogenic inputs of agricultural runoff, wastewater and sewage discharge, and groundwater discharge have all been shown to provide significant sources of nitrogen that have been linked to increased HAB events and/or primary production (Lapointe 1997, 2004, 2005a,b; Glibert et al. 2005a, 2006; Anderson et al. 2002, 2008; Heisler et al. 2008). While many studies have focused on agricultural runoff, wastewater has also been found to promote HABs and increase primary productivity; in some regions, wastewater has been shown to be more important than upwelling as a nitrogen source (Chisholm et al. 1997; Lapointe 1997; Jaubert et al. 2003; Thompson and Waite 2003; Lapointe et al. 2004, 2005b). As the focus of most coastal eutrophication scientific research studies, nitrogen has been shown to be the primary limiting macronutrient for algae in coastal waters and in California (Dugdale 1967; Nixon 1986, 1995; Ryther and Dunstan 1971; Eppley et al. 1979; Kudela and Dugdale 2000). However, recent research has shown that the nitrogen form, not just quantity, plays an important role in

generating HABs and algal blooms (Glibert et al. 2006, Howard et al. 2007, Switzer 2008, Kudela et al. 2008, Cochlan et al. 2008).

There is a general perception that in upwelling systems, such as California, the quantity of anthropogenic nutrient inputs are small relative to upwelling, and therefore they have relatively little effect on the productivity of coastal waters. Upwelling is the process by which deep nutrient-rich water is transported to the surface and replaces nutrient-depleted surface water. There have been no studies to date that have quantified the natural and anthropogenic inputs on regional and local scales in the SCB to verify the accuracy of this perception. However, a growing number of studies have suggested a linkage between anthropogenic nitrogen sources and HABs in California, particularly with regard to anthropogenically-influenced riverine runoff (Kudela and Cochlan 2000, Kudela and Chavez 2004, Beman et al. 2005, Kudela et al. 2008). Additionally, physiological studies have shown several common California HAB species are capable of utilizing anthropogenic nitrogen forms, such as urea (Herndon and Cochlan 2007, Cochlan et al. 2008, Kudela et al. 2008) for growth and toxin production can be increased under these conditions (Howard et al. 2007).

In order to test the hypothesis that natural sources (e.g. upwelling) greatly exceed anthropogenic nutrient sources to the SCB, this study compared the contributions of nitrogen (N) and phosphorus (P) from four major nutrient sources, (1) upwelling (2) treated wastewater effluent discharged to ocean outfalls, (3) riverine runoff, and (4) atmospheric deposition. This comparison was made on both regional (SCB-wide) and sub-regional scales, and this is the first such study to make this comparison on the U.S. west coast.

Methods

Study Area

The Southern California Bight (SCB) lies along the southern part of the Pacific coast of the continental United States. The continental coastline generally runs along a north south gradient beginning at Cape Flattery, Washington (~48° 23'N), until Cape Mendocino in northern California (~40° 15'N), then turns toward a south-southeast direction (Figure III-1). The continuum is broken by a bend or curvature in the coastline between Point Conception (~34° 34'N) and the Mexico international border (~32° 32'N). The SCB includes an ocean area of 78,000 km² (Dailey et al. 1993) and numerous islands offshore. The bottom topography consists of submarine mountains and valleys, neither of which could be considered a classical continental shelf nor a classical continental slope. Emery (1960) called it the Southern California Borderland.

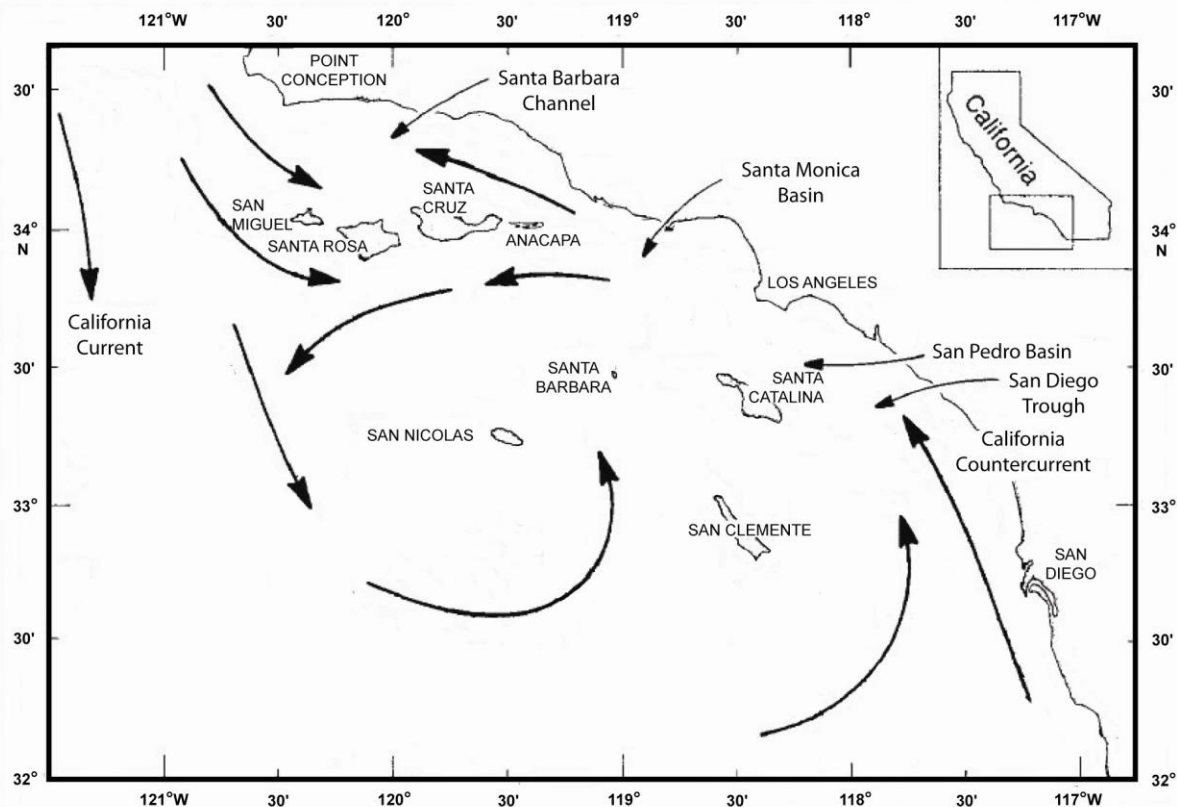


Figure III-1 The circulation patterns in the SCB (adapted from Hickey, 1992).

A ring of coastal mountain ranges defines southern California (SC). The mountain ranges shelter the coastal area from dominating northwesterly winds and create a “coastal basin” where cool, dense air is trapped, resulting in much weaker wind and sea patterns than over the open ocean (Dorman and Winant 1995). Southern California’s climate exhibits a relatively dry summer and wet winter season. During the dry season a semi-permanent eastern Pacific high-pressure area dominates SC. The marine layer is a prominent feature from late spring through early fall. Beginning late fall to early spring (October through March) the high-pressure ridge gets displaced and the southern margin of the polar jet stream affects SC. The probability of rain increases because the marine layer is not dominant anymore and subtropical moisture occasionally feeds cold fronts crossing the SC area from Pacific storms. Over 90% of the precipitation generally occurs during this time period. The migratory nature of the region’s storm fronts causes alternating periods of dry and wet weather during the rainy season.

The ocean region within the SCB is dominated by the equatorward California Current (CC). The CC is a typical broad eastern boundary current (Hickey 1979, Lynn and Simpson 1987) that transports cold Subarctic water from north to south throughout the year along a typically narrow (3 to 6 km) coastal continental shelf. The CC is not steady but migrates seasonally onshore and offshore, producing a rich eddy field (Burkov and Pavlova 1980, Strub and James 2000, Haney et al. 2001). As the CC passes Point Conception, it turns south-southeast along SC’s outer continental slope, then a portion branches (~32°N)

eastward to northward along the coast (Hickey 1992, Harms and Winant 1998, Bray et al. 1999), forming a large gyre known as the Southern California Eddy (Figure III-1). The poleward current along the coast is called the Southern California Countercurrent (Sverdrup and Fleming 1941). It transports warm southern water into Santa Monica Bay and the Santa Barbara Channel.

Surface current flows may not reflect near bottom currents. During spring, the intensity of the equatorward CC increases compared to the poleward Southern California Countercurrent. Its jet migrates onshore, and the eastward branches penetrate into the Southern California Bight through the Santa Barbara Channel and onward south of the Channel Islands (Reid and Mantyla 1976, Hickey 1979, Bray et al. 1999). The islands act as barriers to deflect surface currents in different directions. Near shore, over the continental shelf and borderland slope, the near surface flow is commonly equatorward while the California Undercurrent is poleward (Hickey 1993). Figure III-1 shows the circulation patterns in the SCB.

Study Approach: Estimation and Comparison of Nutrient Sources

The nitrogen and phosphorus loads to the SCB were estimated for (1) upwelling (2) wastewater effluent discharge, (3) riverine runoff and (4) atmospheric deposition. A combination of field measurements, modeling, and remote sensing targeted over a one-year period (January – December 2010) was used to estimate the contribution of each nutrient source on a bightwide scale as well as for six smaller sub-regional areas (Santa Barbara, Ventura, Santa Monica Bay, San Pedro, North San Diego, and San Diego). Nutrient inputs were estimated as annual loads for the bightwide scale and are reported in Metric ton (MT) Year⁻¹. Annual fluxes were calculated for the six sub-regional areas in order to compare sub-regions that vary in spatial area and are reported as MT km⁻² year⁻¹. Table III-1 lists the form of N and P estimated for each source component, Figure III-2 shows regional and sub-regional locations used for the contribution estimates, and Table III-2 provides the area of each sub-region. The combined area of all of the sub-regions is 20% of the total area of the SCB.

Table III-1 List of N and P form analyzed for each nutrient source and analytical reference.

Constituent	Upwelling	Riverine runoff	Large POTW Effluent	Atmospheric Deposition
Total Nitrogen (TN)		X	X	X
Nitrate+ Nitrite (NO _x)	X	X	X	X
Ammonium (NH ₄)	X	X	X	X
Total Dissolved Nitrogen (TDN)		X	X	
Urea		X	X	
Total Phosphorus (TP)		X	X	
Phosphate (PO ₄)		X	X	X
Silicate (SiO ₄)		X	X	

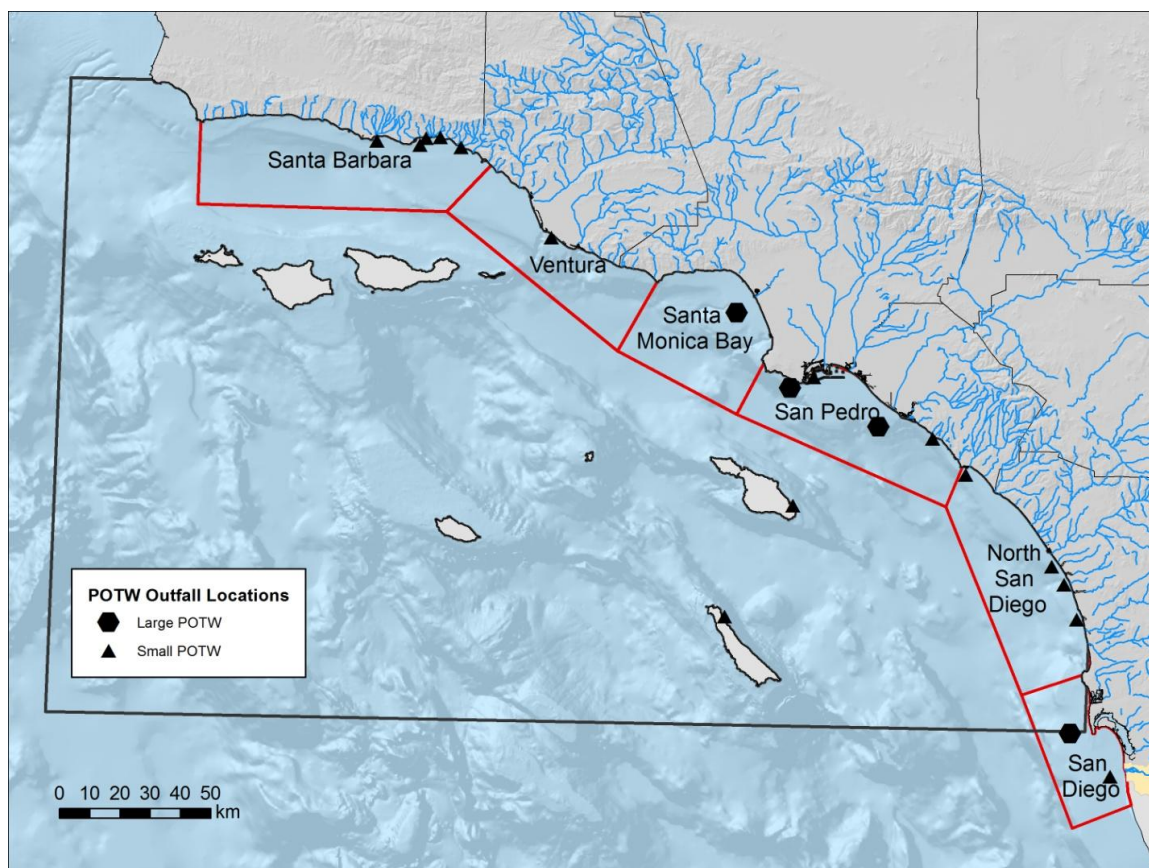


Figure III-2 Regional and sub-regional SCB boundaries used to calculate fluxes of each of the four major sources. The area used for regional estimates is outlined in black; sub-regions are labeled and outlined in red.

Table III-2 Area of Each Sub-region.

Sub-region	Area of Sub-region (km ²)	Percent of total area of SCB
Santa Barbara	2,405	4.6
Ventura	1,449	2.8
Santa Monica Bay	1,571	3.0
San Pedro	1,641	3.1
North San Diego	1,837	3.5
San Diego	1,020	2.0
Total Area (Bightwide)	51,686	

Estimation of Upwelling

Approach. To estimate the upwelling contribution of N and P, the Regional Oceanic Modeling System (ROMS), a three-dimensional ocean circulation model for the US West Coast (Marchesiello et al. 2003), was coupled with an NPZD-type ecosystem-biogeochemistry model (Gruber et al. 2006) to generate a reanalysis of the ocean environment from January – December 2010. This model integration resulted in highly time-resolved output of the three dimensional physical and biogeochemical parameters. The ROMS model saves output of the daily averages of all advection terms in Eq. 1 (Gruber et al. 2006) and the output was integrated over time and space.

$$\frac{\partial B}{\partial t} = \nabla \cdot K \nabla B - \vec{u} \cdot \nabla_h B - (w + w^{\text{sink}}) \frac{\partial B}{\partial z} + J(B), \quad \text{Eq. 1}$$

where K is the eddy kinematic diffusivity tensor, and where ∇ and ∇_h are the 3-D and horizontal gradient operators, respectively. The horizontal and vertical velocities of the fluid are represented by \vec{u} and w respectively. The w^{sink} represents the vertical sinking rate of the biogeochemical components and $J(B)$ represents the source minus sink term. All of these terms are described in detail in Gruber et al. 2006. From this detailed output, periods of upwelling were determined using vertical velocity, lateral advection, and temperature fields, and then the net mass of nitrate and ammonium from lateral and vertical fluxes to the euphotic zone was calculated. Figure III-3 provides a conceptual illustration of the net upwelling flux that was estimated from the model output. The net upwelling flux (U) was determined from the sum of the net lateral flux (U_L) plus the net vertical flux (U_V) as shown by the following equation:

$$U = U_L + U_V \quad \text{Eq. 2}$$

The total vertical flux assimilated by the model includes advection and diffusion while the total lateral flux was assimilated for advection only. Daily estimates were summed to provide an annual estimate. The TN(ammonium and nitrate) and TP (phosphate) estimates were made over a range of spatial scales, from a Bightwide scale (Figure III-2 black line) to smaller sub-regional scales (Figure III-2 red lines).

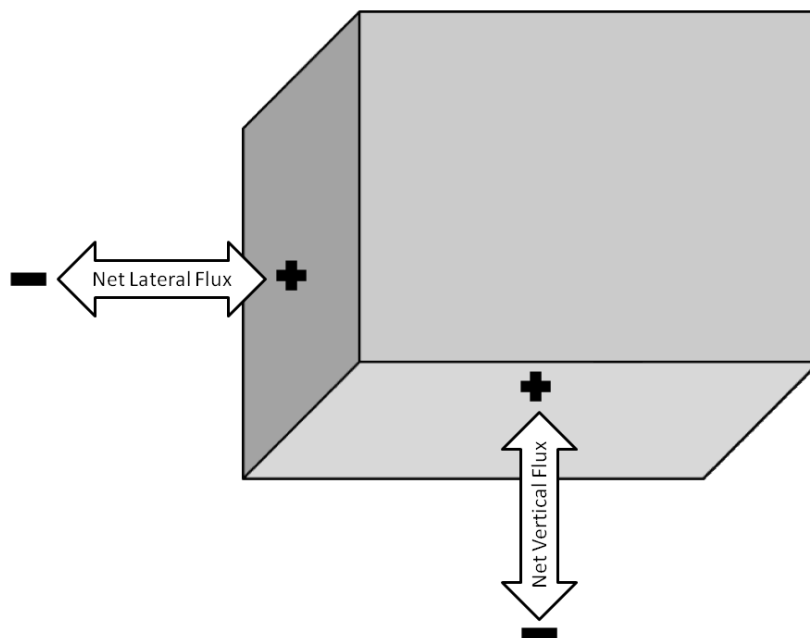


Figure III-3 Conceptualization of a 3-dimensional box illustrating how the net upwelling flux was estimated from the sum of positive and negative vertical and lateral upwelling fluxes for each sub-regional area.

ROMS Hydrodynamic Model Description. ROMS is a free-surface, hydrostatic, three-dimensional primitive equation regional ocean model (Shchepetkin and McWilliams, 2005, 2006; Marchesiello et al. 2001). A description and validation of the ROMS model at the 15km spatial scale has been published (Gruber et al. 2006). This ROMS 3-D model provides both existing “nowcast” and predictive “forecast” assimilations (up to 48 hours in 6-hour increments) of satellite sea surface temperature, HF radar surface current, subsurface temperature, and salinity profiled from Argo floats and gliders. The ROMS output (for the physics-only model runs) is provided at both the JPL ROMS web site (<http://ocean.jpl.nasa.gov/SCB>) and the SCCOOS web site (www.sccoos.org/data/roms).

The ROMS configuration used consists of a single domain covering the southern California coastal ocean from Santa Barbara to San Diego at a resolution of 1 km. With respect to the model grid, the vertical discretization uses a stretched terrain-following coordinate (S-coordinate) on a staggered grid over variable topography (Song and Haidvogel 1994). The stretched coordinate allows increased resolution in areas of interest, such as the thermocline and bottom boundary layers. ROMS uses a sigma-type vertical coordinate in which coordinate surfaces follow the bottom topography. In the SCB configuration, there are 40 unevenly-spaced sigma surfaces used with the majority of these clustered near the surface to better resolve processes in the mixed layer. The horizontal discretization uses a boundary-fitted, orthogonal curvilinear formulation. Coastal boundaries are specified as a finite-discretized grid via land/sea masking. The SCB configuration of ROMS has been tested and used extensively (Dong et al. 2009).

Boundary conditions for the SCB domain are provided from a separate data-assimilating ROMS domain that covers the entire coast of California and northern Baja California at a resolution of 3 km. The tidal forcing is added through lateral boundary conditions that are obtained from a global barotropic tidal model (TPXO.6; Egbert and Erofeeva 2002, Egbert et al. 1994) which has a horizontal resolution of 0.25 degrees and uses an inverse modeling technique to assimilate satellite altimetry cross-over observations. Eight major tide constituents at the diurnal and semidiurnal frequencies (M2, K1, O1, S2, N2, P1, K2 and Q1) are used. The atmospheric forcing required by the ROMS model is derived from hourly output from forecasts performed with a regional atmospheric model, the Weather Research and Forecasting System (WRF). This model has been used in several studies in the SCB region (Conil and Hall 2006; Hughes et al. 2007, 2008). The horizontal resolution is 4 kilometers and the lateral boundary forcing and initial conditions are derived from the NCEP NAM 12-km North American model daily 00GMT forecasts. The surface latent and sensible heat fluxes, as well as surface evaporation rates, are derived from WRF surface air temperatures, surface relative humidity, 10 m winds, solar/terrestrial radiation, and ROMS sea surface temperatures (SSTs), using the bulk formula proposed by Kondo (1975). The fresh water flux is computed as the calculated evaporation rate minus the WRF precipitation rate (E-P). The wind stress is derived from the 10 m winds using the formula of Large and Pond (1982). The variables used for computing the ocean model forcing have been evaluated against buoy data. The surface winds are satisfactorily accurate, with RMS errors of 2-3 m s⁻¹ in speed and 30 degrees in direction. Comparison of modeled versus measured surface air temperatures and relative humidity show good accuracy with errors of 1-2°C and 5-10%.

Biogeochemical Model. The biogeochemical model that was used in this ROMS configuration is a Nutrient-Phytoplankton- Zooplankton-Detritus (NPZD) model based on Fasham et al. (1990). The model was optimized and validated for the US West Coast coastal upwelling region by Gruber et al. (2006). This model has been validated and gives good results in the upwelling dominated coastal zone, but it fails to reproduce observations further offshore in more nutrient-depleted areas (Gruber et al. 2006). A full description of the model can be found in Gruber et al. (2006), but is described briefly here.

The NPZD model includes a single limiting nutrient (nitrogen) and a diatom-like single phytoplankton class. While the model output was only used to calculate nitrate and ammonium lateral and vertical fluxes, a total of twelve state variables are tracked including: nitrate, ammonium, phytoplankton, zooplankton, small and large detritus (both nitrogen and carbon concentrations due to varying C:N ratios), oxygen, dissolved inorganic carbon, calcium carbonate, and total alkalinity. The chlorophyll:carbon ratio in phytoplankton and the organic nitrogen and carbon matter content of the sediment are carried as state variables. The sinking of all particulate pools (i.e., phytoplankton and detritus) is modeled explicitly. Only two parameters were changed from Gruber et al. 2006): the initial slope of the light-response curve for phytoplankton growth and the mortality rate of phytoplankton were both doubled to improve the resulting net primary productivity (Gruber et al. 2011). Model output was not available for phosphate, so upwelled TP (as phosphate) was estimated using the NO₃:PO₄ ratios based on World Ocean Atlas 05 for the Southern California Bight, which averaged 7.69 +/-1.68 for 50 meters depth.

In the absence of a larger domain model with the same NPZD biogeochemical model characteristics, biogeochemical boundary conditions were based on the physical boundary conditions, modeled at daily time steps, and the relationship between physical quantities (either temperature or potential density) and nutrients like nitrate was used to derive initial and boundary conditions for nitrate (NO_3) and ammonium (NH_4), as summarized in Table III-3. Initial and boundary conditions for nitrate concentrations were forced with a polynomial regression that describes the relationship between NO_3 and density (σ_θ), defined for the SCB from temperature, salinity, and nitrate data from the World Ocean Atlas 2005 (Garcia et al. 2006; Figure III-4).

Table III-3 List of polynomial parameters for the biogeochemical boundary conditions in ascending order, e.g. $\text{NO}_3(\sigma_\theta > 26.8) = -20258 + 1484.7 \cdot \sigma_\theta + -27.1422 \cdot \sigma_\theta^2$.

Variable	σ_θ range 1	Polyn. 1	σ_θ range 2	Polyn. 2	σ_θ range 3	Polyn. 3
Nitrate	Up to 24.99	-48.0343 1.9910	25.0 .. 26.79	-371.8125 11.3264 0.1449	Over 26.8	-20258 1484.7 -27.1422
Chl-a (top 50 m)	All values	-547.1559 42.7240 -0.8334	n/a	n/a	n/a	n/a
Chl-a (> 50 m)	All values	17.4953 -0.7332	n/a	n/a	n/a	n/a
Ammonium	Up to 24.82	-1.9986 0.0866	24.82 .. 26.42	-265.6287 20.7761 -0.4056	26.42 .. 27.2	170.3260 -12.5235 0.2302

Because there were no observed data available for ammonium (NH_4), climatological biogeochemical boundary and initial conditions were used to determine a relationship between potential density and NH_4 . As Figure III-4 shows, the scatter is much larger for this relationship than for NO_3 .

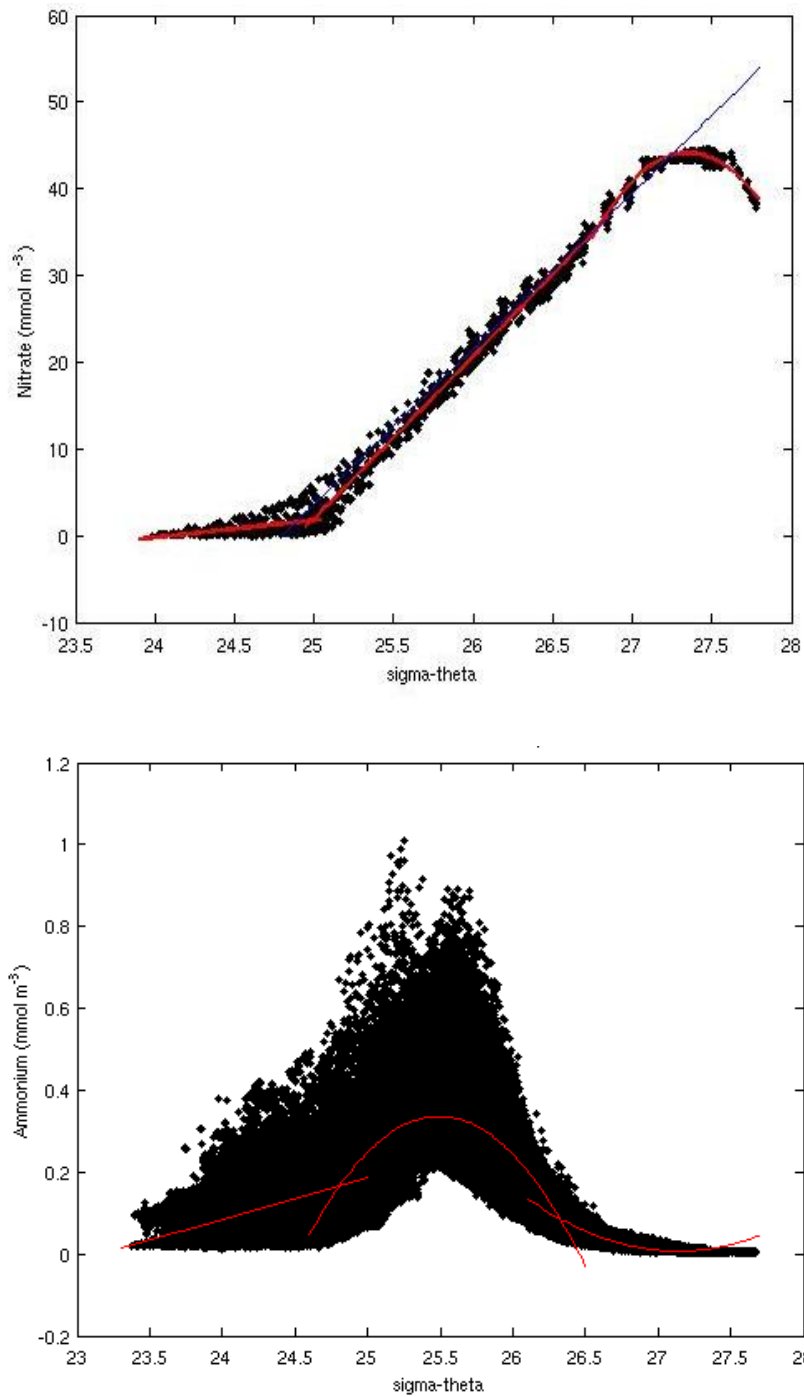


Figure III-4 Relationship between potential density (sigma-theta) and nitrate (top) and ammonium (bottom) in the Southern California Bight. Nitrate and ammonium data (black dots) are derived from the World Ocean Atlas (2005) and ROMS tests run with climatological boundary conditions, respectively. Red lines designate the step-wise polynomial fits.

Wastewater Effluent Discharge

Nutrient loads from wastewater effluent discharged from outfalls to the SCB were estimated for both large (> 100 MGD) and small (< 25 MGD) Publicly Owned Treatment Works (POTWs) in each sub-region (Table III-4). Large POTW nutrient loads were determined and reported for January-December 2010, and small POTW nutrient loads were determined using available data published for 2005 (Lyon and Stein, 2008).

Table III-4 Location and relative size of POTWs used for effluent discharge load estimates by sub-region. S= Small; L = Large.

Sub-region	POTW Name	Size	GPS Coordinates (Latitude/Longitude)
Santa Barbara	Goleta WWTP	S	34.401667/-119.824167
	El Estero WWTP	S	34.391944/-119.668889
	Montecito WWTP	S	34.413333/-119.647778
	Summerland WWTP	S	34.416663/-119.596671
	Carpinteria WWTP	S	34.388333/-119.521654
Ventura	Oxnard WWTP	S	34.126111/-119.190556
Santa Monica Bay	Hyperion Treatment Plant	L	33.911967/-118.52145
San Pedro	Joint Water Pollution Control Plant	L	33.695/-118.327361
	Treatment Plant No. 2	L	33.576667/-118.01
	Terminal Island WWTP	S	33.722111/-118.243389
	Aliso Creek Ocean Outfall	S	33.542778/-117.817222
North San Diego	San Juan Creek Ocean Outfall	S	33.436111/-117.698056
	Oceanside WWTP	S	33.162778/-117.391389
	Camp Pendleton WWTP	S	33.162778/-117.391389
	Fallbrook Public Utility District WWTP	S	33.162778/-117.391389
	Encina Ocean Outfall	S	33.109331/-117.347992
	San Elijo Water Pollution Control Facility	S	33.005833/-117.3025
San Diego	Point Loma Wastewater Treatment Plant	L	32.665278/-117.323611
	Hale Ave. Resource Recovery Facility	S	32.5375/-117.183333
	South Bay Water Reclamation Plant	S	32.5375/-117.183333
	International Wastewater Treatment Plant	S	32.5375/-117.183333

POTW N and P loads were estimated using nutrient concentrations (c , mg L^{-1}), flow - Q ($\text{m}^3 \text{ month}^{-1}$), and a conversion constant k :

$$L = k c Q \quad \text{Eq. 3}$$

A greater emphasis was placed on measuring nutrient concentrations in wastewater effluents from large POTWs than from small POTWs because large facilities represent 90% of the total POTW discharges to the SCB via ocean outfalls. Samples were analyzed for total, total dissolved, and dissolved inorganic N and P, including urea (Table III-1); target analytes and analytical methods are listed in Table III-5.

Samples collected in December 2008 were used to determine inter-laboratory variability related to constituent analysis. The results are summarized in Appendix B.

For each facility below, nutrient concentrations were measured quarterly from December 2008 through December 2009; these quarterly concentrations were combined with monthly discharge flows from 2010 NDPES monitoring reports.

- Hyperion Treatment Plant (HTP) operated by City of Los Angeles (LA)
- Joint Water Pollution Control Plant (JWPCP) operated by LA County Sanitation District
- Treatment Plant No. 2 operated by Orange County Sanitation District
- Point Loma Wastewater Treatment Plant (PLWTP) operated by City of San Diego

Effluent nutrient concentration data for small POTWs relied on existing data from NDPES monitoring reports for 2005 (Lyon and Stein 2008). Small POTW effluent concentration data were compiled for the following nutrient forms: nitrate+nitrite (NO_x), ammonia (NH_3) and total dissolved nitrogen (TDN). No data were available for forms of phosphorus or other constituents of interest.

Table III-5 Targeted analytes and analytical methods by participating agency for wastewater effluents.

Analyte	HTP	JWPCP	OCSD	PLWTP	SCCWRP (CRG)
NO_x	EPA300.0	SM4500 NO ₃ E	N/A	EPA300.0	EPA300.0
NH₃	EPA350.1	SM4500 NH ₃ C & NH ₃ G	EPA350.1	SM4500B-E	N/A
PO₄	N/A	N/A	N/A	EPA300.0	EPA300.0
SiO₄	N/A	N/A	N/A	N/A	SM4500Si-D
Urea	N/A	N/A	N/A	N/A	Goeyens et al. 1998
TN	N/A	N/A	N/A	N/A	SM4500-N
TP	N/A	N/A	N/A	N/A	SM4500P

Riverine Loads

Riverine nutrient loads to the SCB were estimated using empirical wet- and dry-weather data for monitored watersheds in combination with modeled wet-weather loads for unmonitored watersheds for the period of October 2008–December 2010. Methodology and discussion of results are presented in detail in Sengupta et al. (Appendix E), but summarized here.

Field Data Collection. Continuous discharge data and nitrogen (N) and phosphorus (P) concentrations and forms were collected for wet and dry weather (October 2008-2009) by San Diego, Orange, Los Angeles, and Ventura counties through their municipal stormwater NPDES permit monitoring programs and through the Estuarine Eutrophication Assessment study component of the SCB Regional Monitoring Program (McLaughlin et al. in prep). Discharge and water quality samples were collected at 34 wet weather and 57 dry weather mass emission stations by Ventura, Los Angeles, Orange, and San Diego Counties under their National Pollution Discharge Elimination System (NPDES) permits or by SCB Regional Monitoring Program partners during the period of November 2007- October 2009. County NPDES reports were also reviewed for data on wet or dry weather runoff nutrient concentrations to supplement these data. Protocols for dissolved inorganic nutrients and TN and TP were standardized and interagency calibration was conducted for these analytes. Other analytes of interest that are not routinely monitored by the Stormwater Monitoring Collation (SMC) agencies, but were analyzed as part of this study include urea, SiO_4 , and TDN and TDP. Table III-6 provides a summary of the wet- and dry-weather monitoring; target analytes and analytical method used are listed in Table II-7. Analytical methods and the 38 mass loading stations utilized in this study are listed in the Bight'08 Field Operations Manual (Appendix 2; ftp://ftp.sccwrp.org/pub/download/DOCUMENTS/BightPlanningDocuments/Bight08/Bight08_WQ_FieldManual.pdf).

Table III-6 Number of wet- and dry-weather watershed sites and respective monitored events by County/Subregion.

County/Subregion	Wet-Weather Sites	No. of Site-Events	Dry-Weather Sites	No. of Site Events Monitored
Ventura	4	8	3	9
Los Angeles	7	14	7	49
Orange	12	22	11	44
San Diego	11	22	11	11
Bight '08 Estuaries	--	--	25	150
Total	34	66	57	263

Table III-7 Targeted analytes and analytical methods by participating agency for riverine loads.

Analyte	Ventura County	Los Angeles County	Orange County	San Diego County	SCCWRP
NO _x	EPA 300.0	SM 4110 B	*EPA 353.2.0	SM4500-NO3 E SM4500-NO2 B	N/A
NH ₄	SM 4500-NH3 F	SM 4500	4500 NH3 B	SM4500-NH3 D	N/A
PO ₄	N/A	N/A	SM 4500 P B2	N/A	SM4500P C
SiO ₄	N/A	N/A	EPA 200.8	N/A	SM 4500 SiO4
Urea	N/A	N/A	N/A	N/A	Goeyens et al. 1998
TN	N/A	N/A	N/A	N/A	QC 10107044B
TP	SM 4500-P E	SM 4500-P E	SM 4500-P E	N/A	USGS I-2650-03

Modeling Methods. A spreadsheet model based on the Rational Method (O'Loughlin et al. 1996) was used to generate freshwater runoff Q ($\text{m}^3 \text{ day}^{-1}$) and the nutrient loads (N and P) associated with wet weather events. Modeled storm discharge (Q) was calculated as a function of drainage area (A , km^2), mean rainfall intensity (I , mm day^{-1}), hydraulic runoff coefficient (C), and conversion constant (k):

$$Q = A I C k \quad \text{Eq. 4}$$

Hydraulic runoff coefficient (C) varied as a function of land use/cover type (Table III-8). The Ackerman and Schiff model (2003) was improved by refining land use-specific runoff concentrations for NO_x, NH₄, and PO₄, based on previously published values from recently published studies (Stein et al. 2007, Yoon and Stein 2008) and TN and TP runoff concentrations derived from empirical data for this study (Sengupta et al. Appendix E).

Within each watershed, total discharge (Q) was then calculated as the sum of discharge associated with six land use categories: agriculture, commercial, industrial, open space (natural), residential, and other urban. The daily nutrient loads were estimated as the sum of the product of the runoff concentration (c) and Q for each land use, using Eq. 4.

Table III-8 Runoff coefficients (C) for stormwater discharge and average concentrations of ammonium, nitrate, phosphate, TP, and TN in runoff by land-use. Values from Ackerman and Schiff (2003) unless otherwise noted.

Land Use Type	Runoff Coefficient	Ammonium (mg L ⁻¹)	Nitrate (mg L ⁻¹)	Phosphate (mg L ⁻¹)	TP ³ (mg L ⁻¹)	TN ³ (mg L ⁻¹)
Agriculture	0.10	1.34	7.31	3.27 ²	11.31	10.41
Commercial	0.61	0.45	1.30 ²	0.09 ²	0.56	3.56
Industrial	0.64	0.34	1.29 ²	0.32	1.33	3.55
Open	0.06	0.04 ¹	0.34 ¹	0.03 ¹	0.35	2.47
Residential	0.39	0.42	1.65 ²	0.25 ²	1.10	3.96
Other Urban	0.41	0.40	0.80	0.17	0.82	2.99

¹Nutrient concentrations from open land uses are derived from Yoon and Stein (2007)

²Runoff concentration of nitrate and phosphate are derived from Stein et al. (2007)

³Runoff concentration of TN and TP were empirically derived from this study (Sengupta et al. Appendix E).

The drainage area (A) is delineated for each watershed based on hydraulic unit code (HUC) Boundaries. The model domain includes all southern California coastal watersheds in San Diego, Orange, Riverside, Los Angeles, San Bernardino, Ventura and Santa Barbara counties with an initial total watershed area of 27,380 km². Watershed areas larger than 52 km² upstream of dams were excluded in the model domain, in order to mimic the retention of water by dams (Ackerman and Schiff 2003). The final model domain comprised of 98 watersheds with a total area of 14,652 km². Each of the watersheds was populated with land cover data from Stein et al. (2007), and aggregated into the six land use categories.

Daily precipitation data for approximately 200 rain gauge stations were obtained from the National Oceanic and Atmospheric Administration (NOAA), National Environmental Satellite, Data and Information Service (NESDIS), National Climatic Data Center (NCDC) and Climate Data Online (CDO) database. Data from the 200 rain gauge stations were transformed to estimate mean precipitation over the 98 watersheds relevant to the study. Precipitation data was interpolated within each watershed on a regular grid using a Biharmonic Spline Interpolation method (Sandwell 1987).

To estimate the anthropogenic influence on nutrient fluxes to the SCB, a model scenario with 100% open space land-use for the entire Bight, representing a "pre-urbanization" baseline, was run. Because there were no dams withholding potential runoff in the modeled pre-urbanized state, the model domain was expanded to include areas above existing dams. Rainfall data was not available for the period representing the pre-urbanized state; therefore, current rainfall data (2008-2009) were used to estimate

loads. This enables a comparison of pre- and post-urbanization loads without any bias due to differences in precipitation.

Atmospheric Deposition

Approach. Limited data are available on rates of atmospheric deposition of N and P to the SCB. Existing federal networks for estimation of atmospheric deposition (e.g. National Atmospheric Deposition Program; NADP) are focused on land-based wet deposition of nutrients. However, in Southern California, where rainfall typically occurs only 10 to 30 days per year, dry weather can potentially be more important to algal productivity in the Bight nearshore waters than wet deposition (Sabin and Schiff 2008). Therefore, this component of the study focused on dry-deposition sampling.

Because available resources for this component were not sufficient to undertake ocean-based measurements of atmospheric deposition, atmospheric load calculations for the nearshore zone (at sub-regional scale, up to 20 km offshore) were derived from land-based estimates, although these estimates at a sub-regional scale likely represent an overestimate of loads. Atmospheric loads at the regional scale (Bightwide) were not estimated due to lack of confidence in extrapolation of land-based estimates to areas >200 km offshore.

Dry Deposition. Several techniques using surrogate surfaces for estimating nitrogen and phosphorus dry deposition in semi-arid environments, including a water surface sampler and filter surfaces, been developed (Raymond et al. 2004, Moumen et al. 2004). Both of these techniques, used in the present study, use aerodynamic discs, are of short duration (2 to 4 days), and produce reproducible results when evaluated against the atmospheric concentrations and each other. Sampling for dry deposition was conducted three times over a 6 month period at roof-top location at the Hyperion Treatment Plant and the City of Oceanside Library. Samplers were deployed in duplicate for the water collector and triplicate for the filter collectors. Filter samplers were analyzed for NH_4 and NO_3 , and water surface samplers were analyzed for NH_4 , NO_3 , and PO_4 . Concentrations were converted to a deposition rate by incorporating the surface area of the sampler and the duration of the sampling event ($\text{kg km}^{-2} \text{d}^{-1}$). The average deposition rate for the three sampling events was multiplied by the number of dry weather days during the January - December 2010 study year for a Bightwide estimation of dry deposition. Results from the HTP site were applied to the Santa Monica Bay and San Pedro Bay sub-regions, and results from the Oceanside sampler were applied to all other sub-regions.

Wet Deposition. The wet deposition rates for the nitrogen and phosphorus estimates were calculated from the average annual rates for 2009 and 2010 at two NADP sites: (1) Site 42, Los Angeles County (Tanbark Flat, 34.2071, -117.7618) and (2) Site 94 San Bernardino County (Converse Flats, 34.1938, -116.9131). Wet deposition rates for NO_x and NH_4 from these two sites were averaged across sites and years, then applied as rate ($\text{kg km}^{-2} \text{d}^{-1}$) to the total number of wet days for the January - December 2010 study year.

Data Integration

All of the nutrient source estimates described above were converted into MT year⁻¹ for the bightwide source comparison and into MT km⁻² year⁻¹ for the sub-regional source comparison in order to compare sub-regions that vary in spatial area.

Error Analysis in TN and TP Loads

The error associated with the nitrogen and phosphorus loads was determined for the riverine runoff and effluent. Standard deviation of nutrient concentrations was multiplied by the total discharge (annual for effluent and wet or dry weather discharge respectively for the watershed). Total error was calculated as the square root of the squared sums of each of the individual estimates for each watershed, as given in Eq. 5.

$$\text{Total Load Std. Deviation} = (\sum_1^{10} (C_e Q)^2)^{1/2} \quad \text{Eq. 5}$$

where C_e is the standard deviation in nutrient concentration for each watershed or large POTW effluent. Q is the total annual discharge (wet and dry calculated separately for riverine runoff). The error was not calculated for the upwelling loads because the model is not yet fully validated at the spatial scale as used in this study (see "Uncertainty Associated with Nutrient Source Estimates" below).

Results

Bightwide Regional Nitrogen and Phosphorus Loads

Total Nitrogen. At the SCB scale, TN loads differed by an order of magnitude for each source with upwelling contributing the largest load and riverine runoff the smallest (Figure III-5, Table III-8). With respect to nutrient forms, upwelling consisted almost entirely of NOx (98.7%), with very little NH₄ (1.3%). Effluent loads consisted mostly of NH₄ (91.6%), with minor percentages of NOx (7.0%) and ON (1.4%). Despite the small NOx component of effluent, the actual load for this constituent (3.4×10^3 Metric ton (MT) N Year⁻¹) was an order of magnitude larger than the NOx contribution from riverine runoff (1.2×10^3 MT N Year⁻¹). The riverine runoff was comprised mostly of NOx (60%) and ON (35%) with a smaller contribution from NH₄ (5%).

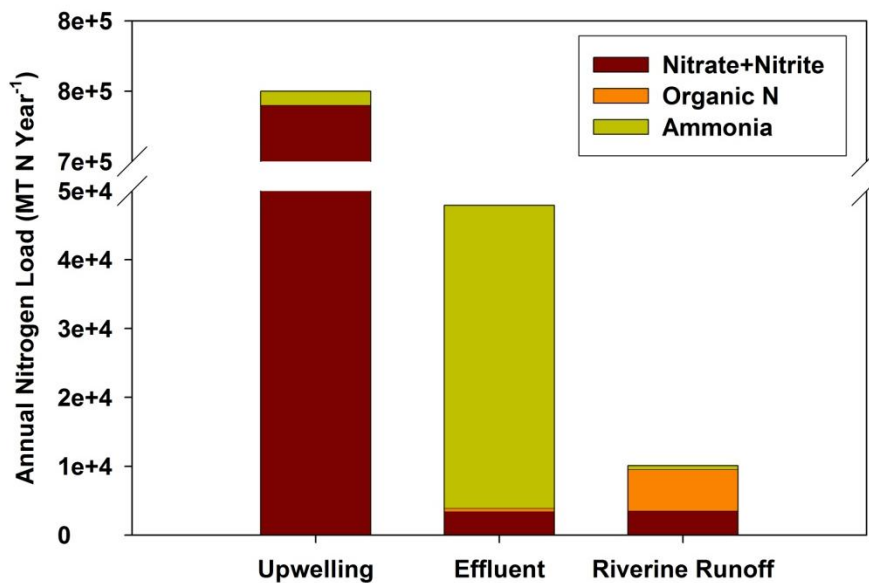


Figure III-5 Annual total nitrogen loads (in MT N Year⁻¹) by source, with total nitrogen components separated into nitrate plus nitrite, organic nitrogen, and ammonia.

Total Phosphorus. Upwelling loads of TP (2.1×10^5 MT TP yr⁻¹) exceeded effluent TP loads by two orders of magnitude (2.1×10^3 MT TP yr⁻¹) and riverine runoff TP loads by three orders of magnitude (2.6×10^3 MT TP yr⁻¹; Figure III-6, Table III-9). Effluent loads consisted mostly of PO₄ (60%), with the remainder consisting of organic P and PP (OP+PP). Riverine loads were more evenly comprised of PO₄ (47%) and OP+PP (53%).

Table III-9 Annual loads of TN and TP and component forms (as percent of total) for each nutrient source (in MT Year⁻¹) and the nitrogen constituents as the percentage of total nitrogen. NA = not analyzed for this source.

Nutrient Form	Upwelling	Effluent	Riverine Runoff
Total Nitrogen	7.5×10^5	4.8×10^4	1.0×10^4
Nitrate + Nitrite	98.7%	7%	35%
Ammonia	1.3%	91.6%	5%
Organic N	NA	1.4%	60%
Total Phosphorus	2.1×10^5	2.1×10^3	2.6×10^3
Phosphate	100%	60%	47%
Other P	NA	40%	53%

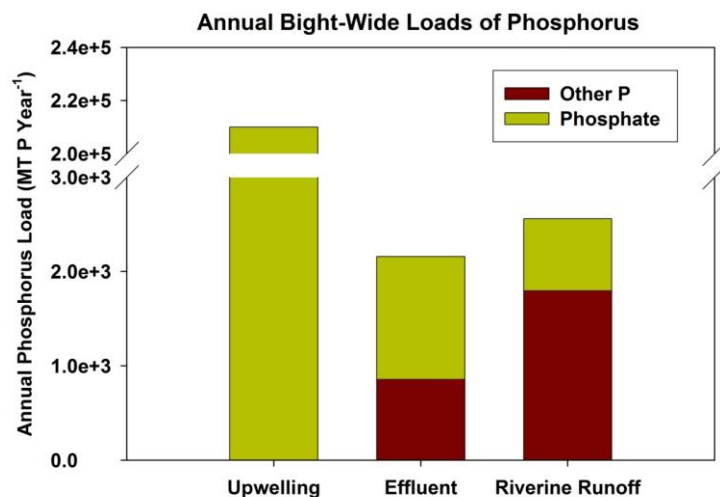


Figure III-6 Annual phosphorus load for each source, with total phosphorus components separated as phosphate and other phosphorus.

Estimates of Error. The error analysis of TN and TP loads for the riverine runoff and effluent ranged from 3.3-23.7% for effluent and 2.4-37.8% for riverine runoff and are summarized in Table III-10. The error was not calculated for the upwelling loads because the model is not yet fully validated at the spatial scale as it was used in this study (see "Uncertainty Associated with Nutrient Source Estimates" below).

Table III-10 Summary of the standard error calculated for nitrogen and phosphorus components of riverine runoff and effluent. Absolute and standard error reported in Kg Year⁻¹.

Component	Riverine Runoff				Effluent	
	Wet Weather		Dry Weather		Standard Error	% Error
	Absolute error	% Error	Absolute error	% Error		
TN	2.2×10^5	8.8	3.0×10^4	2.4	2.0×10^6	4.6
NO ₃ +NO ₂	8.4×10^4	7.5	2.7×10^4	3.6	5.5×10^5	17.6
NH ₄	9.4×10^4	37.8	8.1×10^3	11.6	1.3×10^6	3.3
TP	3.7×10^4	6.3	5.3×10^4	3.5	2.8×10^5	13.2
PO ₄	5.2×10^3	3.4	1.9×10^3	1.8	3.0×10^5	23.7

Sub-regional Nitrogen and Phosphorus Fluxes

Total Nitrogen. Dominant TN sources varied by sub-region. For the three sub-regions with large POTW outfall discharges (Santa Monica Bay, San Pedro, and San Diego), effluent and upwelling had similar annual TN fluxes (Figure III-7, Table III-11). Effluent and upwelling was 9.9 and 10 MT N km⁻² yr⁻¹, respectively for Santa Monica Bay; 12.6 and 24 MT N km⁻² yr⁻¹, respectively for San Pedro Bay; and 2.4

and 7.4 MT N km⁻² yr⁻¹ for south San Diego region. Note that the upwelling flux estimated for San Diego is at the edge of the model boundary; therefore, it has a large amount of uncertainty. For these three regions, riverine runoff and atmospheric deposition were 1-2 orders of magnitude less than upwelling and effluent, respectively, with annual fluxes ranging from 0.1 to 6.0 MT N km⁻² yr⁻¹ for riverine runoff and 0.4 to 0.8 MT N km⁻² yr⁻¹ for atmospheric deposition.

The Santa Barbara and Ventura sub-regions were similar in that both had net annual downwelling rather than net upwelling, ranging from 21 to 107 MT N km⁻² yr⁻¹, respectively. In these sub-regions, the major sources varied between effluent and atmospheric deposition in Santa Barbara (0.1 to 0.4 MT N km⁻² yr⁻¹, respectively) to roughly equivalent fluxes of effluent, riverine runoff and atmospheric deposition in Ventura (0.5, 0.4 and 0.4 MT N km⁻² yr⁻¹, respectively). Only in North San Diego County was upwelling (37 MT N km⁻² yr⁻¹) dominant by an order of magnitude over effluent (1.4 MT N km⁻² yr⁻¹) and by two orders of magnitude over riverine runoff (0.6 MT N km⁻² yr⁻¹) and atmospheric deposition (0.4 MT N km⁻² yr⁻¹).

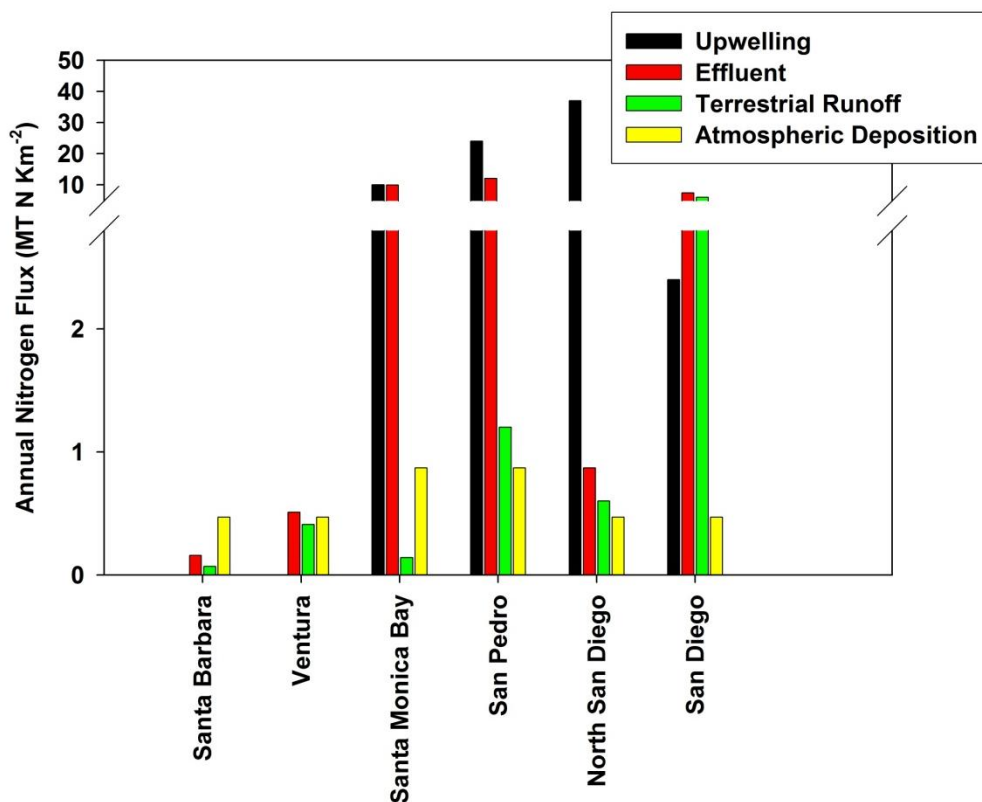


Figure III-7 Annual nitrogen flux for upwelling, effluent, riverine runoff, and atmospheric deposition by sub-region.

Table III-11 Annual TN flux (MT N Km⁻² Year⁻¹) by source for each sub-region.

Source	Santa Barbara	Ventura	Santa Monica Bay	San Pedro	North San Diego	San Diego
Upwelling	-21	-107	10	24	37	2.4
Effluent	0.16	0.5	9.9	12.6	1.4	7.4
Riverine runoff*	0.07	0.4	0.1	1.2	0.6	6.0
Atmospheric Deposition	0.4	0.4	0.8	0.8	0.4	0.4
Sub-regional TN Flux	-20.4	-105.7	21	38.6	39.4	16

Total Phosphorus. Dominant TP sources varied by sub-region. For the three sub-regions with large POTW outfall discharges (Santa Monica Bay, San Pedro and San Diego), upwelling had a larger TP flux than effluent in two of those sub-regions (Santa Monica Bay and San Pedro), by one order of magnitude (Figure III-8, Table III-12). These were 3.1 and 0.6 MT P km⁻² yr⁻¹ welling and effluent respectively for Santa Monica Bay and 6.3 and 0.37 MT P km⁻² yr⁻¹ respectively for San Pedro. The TP flux was the same order of magnitude for upwelling, 0.5 MT P km⁻² yr⁻¹ and effluent, 0.5 MT P km⁻² yr⁻¹ in the San Diego sub-region. Note that the upwelling flux estimated for San Diego is at the edge of the model boundary, therefore, has a large amount of uncertainty. There was no phosphorus data collected for effluent in the, Santa Barbara, Ventura and North San Diego sub-regions.

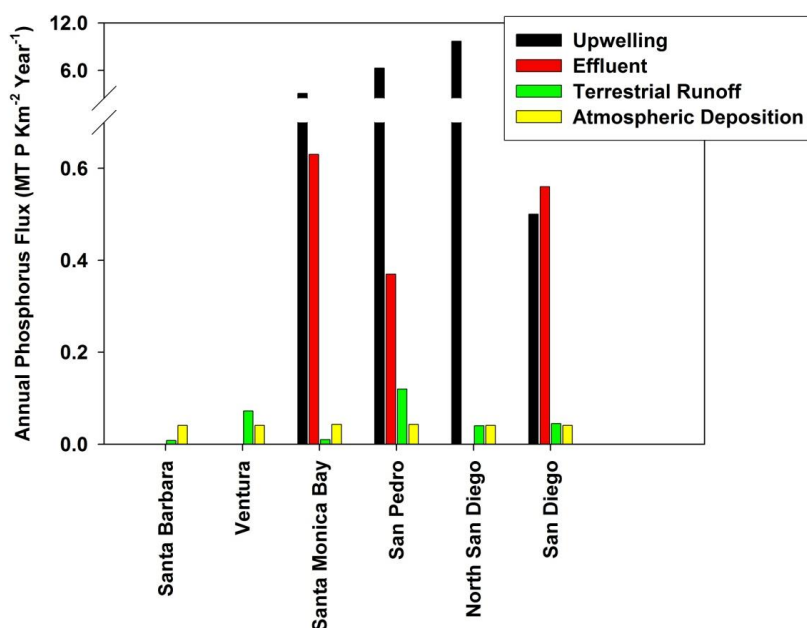


Figure III-8 Annual phosphorus flux (MT P Km⁻² Year⁻¹) for upwelling, effluent, riverine runoff, and atmospheric deposition.

Riverine runoff was the same order of magnitude as effluent in San Pedro with annual fluxes estimated at $0.1 \text{ MT P km}^{-2} \text{ yr}^{-1}$ (compared with $0.3 \text{ MT P km}^{-2} \text{ yr}^{-1}$). Riverine runoff and atmospheric deposition were 1-2 orders of magnitude lower than upwelling in Ventura, Santa Monica Bay, North San Diego and San Diego. The annual fluxes for riverine runoff were $0.008 \text{ MT P km}^{-2} \text{ yr}^{-1}$ for Santa Barbara, $0.07 \text{ MT P km}^{-2} \text{ yr}^{-1}$ for Ventura, $0.01 \text{ MT P km}^{-2} \text{ yr}^{-1}$ for Santa Monica Bay, $0.04 \text{ MT P km}^{-2} \text{ yr}^{-1}$ for North San Diego and $0.04 \text{ MT P km}^{-2} \text{ yr}^{-1}$ for San Diego. The atmospheric deposition fluxes were $0.04 \text{ MT P km}^{-2} \text{ yr}^{-1}$ in Santa Barbara, Ventura, North San Diego and San Diego; whereas the Santa Monica Bay and San Pedro annual fluxes were $0.04 \text{ MT P km}^{-2} \text{ yr}^{-1}$.

Appendix C summarizes the nitrogen and phosphorus loads for each form in all of the subregions.

Table III-12 Annual phosphorus flux ($\text{MT P Km}^{-2} \text{ Year}^{-1}$) for each sub-region. ND = No data.

	Santa Barbara	Ventura	Santa Monica Bay	San Pedro	North San Diego	San Diego
Upwelling*	-5.7	-29	3.1	6.3	9.7	0.5
Effluent	ND		0.6	0.3	ND	0.5
Riverine runoff*	0.008	0.07	0.01	0.1	0.04	0.04
Atmospheric Deposition	0.04	0.04	0.04	0.04	0.04	0.04
Sub-regional TP Flux	-5.6	-29	3.8	6.8	9.8	1.1

*Flux of phosphate

Timing of Loads

Although the data are presented as annual total loads, the timing of those loads to the SCB is quite distinct and relevant for support of phytoplankton blooms. Effluent loads tend to remain relatively constant throughout the year, in contrast to the three source types, which have distinct seasonality.

On average, riverine TN loads were 46% higher and TP loads were 71% higher during storm events, which occur mostly from November to March, than during dry weather. During wet weather, eight watersheds (Los Angeles River, San Gabriel River, Calleguas Creek, San Diego Creek, Tijuana River, Santa Margarita River, Chollas Creek and Santa Ana River) account for 75% of the TN loads, while eight watersheds (Los Angeles River, San Gabriel River, Calleguas Creek, San Diego Creek, Tijuana River, Santa Margarita River, Santa Clara River, and San Marcos River) constituted 71% of the wet weather TP loads (Figure III-9, from Sengupta et al. submitted, Appendix E). The exception to the dominance of storm events to total annual loads was observed in San Gabriel, Los Angeles, and Santa Clara Rivers, where TN and TP loads were comparable or greater during dry weather than during storm events. Thus the San Gabriel River, Los Angeles River, Santa Clara River, and Calleguas Creek watersheds represent the dry

weather "hot spots" for nutrient loading to the SCB, representing 59 % of the dry weather total TN and 62% of the total TP loads to the SCB (Figure III-9).

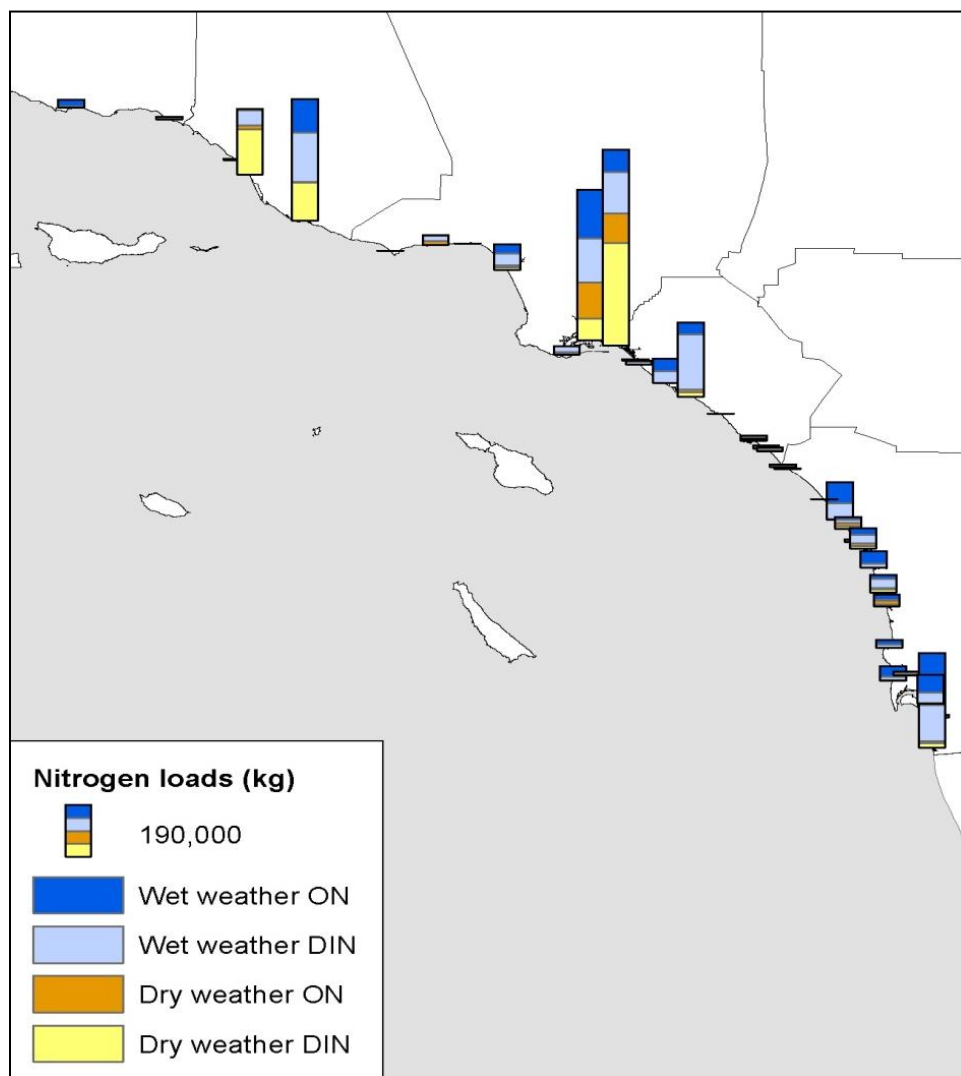


Figure III-9 Nitrogen loads as wet- and dry-weather organic (ON) and dissolved inorganic nitrogen (DIN) for rivers. The height of the bar is the total magnitude of the load.

Estimates of Contribution of Anthropogenic Activities to SCB Nutrient Loads

The contribution of anthropogenic activities to SCB nutrient loads can be calculated based on changes in riverine loads from a pre-urbanization baseline, with the additional of effluent loads, all of which are assumed to be anthropogenic. No estimates of the anthropogenic contribution to atmospheric deposition are available, so this number was not included in the estimate.

Relative to a pre-urbanization scenario of land cover dominated by 100% open space, riverine TN loads increased 4-fold and the TP increased 8-fold on a Bightwide scale (Figure III-10). Dissolved inorganic

nutrients (NO_3 , PO_4 and NH_4) saw a disproportionately higher increase relative to organic or particulate fractions. The largest changes in the sub-regional data were observed for the more heavily urbanized areas of San Pedro and Santa Monica Bay with an approximately 9-fold increase in TN and 15 and 13-fold increase in TP respectively. The smallest changes were observed in Ventura and Santa Barbara with a 2-fold increase in TN and a 5- and 3.5-fold increase in TP, respectively.

While anthropogenic changes to riverine loads are considerable, these loads still represent an order of magnitude less than effluent loads, the major source of anthropogenic loads to the Bight. However, total flux of nitrogen from natural sources (upwelling, atmospheric deposition and pre-urbanization rivers) can be calculated and compared to the total nitrogen flux of all nutrient sources (upwelling, atmospheric deposition, post-urbanization rivers and wastewater effluent discharge). The increase in nitrogen due to anthropogenic sources was found to be largest for the Santa Monica Bay, San Pedro and San Diego sub-regions with increases of 2, 1.5, and 5.5-fold, respectively. These results are summarized in Table III-13.

Table III-13 The total nitrogen flux ($\text{MT N Km}^{-2} \text{ Year}^{-1}$) for natural nutrient sources (upwelling and atmospheric deposition) and for natural and anthropogenic sources (all sources; data from Table III-11) to the SCB .

	Natural Sources	Natural and Anthropogenic Sources
Santa Barbara	-20.5	-20
Ventura	-99.4	-98
Santa Monica Bay	10.8	21
San Pedro	25	38
North San Diego	37.5	39
San Diego	3	16

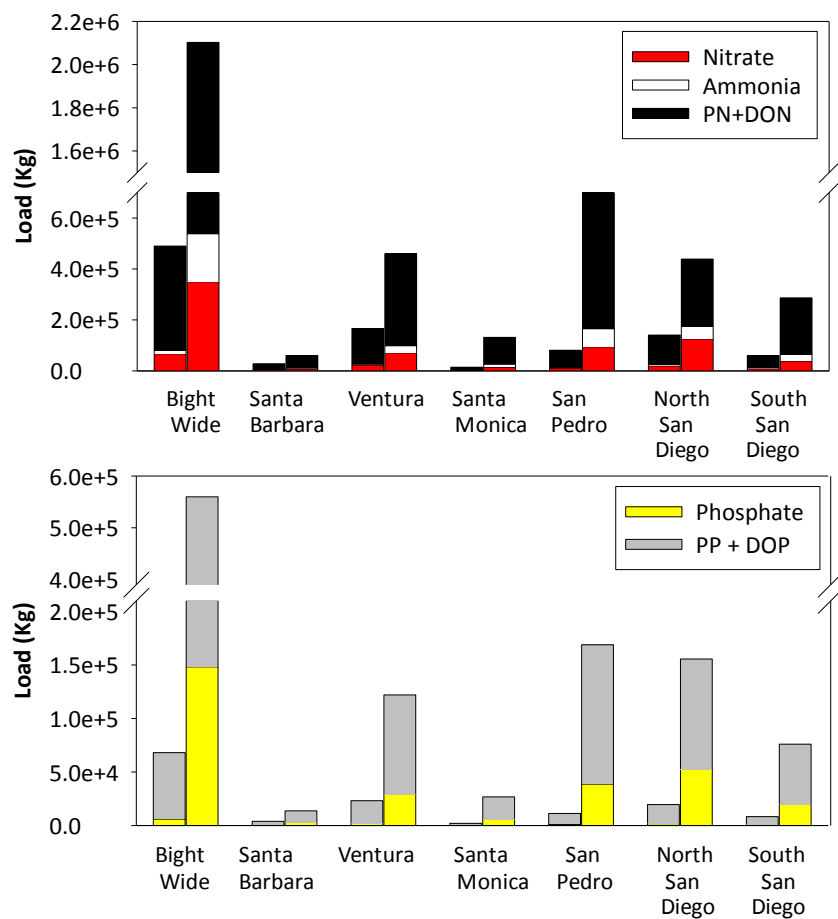


Figure III-10 Net change from 'pre-urbanization' (bars on the left) and post-urbanization (bars on the right) riverine runoff loads of nitrogen and phosphorus on a Bightwide and sub-regional scale for TN (top panel) and TP (bottom panel).

Discussion

Importance of Anthropogenic Nutrients in Upwelling-Dominated Ecosystems

The hypothesis that natural (upwelling) sources of nutrients contribute a substantially larger amount of nutrients to the SCB than anthropogenic sources of nutrients was tested. At the scale of the entire region, the results of this study support this hypothesis; natural sources (i.e. upwelling) dominate and anthropogenic inputs are relatively insignificant by an order of magnitude for N and two orders of magnitude for P. However, at a sub-regional scale and proximal to the coastline (~20 km), anthropogenic N sources, particularly POTW effluent discharged to ocean outfalls, were equivalent to natural nitrogen sources in five of the six sub-regions. In the three sub-regions where effluent TP data were reported or collected, anthropogenic sources were equivalent to natural sources in one of these three sub-regions. These findings contradict the currently held perception that in upwelling-dominated marine ecosystems, anthropogenic nutrient inputs are negligible and are consistent with the growing number of studies that have suggested a linkage between anthropogenic nitrogen sources and HABs in California nearshore waters (Kudela and Cochlan 2000, Kudela and Chavez 2004, Beman et al. 2005, Herndon and Cochlan 2007, Howard et al. 2007, Cochlan et al. 2008, Kudela et al. 2008). Nezhlin et al. (in press; Chapter 2) showed that algal bloom extent has increased over the last decade, with chronic algal bloom 'hotspots' documented in areas of the SCB that have major anthropogenic sources of nutrient loads. These results provide an additional line of evidence supporting the conclusion that anthropogenic nutrients cannot be dismissed as a significant source of nutrients for algal blooms in the SCB.

Importance of Temporal and Spatial Scale of Nutrient Load Delivery

The nutrient loads estimated for the four major sources in this study were calculated using annual time scales. However, it is important to recognize that nutrient delivery to the coastal ocean on shorter, daily to weekly, timescales is more ecologically relevant for primary productivity and HAB development. The timing of these nutrient sources should be considered as some sources are chronic (daily wastewater effluent discharge into oceans and into rivers), whereas other sources are seasonal (riverine runoff and upwelling). Other studies in Southern California have shown that stormwater runoff has been at times the dominant source of nitrogen inputs during non-upwelling periods and provided different proportions of nutrients than upwelling (Warrick et al. 2005, McPhee-Shaw et al. 2007). In Monterey Bay, a more extensive study of this dynamic has shown similar results where riverine inputs of nitrate exceeded upwelling inputs across short, daily to weekly, timescales, (but not monthly or annual scales), as often as 28% of days in a given year (Quay, 2011).

It is important to recognize that the temporal and spatial scales used to evaluate nutrient sources will have a large impact on the results of the comparison of natural and anthropogenic sources. Similarly, the nutrient source loads were estimated for two spatial scales, bightwide and local sub-regional scales. The local spatial scale is more ecologically relevant since it is similar to the scales at which algal blooms develop (meaning, blooms do not develop at the bightwide scale shown in Figure III-2).

Uncertainty Associated with Nutrient Source Estimates

There was a high level of confidence in the load estimates of both TN and TP and related constituents for riverine runoff and effluent sources. The standard error determined for riverine runoff and effluent loads was less than 20% with two exceptions, the riverine runoff (wet weather) ammonia (37.8%) and effluent phosphate (23.7%) loads. Effluent loads from POTWs are monitored on a monthly basis and have been tracked over the last 30 years with a high level of quality assurance (Lyon and Stein, 2008). There were insufficient data to calculate the error for the atmospheric deposition estimates, but this appears to be a very small source at the sub-regional scale. It is useful, therefore, to discuss two components in the uncertainty in the upwelling estimates: 1) methodology to estimate upwelling and 2) modeling uncertainty and validation.

Methodology to Estimate Upwelling. In this study, a coupled hydrodynamic-biogeochemical model (ROMS/NPZD) was used to estimate upwelling. This approach produces a more accurate estimate than the more frequently used upwelling index produced by the NOAA Pacific Fisheries Environmental Laboratory (PFEL). Studies using the PFEL upwelling index typically combine the average volume over time of upwelled water with the average concentration of nitrate to estimate nitrogen flux for a specific area of coastline. For example, Warrick et al. (2005) calculated a nitrate upwelling of 2.1×10^5 MT N year⁻¹ for a 50 km section of the Santa Barbara Channel and the ICF International (2012) reports an estimate using the PFEL upwelling index of 4.3×10^5 MT N Year⁻¹ (30 Km coastline) for Palos Verdes. These estimates differ from the ROMS/Biogeochemistry modeled estimate, 7.5×10^5 MT N year⁻¹ (for 50 km alongshore, 20km offshore and 50m depth) produced by this study for several reasons.

First, an important component of upwelling-- Ekman pumping-- is ignored in the conventional upwelling index. Upwelling can be separated into coastal upwelling and Ekman pumping. The coastal upwelling is associated with non-uniform cross-shore transport for a uniform along-shore wind stress forcing. The Ekman pumping, on the other hand, is associated with the spatial variation of wind stress forcing, more specifically the curl of wind stress. The upwelling index is based on the geostrophic wind computed from sea level pressure from operational weather forecasting models of the U.S. Navy Fleet Numerical Meteorological and Oceanographic Center (FNMOC), which effectively ignores the Ekman pumping component of upwelling.

Second, upwelling is a highly variable process in both space and time. The simple calculations generally cannot account for the variability associated with upwelling. The ROMS model is a three-dimensional, eddy-resolving physical circulation model that is able to address the variability both spatially, across a wide horizontal and vertical area and temporally, by providing highly resolved data.

Third, the PFEL upwelling index characterizes large-scale atmospheric circulation patterns (Bakun 1973) and is based upon Ekman's theory of mass transport of water due to wind stress. However, due to the complex bottom topography and coastal orientation of the SCB, several published studies have concluded that the current variability within the SCB cannot be explained by wind stress (Lentz and Winant 1986, Noble et al. 2002, Hickey et al. 2003) and therefore the PFEL upwelling index is not a good representation of specific upwelling rates in southern California. The results from the remote sensing

analysis of this study (Nezlin et al. in press, Chapter 2) found there was no relationship between the upwelling index and the remotely-sensed variation in sea surface temperature, a further indication that it is not an accurate estimation of specific upwelling in the SCB.

Fourth, the ROMS model performs at a much higher resolution (1 km versus ~100 km) and uses local bathymetry data and therefore reproduces localized upwelling better than the general PFEL index that provides a more regional estimate. The PFEL upwelling index provides a vertical rate of the volume of upwelled water for a specific stretch of coastline, however the upwelling estimates calculated in this study use a 3-dimensional approach to boundary conditions, including both vertical and lateral fluxes. The modeled estimates of upwelling were for an area of approximately 50 km of coastline, combined with a 20km offshore dimension and a 50m depth. The net flux of nitrogen, both laterally and vertically into this 3-D volume was determined for the SCB region and each sub-region. Given the physical circulation patterns associated with the SCB and the presence of the Southern California Eddy (Hickey 1992, Harms and Winant 1998, Bray *et al.* 1999), the lateral component of this estimate is significant, and this alone could explain the difference.

Modeling Uncertainty and Validation. The coupled ROMS/NPZD model has been validated at the 15 km resolution for the entire U.S. West Coast by comparing model results with either remote sensing observations (AVHRR, SeaWiFS) or in-situ measurements from the CalCOFI Program (Gruber et al. 2006). While we have a high level of confidence in our results at an annual and Bightwide scale, we must caveat our results as they become applied to seasonal or sub-regional scales. The 1-km ROMS model and NPZD used for this study has not yet been validated at this spatial scale. For this reason, it is not possible at this time to calculate the error associated with the upwelling estimates from this study. The validation of the ROMS model at 1-km resolution is on-going (but not complete as of this report), and the in-situ data collected during this study will be used as part of that process.

Interannual Variability. The results of this study are focused on the year 2010, however, interannual variations in both anthropogenic and natural nutrient sources were observed. The riverine runoff has been shown by the 13 year model results to vary greatly on an interannual scale depending on precipitation and storm events. Figure III-11 shows 2008–2009 as a relatively dry year, whereas 2009–2010 was characterized by high precipitation and resulted in 3-fold higher riverine runoff loads. Similarly, upwelling is highly variable and certainly large scale climate patterns can affect oceanographic conditions. Several ocean ecosystem indices have been developed to show changes in regional ocean conditions for the California Current System. The Pacific Decadal Oscillation (PDO) shifts every 20–30 years between a colder, negative phase and a warmer, positive phase. Whereas the El Niño/Southern Oscillation (ENSO) occurs about every 5 years, can last 6–18 months, and is characterized by variations in temperature. Indices of each of these patterns (Figures III-12 and III-13) show that the 2010 study period was characterized by a warm oceanographic regime (PDO), strong El Niño conditions (ENSO), and weak upwelling conditions (PFEL Upwelling Index).

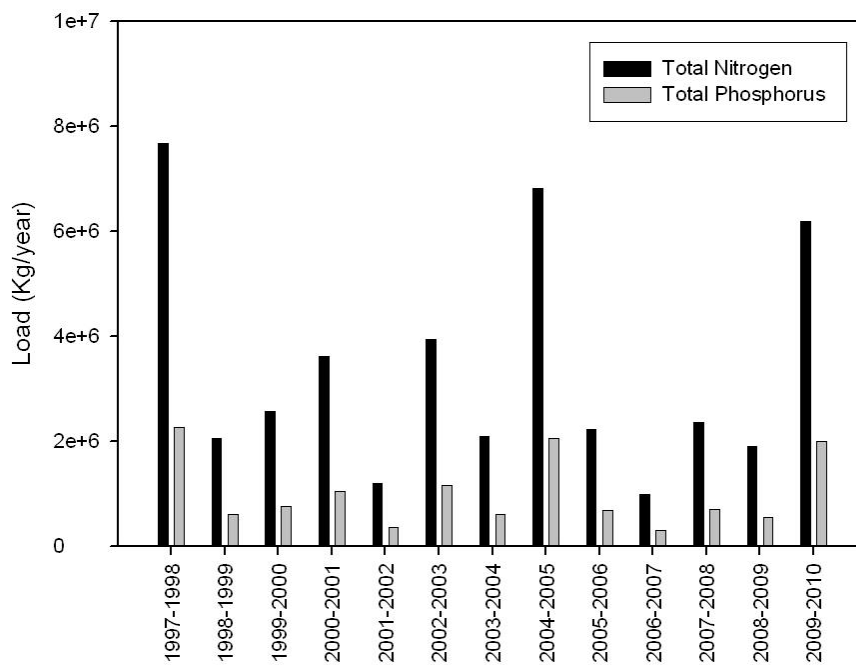


Figure III-11 Total nitrogen and total phosphorus loads for the 13-year model analysis for riverine runoff.

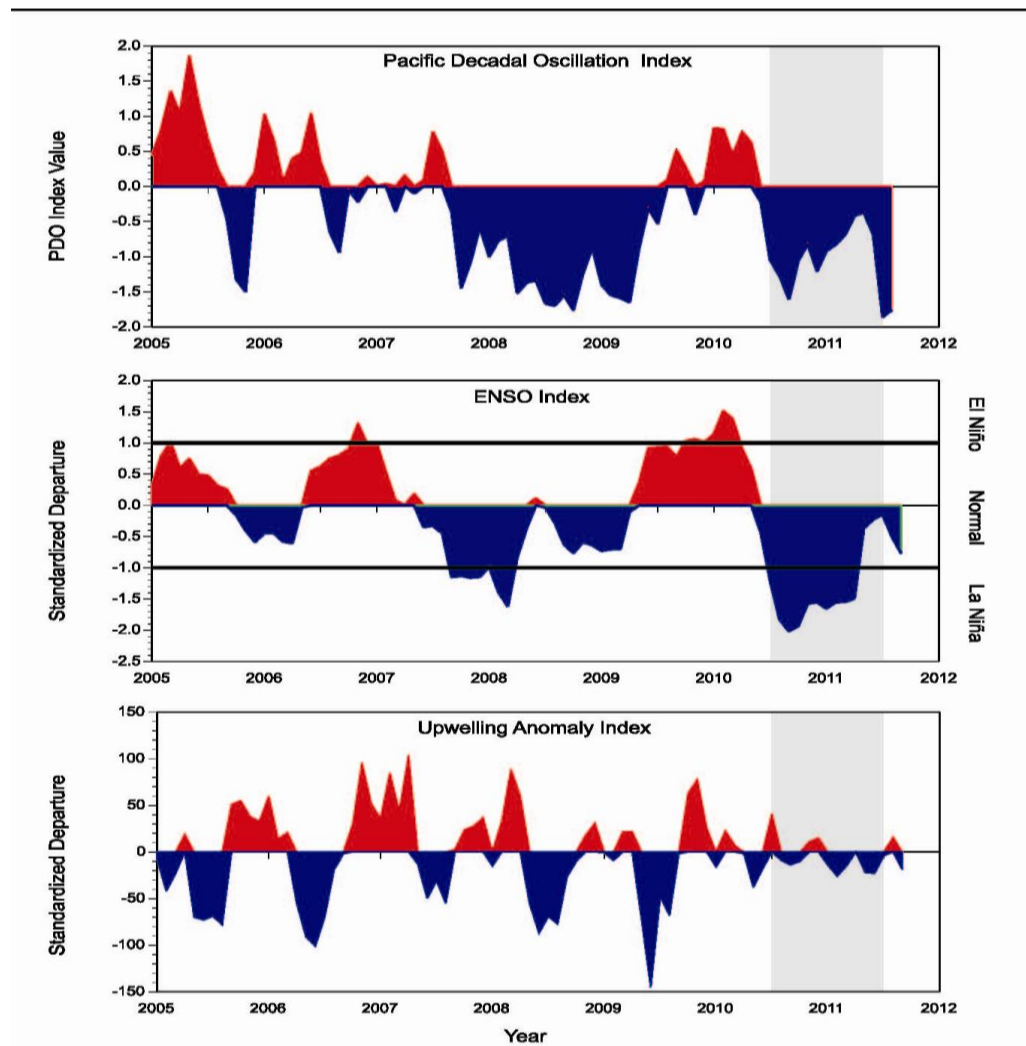


Figure III-12 Ecosystem indices 2005 to 2012 for the Pacific Decadal Oscillation (PDO) Index, the El Niño/Southern Oscillation (ENSO) Index, and the PFEL Upwelling Anomaly Index (from the Orange County Sanitation District Annual Report, 2011).

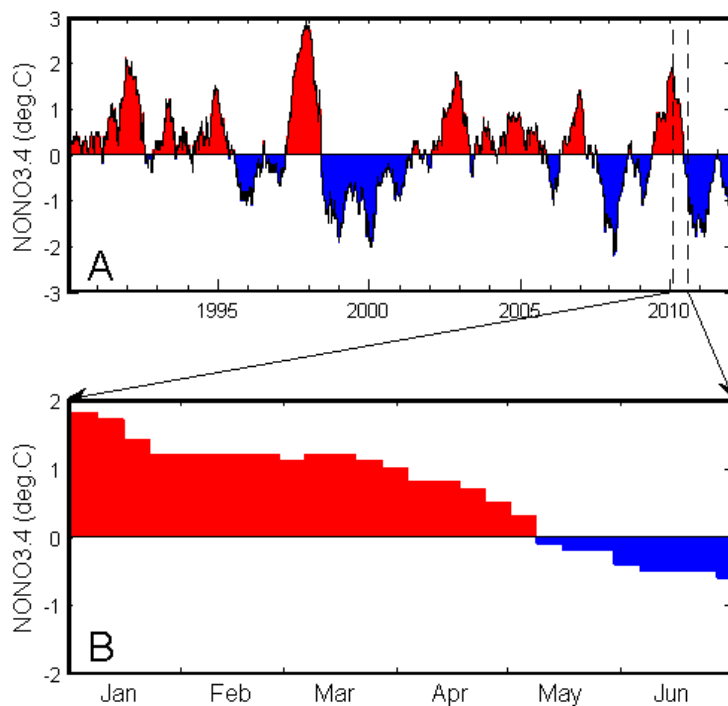


Figure III-13 El Niño index (NINO3.4 is sea surface temperature anomaly in the equatorial Pacific region 5°N–5°S:170–120°W) (A) during 1990–2011 and (B) in January–June 2010.

The Importance of Nutrient Ratios and Forms

Nitrogen is considered to be the primary limiting macronutrient for the growth of algae in coastal waters (Dugdale, 1967, Nixon, 1986, 1995; Ryther and Dunstan, 1971, Eppley et al. 1979; Kudela and Dugdale, 2000). The results from this study are consistent with previous studies in that N:P ratios calculated from the ambient nutrients measured during the ship surveys indicate nitrogen limitation in most regions (see Section IV).

Recent studies have shown that the form of nitrogen, not just the quantity, is important for HABs and algal blooms (Howard et al. 2007, Switzer, 2008, Kudela et al. 2008, Cochlan et al. 2008). The sources of nitrogen to the SCB are comprised of different forms of nitrogen, mainly nitrate (plus nitrite), ammonia, and organic nitrogen (including urea). Dissolved inorganic nitrogen (DIN) was the dominant form in most natural and anthropogenic sources, except a few of the river systems, where organic nitrogen was close to equivalent (i.e. riverine runoff was 60% organic nitrogen). When we examine the forms of nitrogen that comprise each of these sources, it was surprising that effluent provides a similar nitrate (plus nitrite) load as riverine runoff to the SCB even though this form only comprises 7% of the TN load for effluent. As expected, upwelling was mostly comprised of nitrate, effluent was mostly comprised of

ammonia, and riverine runoff was comprised of a mixture of inorganic and organic nitrogen forms. Organic nitrogen was mostly derived from riverine runoff (60% on a bightwide scale).

Urea, an organic nitrogen form used as an indicator of coastal runoff (Kudela and Cochlan, 2000) has been found to sustain HABs in central and southern California, and California HAB species have been shown to utilize urea for growth (McCarthy, 1972, Eppeley et al. 1979, Kudela and Cochlan, 2000, Herndon and Cochlan, 2007, Howard et al. 2007, Cochlan et al. 2008, Kudela et al. 2008). Despite these studies, urea concentrations in California's coastal waters and the importance of urea as a nitrogen source for algal growth is often overlooked and understudied. The main source of urea to the SCB was determined to be riverine runoff as urea comprised 1% or less of the large POTW effluent loads.

Conclusions

At a regional, bightwide scale, natural nutrient sources make a much larger contribution of nutrients than anthropogenic sources. At smaller sub-regional spatial scales, which are more ecologically relevant to the development of algal blooms, the quantity of anthropogenic and natural nitrogen sources (but not phosphorus) are comparable in orders of magnitude. The anthropogenic nutrient sources were mostly comprised of dissolved inorganic nitrogen. The organic nitrogen was only evaluated in two sources (riverine runoff and effluent) and the riverine runoff was the main source of organic nitrogen to the SCB. Urea was a measurable source of nitrogen in the SCB but a minor component of the overall nitrogen load. These results suggest that the spatial scale used in the analysis will affect the relative comparison between anthropogenic and natural nutrient sources. While this study was designed to be a first order estimation of nutrient sources, the results suggest that anthropogenic nutrients relevant to algal blooms are also significant at spatial scales. The coastal waters in the SCB are generally nitrogen limited; consequently, any nitrogen inputs to the coastal oceans will likely have an impact on biological productivity.

Future Studies and Recommendations

Future studies are needed to determine the amount of biological productivity that is attributable to anthropogenic nutrient sources to the SCB. A multi-year source analysis should be conducted in order to determine interannual variability for each source. Existing data could be used for a multiyear analysis of effluent and riverine sources. Upwelling could be estimated by hindcasting the ROMS Hydrodynamic Model over several years. A multi-year analysis would be particularly appropriate for atmospheric deposition because a source signature was detected in surface waters (see Appendix E). However, additional studies are needed in order to provide a sufficient amount of deposition-rate data for a multi-year analysis and to further investigate atmospheric deposition as a nutrient source in coastal waters.

The models used in this study are in the process of being validated. Once validation is completed, these models can be used for a variety of purposes. First, a multi-year source comparison can be conducted using the ROMS coupled with the NPDZ model to determine interannual variability among sources. Second, the models can be used to assess various nutrient source scenarios and to determine the biological productivity that results from anthropogenic nutrients. Third, the models can also be used to

assess coastal hypoxia and ocean acidification. Fourth, the models can be used to generate seasonal estimates of anthropogenic and natural nutrients sources and provide insight into the effect of anthropogenic nutrients on productivity.

References

Ackerman, D. and Schiff. K., 2003. Modeling stormwater mass emissions to the southern California Bight. *Journal of the American Society of Civil Engineers* 129: 308-323.

Anderson, D.M., Glibert, P.M., and Burkholder, J.M., 2002. Harmful algal blooms and eutrophication: Nutrient sources, composition, and consequences. *Estuaries* 25: 704-726.

Anderson, D.M., Burkholder, J.M., Cochlan, W.P., Glibert, P.M., Gobler, C.J., Heil, C.A., Kudela, R.M., Parsons, M.L., Rensel, J.E., Townsend, D.W., Trainer, V.L., Vargo, G.A., 2008. Harmful algal blooms and eutrophication: Examining linkages from selected coastal regions of the United States. *Harmful Algae* 8: 39-53.

Bakun, A., 1973. Coastal upwelling indices, west coast of North America, 1946–1971. NOAA Tech. Rep. NMFS SSRF-671. U.S. Department of Commerce. Washington, DC.

Barron, J.A., Bukry, D., Field, D., 2010. Santa Barbara Basin diatom and silicoflagellate response to global climate anomalies during the past 2200 years. *Quaternary International* 215: 34-44.

Beman, M., Arrigo, K., Matson, P., 2005. Agricultural runoff fuels large phytoplankton blooms in vulnerable areas of the ocean. *Nature* 434: 211–214.

Bray, N.A., A. Keyes and W.M.L. Morawitz, 1999. The California Current system in the Southern California Bight and the Santa Barbara Channel. *Journal of Geophysical Research-Oceans* 104: 7695-7714.

Brzezinski, M.A., 1985. The Si:C:N ratio of marine diatoms: interspecific variability and the effect of some environmental variables. *Journal of Phycology* 21: 347–357

Burkov, V.A. and Y.V. Pavlova, 1980. Description of the eddy field of the California Current. *Oceanology*. English Translation 20: 272-278.

Busse, L.B., Venrick, E.L., Antrobus, R., Miller, P.E., Vigilant, V., Silver, M.W., Mengelt, C., Mydlarz, L., Prezelin, B.B., 2006. Domoic acid in phytoplankton and fish in San Diego, CA, USA. *Harmful Algae* 5: 91–101.

Caron, D.A., M.E. Garneau, E. Seubert, M.D.A. Howard, L. Darjany, A. Schnetzer, I. Cetinic, G. Filteau, P. Lauri, B. Jones, and S. Trussell, 2010. Harmful algae and their potential impacts on desalination operations off southern California. *Journal of Water Research* 44: 385-416.

Chisholm, J.R.M., Fernex, F.E., Mathieu, D., Jaubert, J.M., 1997. Wastewater discharge, seagrass decline and algal proliferation on the Cote d'Azur. *Mar. Poll. Bull.* 34: 78–84.

Cochlan, W.P., Herndon, J., Kudela, R.M., 2008. Inorganic and organic nitrogen uptake by the toxigenic diatom *Pseudo-nitzschia australis* (Bacillariophyceae). *Harmful Algae* 8: 111–118.

Dailey, M.D., J.W. Anderson, D.J. Reish and D.S. Gorsline. 1993. The Southern California Bight: Background and setting. Berkeley, CA. *in*: M. D. Dailey , D. J. Reish and J. W. Anderson (Eds.), *Ecology of the Southern California Bight*. University of California Press. 1-18

Dong, C., E.Y. Idica, and J.C. McWilliams. Circulation and multiple-scale variability in the Southern California Bight. *Progress in Oceanography* 82: 168-190.

Dorman, C.E. and C.D. Winant, 1995. Buoy observations of the atmosphere along the west coast of the United States. *Journal of Geophysical Research-Oceans* 100: 16029-16044.

Dugdale, R. C., 1967. Nutrient limitation in the sea: Dynamics, identification and significance. *Limnology and Oceanography* 12: 685–695.

Emery, K.O., 1960. *The Sea off Southern California*. John Wiley and Sons, Inc. New York, NY.

Eppley, R., Renger, E., Harrison, W., 1979. Nitrate and phytoplankton production in California coastal waters. *Limnology and Oceanography* 24: 483–494.

GEOHAB, 2006. Global ecology and oceanography of harmful algal blooms. *Harmful Algal Blooms in Eutrophic Systems* 74.

Glibert, P.M., Anderson, D.M., Gentien, P., Granéli, E., and Sellner, K.G., 2005a. The global, complex phenomena of harmful algal blooms. *Oceanography* 18: 137-147.

Glibert, P.M., Seitzinger, S., Heil, C.A., Burkholder, J.M., Parrow, M.W., Codispoti, L.A., and Kelly, V., 2005b. The role of eutrophication in the global proliferation of harmful algal blooms. *Oceanography* 18: 198-209.

Glibert, P.M., Harrison, J., Heil, C., and Seitzinger, S., 2006. Escalating worldwide use of urea- a global change contributing to coastal eutrophication. *Biogeochemistry* 77: 441-463.

Gruber, N. Frenzel, H., Doney, S.C., Marchesiello, P., McWilliams, J.C., Moisan, J.R., Oram, J.J., Plattner, G.K., Stolzenbach, K.D. 2006. Eddy-resolving simulation of plankton ecosystem dynamics in the California Current System. *Deep Sea Research I* 53: 1483-1516.

Gruber, N. , Z. Lachkar, H. Frenzel, P. Marchesiello, M. Münnich, J. C. McWilliams, T. Nagai, and G.-K. Plattner, 2011. Eddy-induced reduction of biological production in eastern boundary upwelling systems, *Nature Geoscience* 4(11): 787-792.

Hallegraeff, G.M., 1993. A review of harmful algal blooms and their apparent global increase. *Phycologia* 32: 79-99.

Hallegraeff, G.M., 2004. Harmful algal blooms: a global overview. *In*: *Manual on Harmful Marine Microalgae*. Hallegraeff, G.M., Anderson, D.M., and Cembella, A.D. (Eds.), UNESCO Publishing, France 25-49.

- Haney, R.L., R.A. Hale and D.E. Dietrich, 2001. Offshore propagation of eddy kinetic energy in the California Current. *Journal of Geophysical Research-Oceans* 106: 11709-11717.
- Harms, S. and C.D. Winant, 1998. Characteristic patterns of the circulation in the Santa Barbara Channel. *Journal of Geophysical Research-Oceans* 103: 3041-3065.
- Heisler, J., Glibert, P., Burkholder, J., Anderson, D., Cochlan, W., Dennison, W., Gobler, C., Dortch, Q., Heil, C., Humphries, E., Lewitus, A., Magnien, R., Marshall, H., Sellner, K., Stockwell, D., Stoecker, D., Suddleson, M., 2008. Eutrophication and harmful algal blooms: a scientific consensus. *Harmful Algae* 8: 3-13.
- Hamilton, P., Noble, M.A., Largier, J., Rosenfeld, L.K., and Robertsone, G., 2006. Cross-shelf subtidal variability in San Pedro Bay during summer. *Continental Shelf Research* 26: 681-702
- Herndon, J., Cochlan, W.P., 2007. Nitrogen utilization by the raphidophyte *Heterosigma akashiwo*: growth and uptake kinetics in laboratory cultures. *Harmful Algae* 6: 260-270.
- Hickey, B.M., 1979. The California Current system: Hypotheses and facts. *Progress in Oceanography* 8: 191-279.
- Hickey, B.M., 1992. Circulation over the Santa Monica-San Pedro basin and shelf. *Progress in Oceanography* 30: 37-115.
- Hickey, B.M., E.L. Dobbins and S.E. Allen, 2003. Local and remote forcing of currents and temperature in the central Southern California Bight. *Journal Phytoplankton blooms detected by SeaWiFS - 320 of Geophysical Research-Oceans* 108: 3081, doi:3010.1029/2000JC000313.
- Howard, M.D.A., W.P. Cochlan, R.M. Kudela, and N. Ladizinsky, 2007. Nitrogenous preference of toxic *Pseudo-nitzschia australis* (Bacillariophyceae) from field and laboratory experiments. *Harmful Algae* 6: 206-217.
- Howarth, R.W., 2008. Coastal nitrogen pollution: a review of sources and trends globally and regionally. *Harmful Algae* 8: 14-20.
- Howarth, R.W., Walker, D., Sharpley, A., 2002a. Sources of nitrogen pollution to coastal waters of the United States. *Estuaries* 25: 656-676.
- Howarth, R.W., Boyer, E.W., Pabich, W.J., Galloway, J.N., 2002b. Nitrogen use in the United States from 1961 to 2000 and potential future trends. *Ambio* 31: 88-96.
- ICF International, 2012. Preliminary Screening Analysis for the Clearwater Program. (ICF 00016.07.) Irvine, CA. Prepared for the Sanitation Districts of Los Angeles County, Whittier, CA.
- Jaubert, J.M., Chisholm, J.R.M., Minghelli-Roman, A., Marchioretti, M., Morrow, J.H., Ripley, H.T., 2003. Re-evaluation of the extent of *Caulerpa taxifolia* development in the northern Mediterranean using airborne spectrographic sensing. *Mar. Ecol. Progr. Ser.* 263: 75-82.

Kudela, R., Dugdale, R., 2000. Nutrient regulation of phytoplankton productivity in Monterey Bay, California. *Deep-Sea Research II* 47, 1023–1053.

Kudela, R.M., Cochlan, W.P., 2000. The kinetics of nitrogen and carbon uptake and the influence of irradiance for a natural population of *Lingulodinium polyedrum* (Pyrrophyta) off southern California. *Aquat. Microbial Ecol.* 21: 31–47.

Kudela, R.M. and Chavez, F.P., 2004. The impact of coastal runoff on ocean color during an El Nino year in central California. *Deep Sea Research* 51(10-11): 1173-1185.

Kudela, R.M., Lane, J.Q., Cochlan, W.P., 2008. The potential role of anthropogenically derived nitrogen in the growth of harmful algae in California, USA. *Harmful Algae* 8: 103–110.

Lange, C.B., Reid, F.M.H., Vernet, M., 1994. Temporal distribution of the potentially toxic diatom *Pseudo-nitzschia australis* at a coastal site in southern California. *Mar. Ecol. Prog. Ser.* 104: 309–312.

Lapointe, B.E., 1997. Nutrient thresholds for bottom-up control of macroalgal blooms on coral reefs in Jamaica and southeast Florida. *Limnol. Oceanogr.* 42 (5, part 2): 1119–1131.

Lapointe, B.E., Barile, P.J., Wynne, M.J., Yentsch, C.S., 2005a. Reciprocal Invasion: Mediterranean native *Caulerpa ollivieri* in the Bahamas supported by human nitrogen enrichment. *Aq. Invad.* 16(2): 2–5.

Lapointe, B., Peter J. Barile, Mark M. Littler, Diane S. Littler. 2005b. Macroalgal blooms on southeast Florida coral reefs II. Cross-shelf discrimination of nitrogen sources indicates widespread assimilation of sewage nitrogen. *Harmful Algae* 4: 1106-1122.

Lapointe, B.E., Barile, P.J., Matzie, W.R., 2004. Anthropogenic nutrient enrichment of seagrass and coral reef communities in the lower Florida keys: discrimination of local versus regional nitrogen sources. *J. Exp. Mar. Biol. Ecol.* 308(1): 23–58.

Lentz, S.J. and C.D. Winant, 1986. Subinertial currents on the southern California shelf. *Journal of Physical Oceanography* 16: 1737-1750.

Lewitus, A.J., Horner, R.A., Caron, D.A., Garcia-Mendoza, E., Hickey, B.M., Hunter, M., Huppert, D.D., Kudela, R.M., Langlois, G.W., Largier, J.L., Lessard, E.J., RaLonde, R., Rensel, J.E.J., Strutton, P.G., Trainer, V.L., Tweddle, J.F., 2012. Harmful algal blooms along the North American west coast region: History, trends, causes and impacts. *Harmful Algae* 19:133-159.

Lynn, R.J. and J.J. Simpson, 1987. The California Current System: The seasonal variability of its physical characteristics. *Journal of Geophysical Research-Oceans* 92: 12947-12966.

Lyon, G.S. and Stein, E.D., 2008. Effluent discharges to the Southern California Bight from small municipal wastewater treatment facilities in 2005. 2008. GS Lyon, ED Stein. pp. 1-14 in: SB Weisberg and K Miller (eds.), Southern California Coastal Water Research Project 2008 Annual Report. Southern California Coastal Water Research Project. Costa Mesa, CA.

- Marchesiello, P., McWilliams, J.C., Shchepetkin, A.F., 2003. Equilibrium structure and dynamics of the California Current system. *Journal of Physical Oceanography* 33: 753–783.
- McCarthy, J.J., 1972. The uptake of urea by natural populations of marine phytoplankton. *Limnology and Oceanography*, 17: 738-748.
- McPhee-Shaw, E.E., David A. Siegel, Libe Washburn, Mark A. Brzezinski, Janice L. Jones, Al Leydecker, and John Melack, 2007. Mechanisms for nutrient delivery to the inner shelf: Observations from the Santa Barbara Channel. *Limnol. Oceanogr.*, 52(5): 1748–1766.
- Moumen, Nadjoua, Seung-Muk Yi, Heather A. Raymond, YoungJi Han, Thomas M. Holsen, 2004. Quantifying the dry deposition of ammonia in ammonia-rich and ammonia-poor environments using a surrogate surface approach. *Atmospheric Environment* 38: 2677–2686.
- Nixon, S. W. (1986). Marine end Environmental Pollution. In *Nutrient dynamics and the productivity of marine coastal waters* (Halwagy, R., Clayton, D., and Behbehani, M., eds.). Oxford, UK. Alden Press 97–115.
- Nixon, S. W., 1995. Coastal marine eutrophication: A definition, social causes, and future concerns. *Ophelia* 41: 199–219.
- Nezlin, N.P., Sutula, M.A., Stumpf, R.P., Sengupta, A., 2012. Phytoplankton blooms detected by SeaWiFS along the central and southern California Coast. *Journal of Geophysical Research*, 117, (C07004). 1-14.
- Noble, M.A., H.F. Ryan and P.L. Wiberg, 2002. The dynamics of subtidal poleward flows over a narrow continental shelf, Palos Verdes, CA. *Continental Shelf Research* 22: 923-944.
- O’Loughlin, G., W. Huber and B. Chocat., 1996. Rainfall-runoff processes and modeling. *Journal of Hydraulic Research* 34: 733-751.
- Paerl, H.W. and M.F. Piehler, 2008. Nitrogen and marine eutrophication. In: *Nitrogen in the Marine Environment*. EDS. D. Capone, D. Bronk, M. Mulholland, E. Carpenter. Burlington, Massachusetts. 2nd Edition. Elsevier Inc., 529-567.
- Parsons, M.L., Dortch, Q., Turner, R.E., 2002. Sedimentological evidence of an increase in *Pseudo-nitzschia* (Bacillariophyceae) abundance in response to coastal eutrophication. *Limnology and Oceanography* 47: 551–558.
- Quay, J., 2011. New Tools and Insight for the Recognition of *Pseudo-nitzschia* blooms and Toxin Incidence. Doctor of Philosophy, Ocean Science, University of California, Santa Cruz.
- Raymond, H.A, Seung-Muk Yi, Nadjoua Moumen, YoungJi Han, Thomas M. Holsen, 2004. Quantifying the dry deposition of reactive nitrogen and sulfur containing species in remote areas using a surrogate surface analysis approach *Atmospheric Environment* 38: 2687–2697
- Reid, J.L., Jr. and A.W. Mantyla, 1976. The effect of the geostrophic flow upon coastal sea elevations in the northern North Pacific ocean. *Journal of Geophysical Research* 81: 3100-3110.

Ryther, J., and Dunstan, W., 1971. Nitrogen, phosphorus and eutrophication in the coastal marine environment. *Science* 171: 1008–1112.

Sabin, L.D. and Schiff, K.C., 2008. Dry atmospheric deposition rates of metals along a coastal transect in southern California. *Atmospheric Environment* 42: 6606-6613.

Shchepetkin, A.F. And McWilliams, J.C., 2005 The regional oceanic modeling system (ROMS): A split-explicit, free-surface, topography-following-coordinate oceanic model. *Ocean Modeling* 9: 347-404.

Shchepetkin, A.F. And McWilliams, J.C., 2008. Computational kernel algorithms for fine-scale, multi-process, long-term oceanic simulations, in: Temam, R., Tribbia, J. (Eds.), *Handbook of Numerical Analysis: Computational Methods for the Ocean and the Atmosphere*. Elsevier Science.

Smayda, T.J., 1990. Novel and nuisance phytoplankton blooms in the sea: evidence for a global epidemic. Granéli, E., Gundström, B., Edler, L., and Anderson, D.M., eds. Elsevier, New York, New York, USA. *In: Toxic Marine Phytoplankton* 29-40,

Strub, P.T. and C. James, 2000. Altimeter-derived variability of surface velocities in the California Current System: 2. Seasonal circulation and eddy statistics. *Deep-Sea Research II* 47: 831-870.

Sverdrup, H.U. and R.H. Fleming, 1941. The waters off the coast of southern California, March to July 1937. *Bulletin of the Scripps Institution of Oceanography* 4: 261-378.

Switzer, T. Urea loading from a spring storm - Knysna estuary, South Africa. *Harmful Algae*, 8: 66-69.

Thompson, P. and Waite, Anya, 2003. Phytoplankton responses to wastewater discharges at two sites in Western Australia. *Marine and Freshwater Research* 54: 721-735.

Thompson, P., Waite, A., 2003. Phytoplankton responses to wastewater discharges at two sites in Western Australia. *Marine and Freshwater Research* 54: 721-735.

Warrick, J., Washburn, L., Brzezinski, M., Siegel, D., 2005. Nutrient contributions to the Santa Barbara Channel, California, from the ephemeral Santa Clara River. *Estuarine, Coastal and Shelf Science* 62: 559–574.

IV. CHARACTERIZATION OF ALGAL BLOOMS AND MONITORING COASTAL OCEAN DYNAMICS WITHIN THE SOUTHERN CALIFORNIA BIGHT

Introduction

Algal blooms occur in coastal waters in response to a variety of environmental conditions (temperature, light availability, physical dynamics), however, nutrients, in particular, are critical to the development and/or maintenance of algal blooms. Most blooms are harmless, necessary, and beneficial to the function of marine and freshwater ecosystems; however, some blooms can be indicative of eutrophication, ecosystem disruption, or altered states. There is increasing awareness that some algal blooms can have negative impacts to the environment, human health, and the economy (such as aquaculture, fisheries and tourism); these blooms are referred to as “harmful algal blooms” (HABs) (Hallegraeff 1993, 2004). Globally, HAB occurrences are increasing in both frequency and intensity in coastal waters, and most coastal states in the United States have reported increasing HAB occurrences (Smayda 1990; Hallegraeff 1993; Anderson et al. 2002; Hallegraeff 2004, Glibert et al. 2005a,b; Anderson et al. 2008; see summary www.whoi.edu/redtide/page.do?pid=14898). Many harmful algal species are regularly observed in southern California coastal waters (www.sccoos.org/data/habs/species.php), including: *Akashiwo sanguinea*, *Alexandrium* spp., *Cochlodinium* spp., *Dinophysis* spp., *Lingulodinium polyedrum*, *Phaeocystis* spp., *Prorocentrum* spp., and *Pseudo-nitzschia* spp. (see Caron et al. 2010 for review).

Many of these species are considered harmful because they produce neurotoxins that can cause mortality in marine wildlife and humans. From a management perspective, *Pseudo-nitzschia* spp. and *Alexandrium* spp. are the species that raise the most concern because of their ability to produce the potent neurotoxins domoic acid and saxitoxin, respectively. Domoic acid poisoning can cause memory loss, brain damage, and fatality; saxitoxin poisoning can lead to numbness, respiratory failure, and fatality. Due to the public health implications of these toxins, the California Department of Public Health (CDPH) monitors toxin levels in shellfish. To avoid outbreaks of shellfish poisoning, the CDPH will close both commercial and recreational harvesting when specific alert levels are exceeded (see Caron et al. 2010 for review). In addition to human health impacts, bioaccumulation of algal toxins through the food web (via contaminated fish and shellfish) has been linked to erratic behavior in birds and marine mammals, as well as marine animal mortality events. In recent years, domoic acid has been the most frequently observed neurotoxin in the Southern California Bight (SCB) (Langlois 2007, Schnetzer et al. 2007, Caron et al. 2010), and therefore of the most concern for research, monitoring, and management.

Benign and harmful algal blooms are highly variable both spatially (horizontally and vertically) and temporally. Spatially, algal blooms can occur locally (10s of meters), regionally (100s of kilometers), and vertically in the water column (on centimeter to meter scales); temporally, blooms may vary on a wide range of temporal scales including hours, days, weeks, and months. Most algal blooms are sampled opportunistically with limited synoptic sampling over a large area; higher frequency sampling is typically limited to a single fixed location (such as piers). The subsurface areas in particular, are often undersampled due to difficulty and expense of sampling this area. As a result, algal bloom initiation and

evolution are poorly understood, despite the variety of HAB programs in the U.S. and regular sampling sites (i.e. SCCOOS and CeNCOOS pier stations) in California coastal waters.

To identify the physical, chemical and biological conditions that lead to HAB formation, a variety of models are currently being applied to HABs in California (Anderson et al. 2008, 2010; Lane et al. 2009). However, due to the limited empirical observations and understanding of bloom initiation and formation, these models are limited in their predictive power (Anderson et al. 2009, 2011; Lane et al. 2009). Improving the knowledge of subsurface algal bloom dynamics has been suggested as a critical aspect required to substantially improve model capacity to predict and forecast algal blooms (Anderson et al. 2011). The goal of the Bight '08 Offshore Water Quality Program was to capture the development, progression, and dissipation of spring algal blooms in order to better understand the oceanographic conditions leading to algal bloom formation and development. Due to the limited existing observational data and the statewide movement to model HABs, the location of bloom development in the water column was a focal point of this study.

The purpose of this component was to characterize the spatial and temporal patterns of a spring algal bloom and determine the origin of bloom development. Characterizing the physical, chemical, and biological oceanographic features associated with the development, evolution, and dissipation of a spring algal blooms will provide insight as to which nutrient sources might be available to the algal community.

Methods

The field study was designed to determine where blooms developed, both within the water column (either at the surface, or deeper in the water column) and within either a nearshore (<1 km) area or farther offshore (1 km to 10 km). The intention was that determining where algal blooms were originating would be suggestive of the main nutrient sources available for algal utilization. Blooms developing in the surface and nearshore waters suggest land-based runoff as the proximal nutrient source to that location. Alternatively, blooms developing farther offshore suggest upwelling- or effluent-based nutrient sources.

Field Study Components

The spatial and temporal patterns of algal blooms were characterized using a multi-disciplinary field based approach utilizing a variety of observation methods, including: ship surveys, modeling, high-frequency radar, remote sensing, continuous automated sampling, and weekly pier-based sampling (Figure IV-1). On the San Pedro Shelf, a more intensive investigation was conducted using Slocum Webb gliders, two environmental sample processors (MBARI), and several additional ship surveys. Each of these components is discussed in detail below.

For the purposes of this component of the Bight '08 WQ study, the term “nearshore” was meant to include 1 km or less spatial extent from the coast (meaning detectable at the coastal pier sites), whereas the term “offshore” was meant to include 1 km to 15 km from the coast.

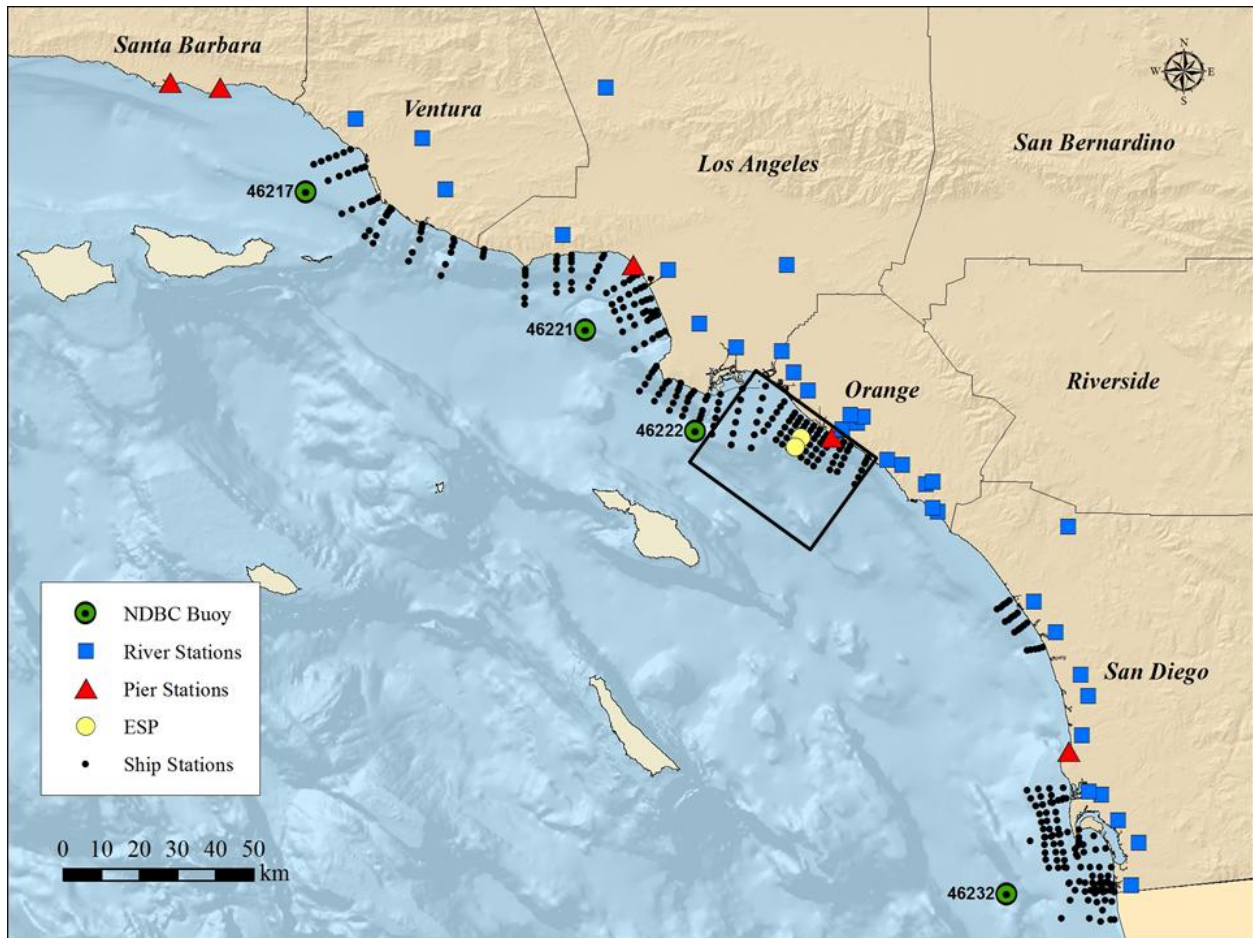


Figure IV-1 Sampling locations for the ocean field components collected as part of this study. Pier Stations were monitored as part of the SCCOOS program; ESP sites indicate MBARI Environmental Sample Processors. The black lines indicate the area where the Slocum Webb gliders were deployed.

Ship Surveys

Sampling took place along a series of preselected transects located close to input sources to the SCB; five surveys conducted in each of four subregions. Two of these surveys were conducted by the Central Bight Water Quality (CBWQ) group and City of San Diego (SD) as part of their NPDES permit monitoring programs. While these surveys are usually conducted on preselected dates regardless of oceanographic conditions, for the Bight '08 field study the timing of the ship surveys were adjusted to coincide with oceanographic triggers while still meeting the permit requirements (e.g. winter and spring sampling) of the agencies involved. In addition to the regular permit monitoring surveys, three "bloom event" surveys designed to follow the onset of an upwelling or bloom event were conducted.

The station location information for the two NPDES quarterly surveys and the three event surveys is listed in the Bight '08 OWQ Field Operations Manual, in Appendices 7-22 (<http://www.sccwrp.org/Documents/BightDocuments/Bight08Documents/Bight08PlanningDocuments.aspx>). Along each transect, 5-6 CTD profiles were collected with discrete samples collected at a subset (three) of those stations.

The Timing of Ship Surveys. The timing of the ship surveys was determined by the presence of several oceanographic 'triggers' which consist of (1) temperature drops below 13.5°C, (2) an increase in overall chlorophyll, (3) presence of *Pseudo-nitzschia*, (4) presence of subsurface algal population (identified by the Webb gliders), and (5) prediction of wind events and upwelling. Weekly meetings (i.e. conference calls) were held every Friday from February through May to review all oceanographic conditions, to determine the presence or absence of triggers, and to recommend whether to conduct a ship survey the following week. Table IV-1 lists all participants and respective data product/topic reporting responsibilities.

Table IV-1 Data products discussed and participants in weekly trigger meetings.

Role/Data Product	Person	Agency
Bight '08 Offshore Water Quality Co-Chair	George Robertson	Orange County Sanitation District
Bight '08 Offshore Water Quality Co-Chair	Meredith Howard	Southern California Coastal Water Research Project
Gliders	Burt Jones	University of Southern California
SCCOOS HAB Pier and ESP	Dave Caron & Erica Seubert	University of Southern California
Remote Sensing	Nick Nezlin	SCCWRP
ROMS Modeling	Yi Chao	JPL/UCLA
Presentation coordination	Bridget Seegers	University of Southern California/Jones Laboratory

Ship Survey Measurements. These offshore field surveys collected CTD (conductivity, temperature, depth) data and bio-optical (transmissivity, chlorophyll, and Colored Dissolved Organic Material (CDOM), fluorometry) vertical profiles. Profiles extended from the surface (≤ 1 m) to within 2-3 m of the bottom, except in water depths greater than 100m, where only the upper 100 meters (75 m for Orange County Sanitation District Surveys) of the water column was sampled.

Discrete water samples were collected at three stations per transect at the surface and at the maximum chlorophyll-fluorescence, (subsurface and chlorophyll-*a* maximum) for measurements of domoic acid, chlorophyll-*a*, particulate nitrogen and phosphorus, and total and dissolved nutrients. The ship-based indicators that were collected are listed in Table IV-2.

Discrete chlorophyll-*a* measurements were used to calibrate CTD-based fluorescence measurements to chlorophyll-*a*. A summary of the calibration is provided in Appendix D.

Table IV-2 Parameters collected during the ship based surveys.

Component	Indicator/Analyte	
	Required	Optional
CTD profile	Conductivity Temperature Depth Dissolved Oxygen Percent Light Transmittance Chlorophyll fluorescence pH	Irradiance Fluorescence (Color Dissolved Organic Matter)
Discrete water samples	Chlorophyll-a Nitrate Nitrite Phosphate Silicate Urea Ammonium Particulate Nitrogen (PN) Particulate Phosphorus (PP) Total Nitrogen (TN) Total Phosphorus (TP) <i>Pseudo-nitzschia</i> cell counts (whole water, WW) Domoic Acid (DA)	

Additional Types of Ocean Sampling

Southern California Coastal Ocean Observing System (SCCOOS) Pier-based Sampling. The weekly pier based SCCOOS HAB sampling program was used to determine if HAB species were present (particularly *Pseudo-nitzschia* spp.) in the SCB. There are four piers used for the Bight '08 study were located in Santa Barbara, Santa Monica, Newport Beach, and La Jolla (Table IV-3). The piers have mounted sensors for collecting continuous time-series data of temperature, salinity, and chlorophyll fluorescence; weekly discrete water samples were also collected analyzed for the constituents listed in Table IV-4.

Table IV-3 SCCOOS Pier sampling locations and responsible participants.

Pier	City	Latitude	Longitude	Institution/PI Responsible
Stearn's Wharf	Santa Barbara	34° 24.48' N	119° 41.10' W	University of California Santa Barbara
Santa Monica Pier	Santa Monica	34° 0.48' N	118° 29.94' W	University of California, Los Angeles
Newport Pier	Newport Beach	33° 36.37' N	117° 55.87' W	University of Southern California
Scripps Pier	La Jolla	32° 52.02' N	117° 15.42' W	University of California, San Diego - Scripps Institution of Oceanography

Table IV-4 Continuously sampled SCCOOS Pier-based indicators and discrete water sample analytes collected weekly discrete water.

Collection Method	Indicator/Analyte
Continuous sensor	Temperature Salinity Fluorescence
Discrete water samples	Chlorophyll-a Nitrate Ammonium Phosphate Silicate Domoic acid Temperature HAB species counts <i>Pseudo-nitzschia</i> <i>Alexandrium</i> <i>Lingulodinium polyedrum</i> <i>Prorocentrum</i> <i>Dinophysis</i> <i>Akashiwo sanguineum</i> <i>Cochlodinium</i> <i>Phaeocystis</i>

Gliders. Autonomous gliders that transmitted data to shore every ~6 hours were deployed in San Pedro Bay. These data provided trigger information for the offshore and subsurface locations that were used to evaluate the potential onset of algal blooms; additional pier and ship surveys were initiated when triggers were observed. Additionally, two USC Webb gliders were used and exchanged approximately every three weeks, in order to maintain a nearly continuous presence for the entire field study period.

The gliders were equipped to measure temperature, salinity, chlorophyll fluorescence, CDOM fluorescence, phycoerythrin fluorescence, and optical backscatter at three minimally absorbing wavelengths (550, 650, and 880 nm). Glider mapping along several sentinel lines was used to monitor for the development of blooms and/or precursor events such upwelling or stormwater runoff events. The region of observation was the San Pedro Bay between Los Angeles Harbor and the Newport Pier. The gliders were equipped with a GPS and satellite phone, which allows daily data transmission. Throughout the deployment period gliders were recovered monthly for calibration, cleaning, and battery change.

Environmental Sample Processors. A pair of Monterey Bay Aquarium Research Institute (MBARI) Environmental Sample Processors (ESPs, <http://www.mbari.org/esp>) were deployed from April 2nd until April 28th, 2010. These processors collected and analyzed water samples of water *in situ* and provided real time information on *Pseudo-nitzschia* species presence and domoic acid detection. The ESP's were moored near the glider transects in 2 locations: one (nearshore location) 4 km from shore at the 30m

isobath and the other (offshore location) 7 km from shore at the 60m isobath. Each ESP was attached to a mooring and set at 17 m depth in order to sample the most likely occurrence of a subsurface chlorophyll maximum.

ROMS Modeling. The JPL ROMS 3–D model (0–2000 m) provided both existing (“nowcast”) and predictive (up to 48 hours in 6–hour increments) representations of temperature, salinity, sea surface height, and currents. The model outputs were used to identify changes in ocean temperature that indicated in-progress or predicted coastal upwelling events. This model is discussed in more detail in Section III.

High-Frequency Radar. High frequency (HF) radar was used to measure surface current velocity near the coast. Daily (25-hour averaged) vector plots were used in conjunction with satellite and ROMS model output, which allowed mesoscale features, like coastal eddies, to be resolved with a great degree of accuracy.

Remote Sensing. Daily satellite imagery was used to identify surface algal blooms (using chlorophyll-*a*) as well as spatial patterns in sea surface temperature. Satellite data products that were used include (1) Chlorophyll-*a* measured by SeaWiFS, MODIS and MERIS and (2) SST measured by satellites (AVHRR, MODIS and GOES).

Data Analysis

Comparison of Chlorophyll among Subregions. Chlorophyll-*a* was used as an indicator of algal biomass and compared both regionally and locally among the sub-regions using two sources: (1) remotely sensed chlorophyll from satellite imagery and (2) chlorophyll fluorescence collected from ship surveys (CTD casts). Collected ship survey data was subsequently calibrated using discrete chlorophyll-*a* samples (see Appendix D for details).

The remotely sensed chlorophyll from satellite imagery was analyzed using the same geographical areas and coordinates as the nutrient source comparison (Section III, Figure III-2) over the (1) bightwide and (2) sub-regional spatial scales. The monthly averages for remotely sensed chlorophyll-*a* were compared to monthly climatologies. The monthly climatologies were determined from average values of 9 years of observations from 2002–2011. Algal biomass variations in the SCB were analyzed on the basis of ocean color data collected by MODerate resolution Imaging Spectroradiometer (MODIS) on Aqua platform (Esaías et al. 1998). Sea surface reflectance measured by MODIS were converted to chlorophyll-*a* concentrations (CHL) at Goddard Space Flight Center using standard algorithm (O'Reilly et al. 1998). Chlorophyll-*a* data for the SCB were extracted from Level 3 standard mapped images at 4.5-km resolution (8-day composites for January–June 2010 and monthly climatologies averaged over the MODIS-Aqua operation period, i.e., 2002–2011). Data within the regions used for Bight'08 modeling analysis were averaged as medians. Medians were preferred to arithmetic means because CHL distribution in the ocean is asymmetric (Banse and English 1994, Campbell 1995) and medians better correspond to modal values.

Chlorophyll fluorescence and discrete chlorophyll-*a* data was collected during the ship surveys. The discrete chlorophyll-*a* measurements were used to calibrate the chlorophyll fluorescence data (see Appendix D for details) in order to compare algal biomass and biological response to upwelling events. The calibrated chlorophyll fluorescence data was binned by date, binned into the following depth strata: (1) 0-50m, (2) 0-15m, (3) 15-30m, (4) 30-45m and (5) 45-100m. The average chlorophyll-*a* fluorescence concentration was determined for each sub-region by survey date and for each depth bin.

Nutrient Ratios. The Redfield Ratio is an empirically derived atomic ratio of carbon (C), nitrogen (N) and phosphorus (P) found in plankton as well as in dissolved fractions in marine water. This stoichiometric ratio, C:N:P = 106:16:1, is used to determine which nutrients are limiting the growth of algae in an ecosystem. The Redfield-Brzezinski ratio was determined specifically for diatoms due to their silicate requirement, of Si:N:P = 15:16:1 (Brzezinski, 1985).

Nutrient ratios were calculated from the nutrient samples collected as part of the ship surveys in order to compare SCB specific ratios to Redfield Ratios. The dissolved inorganic nutrients, DIN, (nitrate plus nitrite, NO_x and ammonium, NH₄) were used for nitrogen, PO₄ concentrations and SiO₄ to calculate DIN:PO₄, DIN:SiO₄ and SiO₄:PO₄ ratios. The average concentration of DIN, PO₄, and SiO₄ were calculated for surveys that occurred before upwelling events (pre-upwelling); separate averages were calculated for surveys that occurred after upwelling events (post-upwelling).

Results

Regional Comparison of Upwelling

Upwelling in each subregion was compared using temperature data from 2 sources, (1) the land-based SCCOOS pier stations and (2) the offshore National Data Buoy Center (NDBC) buoys. Figure IV-2 shows temperature data from both sources. The temperature patterns were similar at the land-based stations for the three southernmost sites, Santa Monica Bay, Newport Pier and Scripps Pier. However, the temperatures at Stearns Wharf in Santa Barbara were consistently colder and showed different temperature patterns; mainly more drops in the temperature, than the other areas. All areas had a temperature drop in mid-March and at the end of April/early May. The Santa Barbara subregion had additional temperature decreases in the beginning of April and mid-May. The Scripps pier consistently had the highest temperatures while Santa Barbara had the coldest.

The NDBC buoy data show similar results in that the Ventura region had consistently colder water than the other areas. All areas had a decrease in temperature in mid-March, and at the end of April/early May. The end of March, the beginning of April, and mid-May showed large differences in temperature patterns across all of the buoy sites. Overall, San Diego consistently had the warmest water temperatures while Ventura had the coldest.

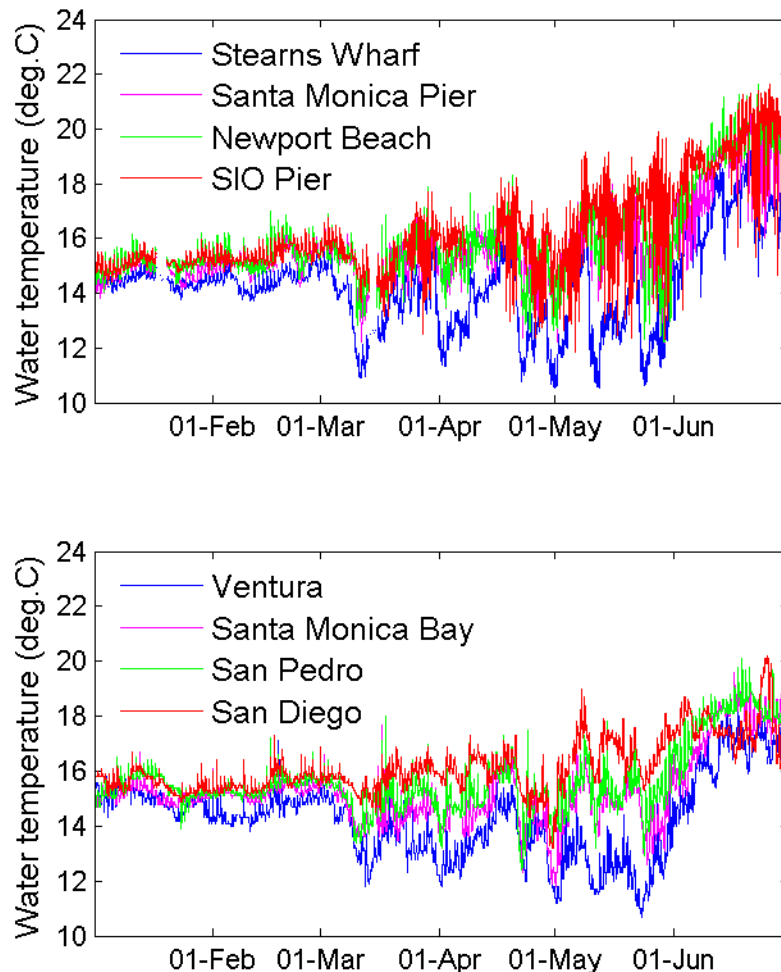


Figure IV-2 Regional Comparison of upwelling in SCB in 2010 from automated sensors on the SCCOOS Piers (top) and NDBC Buoys (bottom). SIO stands for Scripps Institute of Oceanography.

Regional and Sub-regional Comparison of Chlorophyll

Chlorophyll-*a* was used as an indicator of algal biomass and compared both regionally and locally among the sub-regions using 2 sources: (1) remotely sensed chlorophyll from satellite imagery, which measures surface concentrations only, and (2) chlorophyll fluorescence collected from ship surveys, which measures concentrations throughout the water column. Collected data was then calibrated using discrete chlorophyll-*a* samples (see Appendix D for details).

Remotely Sensed Chlorophyll. In 2010, two upwelling events affected the entire SCB: (1) in mid-March and (2) in late April/early May (Figure IV-2 above). Both events were associated with an increase of chlorophyll-*a* across the entire SCB as shown by Figure IV-3. The remotely sensed chlorophyll concentrations during both these periods were comparable with concentrations observed at the end of January and the end of June, when water temperature demonstrated no evidence of upwelling. Additionally, the magnitude of these blooms was lower than monthly climatologies (determined from average values of 9 years of observations from 2002-2011). The low chlorophyll in the open SCB area (Figure IV-3) was due to the much larger offshore area used in the analysis which contained much lower average chlorophyll levels compared to the sub-regional analysis.

The localized sub-regional analysis revealed increased chlorophyll-*a* across all areas in mid-March and early May (Figure IV-4) consistent with time periods of lowered temperatures measured at the NDBC and SCCOOS Pier stations indicating region-wide upwelling events (Figure IV-2). There was one exception in San Pedro, where there was no obvious remotely sensed response to the early May upwelling event. The periods of high chlorophyll exceeded monthly climatic values. The highest remotely sensed chlorophyll concentrations were in the northern SCB (Santa Barbara and Ventura) and concentrations gradually decreased to the south.

The remotely sensed chlorophyll patterns were not consistent across sub-regional areas during periods when regional (bightwide) upwelling events were not observed.

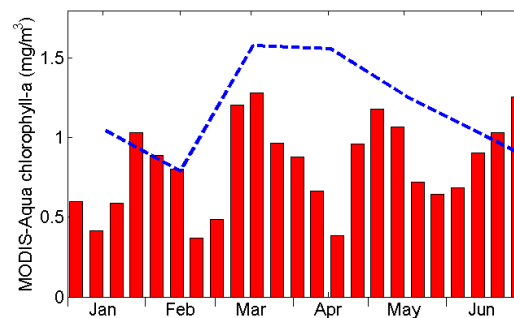


Figure IV-3 Remotely-sensed chlorophyll concentration averaged over open SCB from January through June 2010 (red bars) and monthly climatologies (blue dashed line).

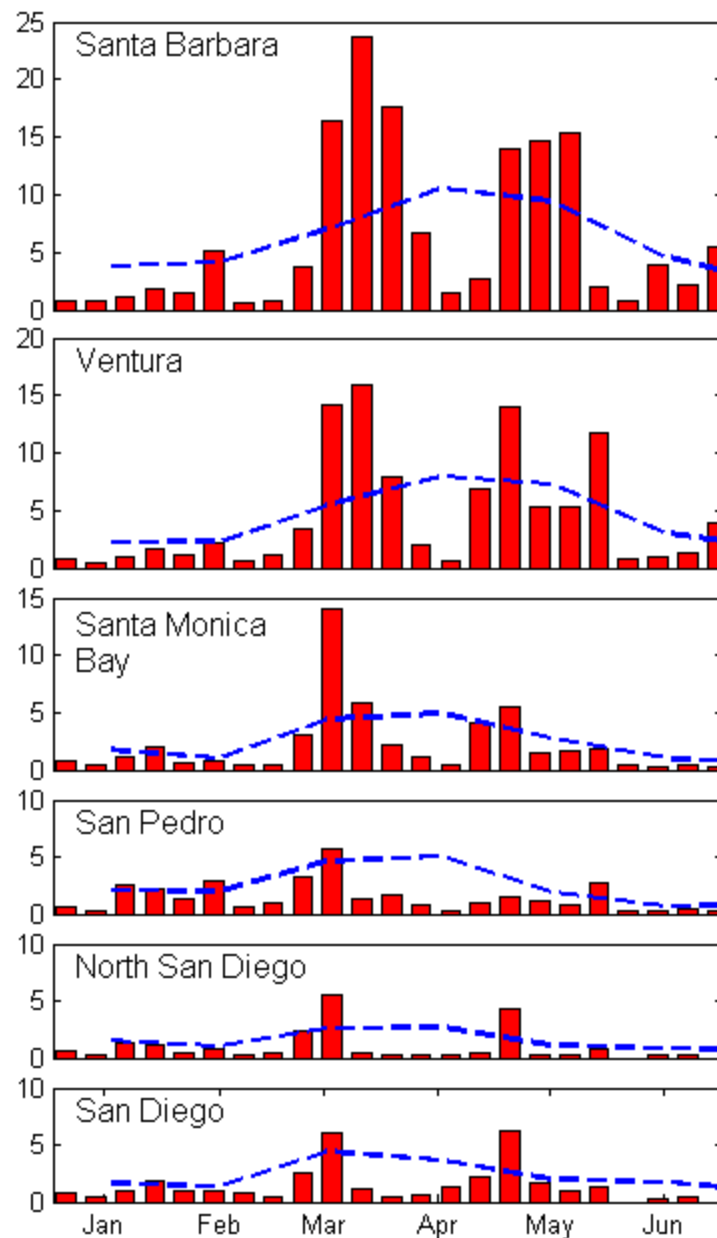


Figure IV-4 Remotely-sensed chlorophyll concentration (mg m^{-3}) for each sub-region from January through June 2010 (red bars) and monthly climatologies (blue dashed line).

Chlorophyll Fluorescence. A comparison using the calibrated chlorophyll fluorescence data from the ship surveys was also conducted. The results are summarized in Figures IV-5 and IV-6. The results of the chlorophyll-*a* analysis from the surface to 50m (Figure IV-5) show that there was relatively low algal biomass in the beginning of April; however, biomass increased across all regions by May after the upwelling event in late April/early May. The results of the analysis of chlorophyll-*a* binned by depth (Figure IV-6) show that across all regions the highest chlorophyll concentrations were in the upper 30m

of the water column. The pattern in the 0-15 m and 15-30 m is very similar to the 0-50 m results, where chlorophyll concentrations increase in the beginning of May in response to a bightwide upwelling event in late April. The 30-45 m binned data do not show as large of a response to the upwelling event. The 45-100 m binned data do not show any change for any of the subregions except Santa Monica Bay.

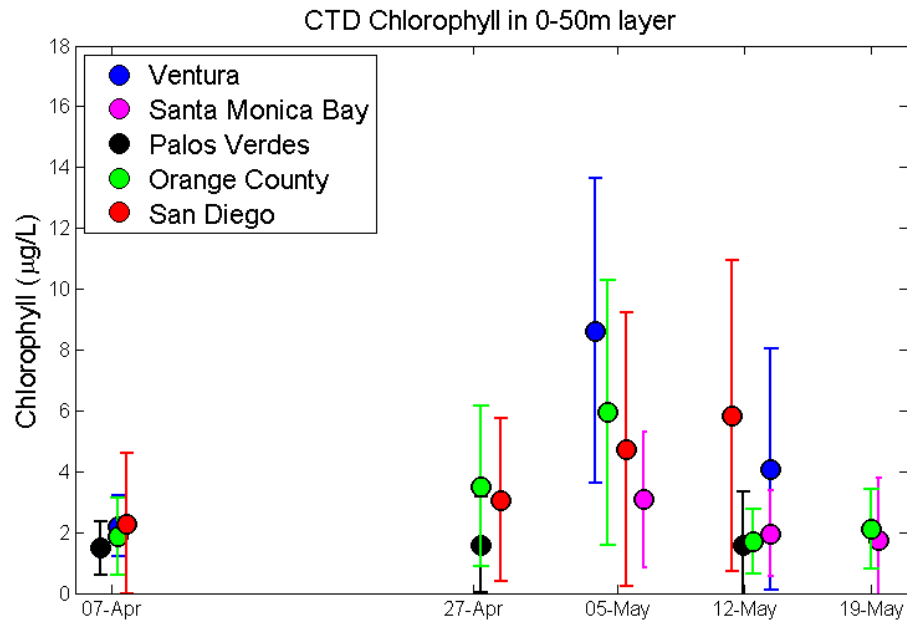


Figure IV-5 Calibrated chlorophyll fluorescence data from the ship surveys averaged for each survey in each subregion for all depths from surface to 50m.

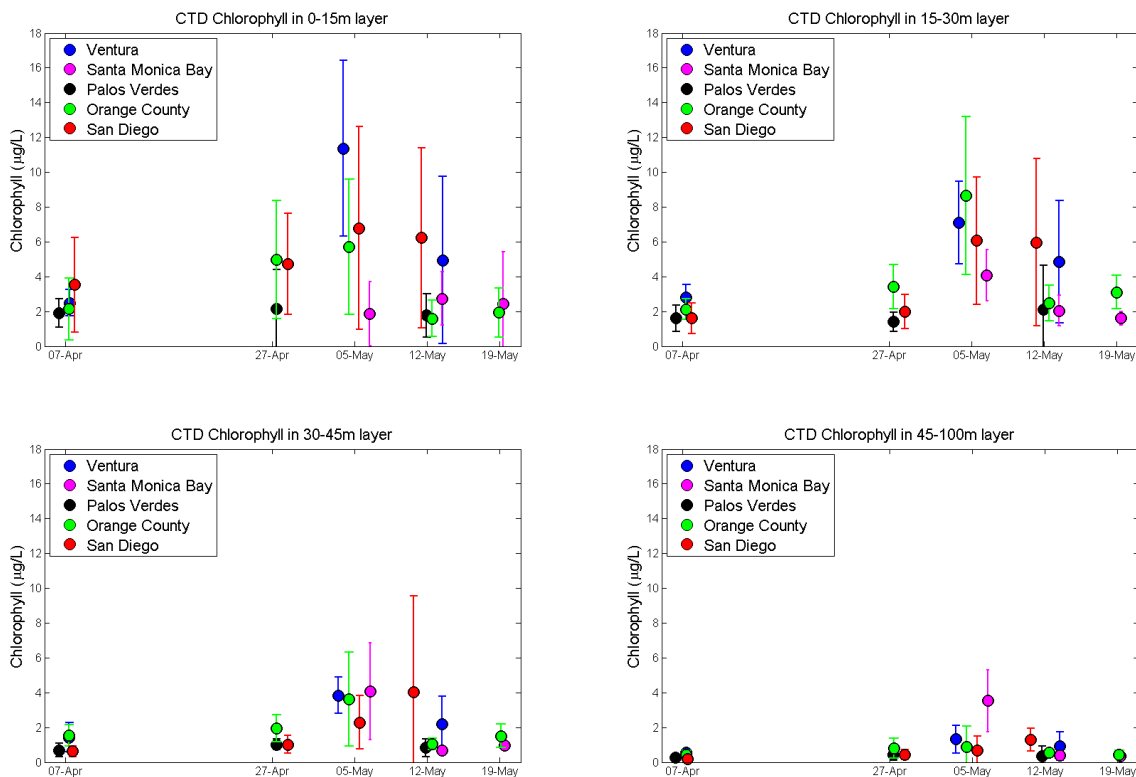


Figure IV-6 Calibrated chlorophyll fluorescence data from the ship surveys averaged for each survey in each subregion for different depths. The top left panel is the surface to 15m averages, the top right panel is the 15-30m chlorophyll-a averages, the lower left panel is the 30-45m chlorophyll-a averages and the lower right panel is the >45m chlorophyll-a averages.

Subregion Results of Observational Measurements

The observational results from the ship surveys, SCCOOS pier sites, and NDBC buoys are summarized for each subregion. Because extensive ship survey data were collected, only the highlights of each sub-regional dataset are presented in this section; the remaining data are presented in Appendix D.

San Pedro Area. San Pedro was the most intensively characterized sub-regional area relative to the other regions due to the presence of the Slocum Webb gliders, Environmental Sample Processors, and additional ship surveys.

March Observations. The observations in March are from the SCCOOS sampling site, Newport Pier, the NDBC buoy, and the ship surveys. The temperatures at Newport Pier dropped slightly on March 5th (down to 14.8°C), on March 9th they slightly decreased again (down to 14.8°C), and on March 10th the lowest temperature was observed of 12.9°C, which was below the 13.5°C trigger temperature (Figure IV-7). There was a simultaneous increase in nitrate (an indication of upwelling) observed from the Newport pier samples from 1.9 µM on March 1 to 5.0 µM on March 8th (Figure IV-8). The total phytoplankton cell

counts increased 12-fold 1 week after the nitrate pulse from 129,992 cells L⁻¹ on March 8 to 1,591,105 cells L⁻¹ on March 15. The phytoplankton community consisted of 99% diatoms, with 14% of the diatom assemblage comprised of *Pseudo-nitzschia* spp.

The ship surveys (both OCSD and LACSD) in March were conducted on March 2 and 3rd and then again three weeks later on March 23rd and 24th; these results are shown in Appendix D. There was a subsurface chlorophyll feature observed in the March 2nd and 3rd survey in Orange County, however, the Los Angeles survey showed low chlorophyll-a and no discernible feature (the raw uncorrected data does exhibit a subsurface feature). The surveys at the end of March showed chlorophyll observed at multiple depths in the LA transects and no discernible features in the Orange County transects.

The nutrient ratios and average nutrient concentrations observed before the upwelling event (pre-upwelling, March 2nd and 3rd) and after the upwelling event (post-upwelling, March 23rd and 24th) are summarized in Table IV-5. The DIN:PO₄ ratios indicate nitrogen limitation, even post upwelling, whereas the SiO₄:PO₄ indicate silicate limitation. The concentrations of all nutrients (except urea) doubled after upwelling events.

Table IV-5 The nutrient ratios and average concentrations summarized for the March surveys pre-upwelling (March 2 & 3, 2010) and post-upwelling (March 23 & 24, 2010) for OCSD and LACSD ship surveys. The Redfield Ratios are listed in parenthesis.

	Nutrient Ratios			Nutrient Concentrations (μM)				
	DIN:PO ₄ (16:1)	DIN:SiO ₄ (16:15)	SiO ₄ :PO ₄ (15:1)	NO _x	NH ₄	Urea	PO ₄	SiO ₄
Pre-upwelling	5.8	1.0	7.3	1.5	0.6	0.6	0.3	2.3
Post-upwelling	8.0	1.3	8.4	3.4	1.2	0.7	0.7	4.8

April and May Observations. In April the Slocum Webb gliders and ESPs were deployed providing intensive coverage in this area. An upwelling event was observed in late April from both the NDBC buoy and Newport Pier temperature data shown in Figure IV-7. At Newport Pier, temperatures changed from approximately 18°C on April 17, 2010 to below 13°C on April 22, 2010 and then briefly warmed until April 30, 2010, when they again dropped below 13°C. The Newport Pier discrete observations, summarized in Figure IV-8, showed a corresponding peak in nitrate on April 26 of 7.0 μM, another indication of an upwelling event. Chlorophyll concentrations increased simultaneously with nitrate, from 3.7 μg L⁻¹ on April 18, 2010 to 11.42 μg L⁻¹ on April 26, 2010. Consistent with chlorophyll observations, the total phytoplankton cell counts increased simultaneously with nitrate concentrations, from 72,796 cells L⁻¹ on April 18, 2010 to 563,299 cells L⁻¹ on April 26, 2010, a 7-fold increase. The phytoplankton community was dominated by diatoms (74%), and *Pseudo-nitzschia* spp. comprised 31% of those diatoms on April 26, 2010. By May 3, 2010, *Pseudo-nitzschia* spp. became 49% of the diatom assemblage and then dissipated by May 24, 2010 when no *Pseudo-nitzschia* spp. were detected at the Newport Pier.

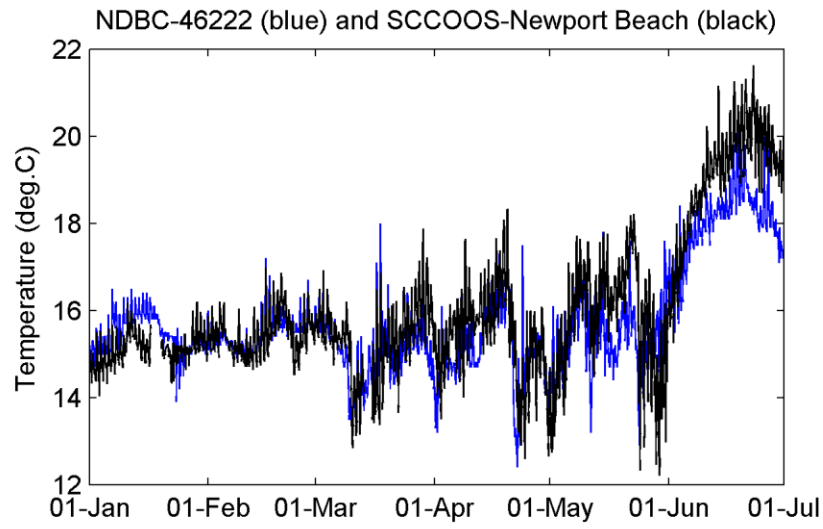


Figure IV-7 Temperature observations from the NDBC buoy and the Newport Pier in 2010.

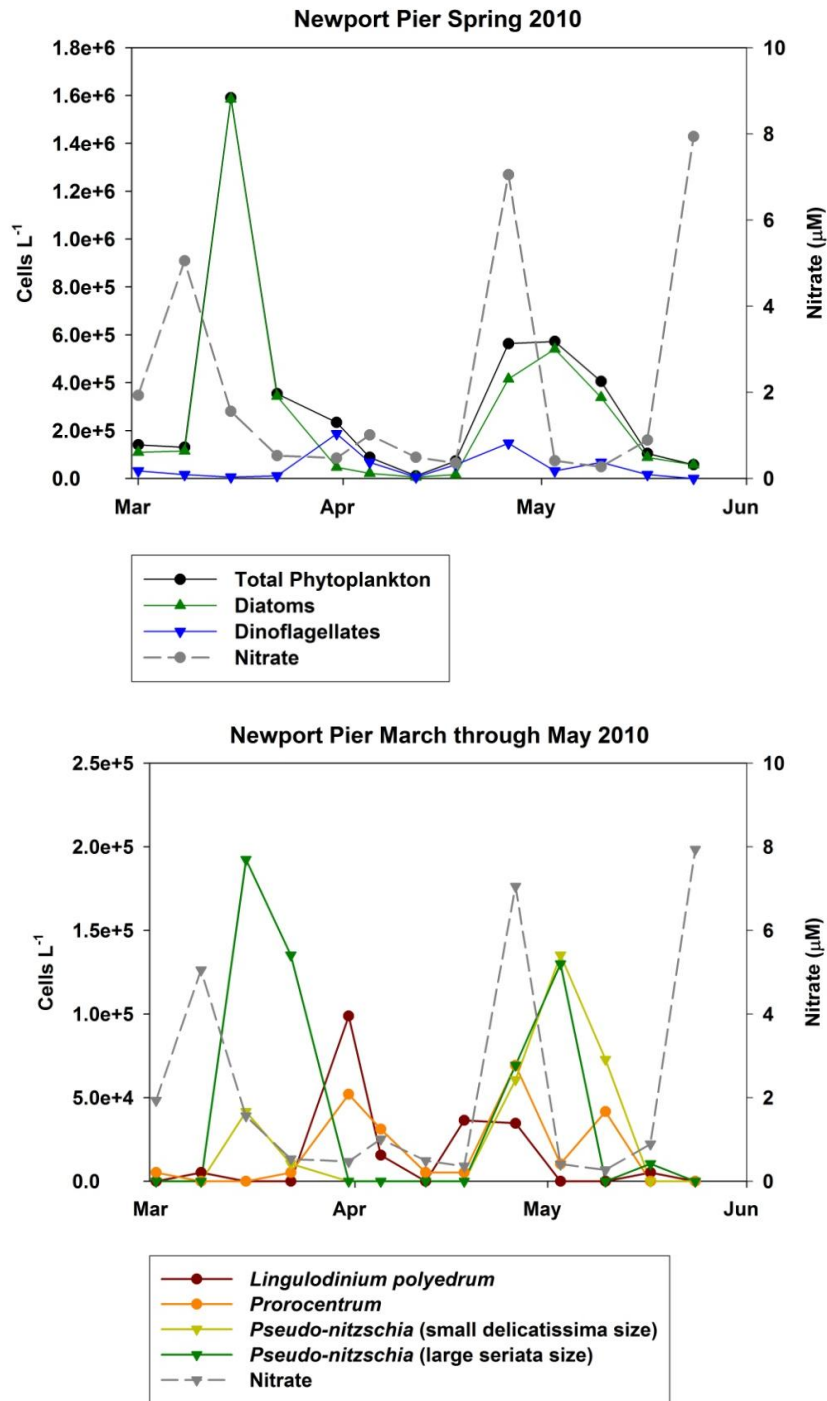


Figure IV-8 SCCOOS Newport Pier data summarized for the spring of 2010. The top graph shows cell counts), and the bottom graph summarizes the HAB species cell counts and nitrate concentrations.

The glider observations of these oceanographic dynamics began on April 23, 2010 (the gliders were recovered for calibration during the majority of mid-April). Figure IV-9 summarizes the glider results for late April and early May. The first time period, April 23-27, 2010, was characterized by a stratified water

column with highest temperatures at the surface and colder temperatures in the subsurface layers, indicating a non-upwelling period. There was a strong subsurface chlorophyll signature observed indicating high algal biomass. The April 28-May 2, 2010 time period showed an upwelling event indicated by the low observed temperatures observed inshore and in surface waters, a decrease from the April 23-27th time period. There was also a corresponding high chlorophyll signal at the surface and inshore. By May 3-7, 2010, a relaxation event was observed by the stratified water column and high chlorophyll detected across a larger area in the surface waters.

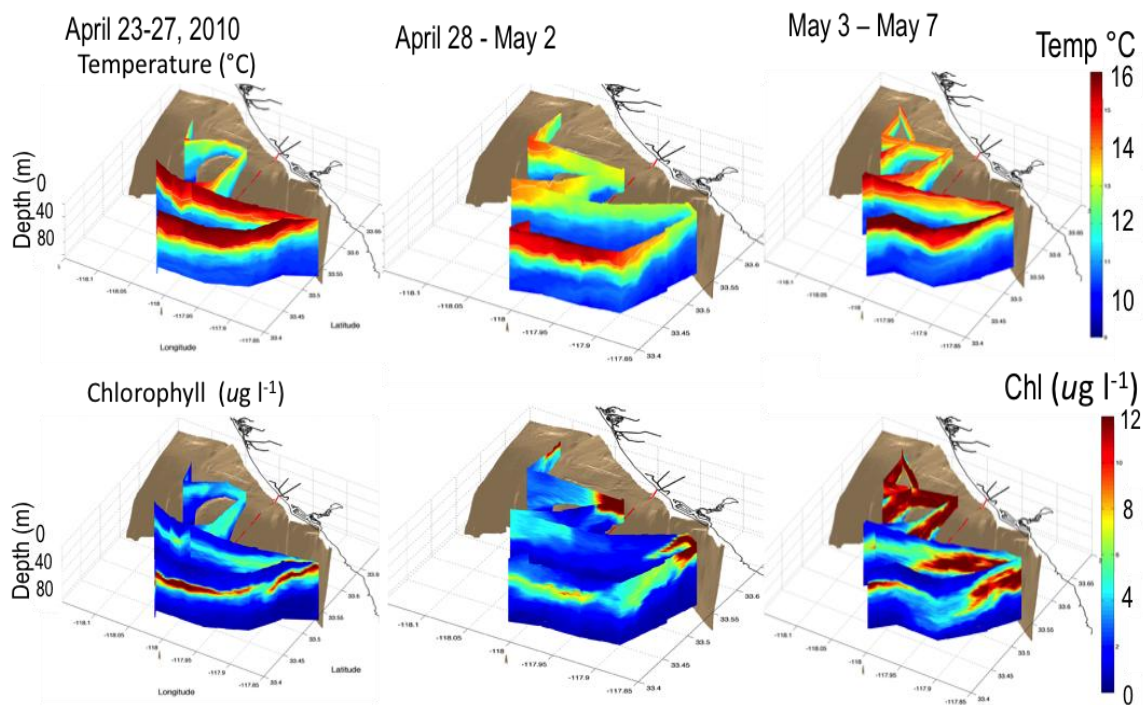


Figure IV-9 Glider Observations in late April and early May. The glider moved in a zig-zag pattern up the coast with LA harbor to the north (but not shown) and Newport to the east (shown). Temperature is shown in the top panel and chlorophyll fluorescence data is shown in the bottom panel.

There were three ship surveys conducted in Orange County (but not Los Angeles County) that coincided with the glider observations in the late April to early May time period. The ship survey results for temperature and chlorophyll-*a* are summarized in Figure IV-10, and all other observations are summarized in Appendix D. The ship survey data show similar patterns as the glider. On April 20, 2010 the temperature data show a stratified water column and a subsurface chlorophyll signature, though the concentrations were lower than those observed by the glider on April 23, 2010. By April 27, 2010, the decreased surface temperatures indicated an upwelling event and the corresponding high chlorophyll signature had moved inshore and into surface waters. By May 4, 2010, a relaxation event was characterized by the stratified water column and increased concentration and geographic extent of chlorophyll. By the May 12, 2010 survey, the algal bloom had dissipated (see Appendix D).

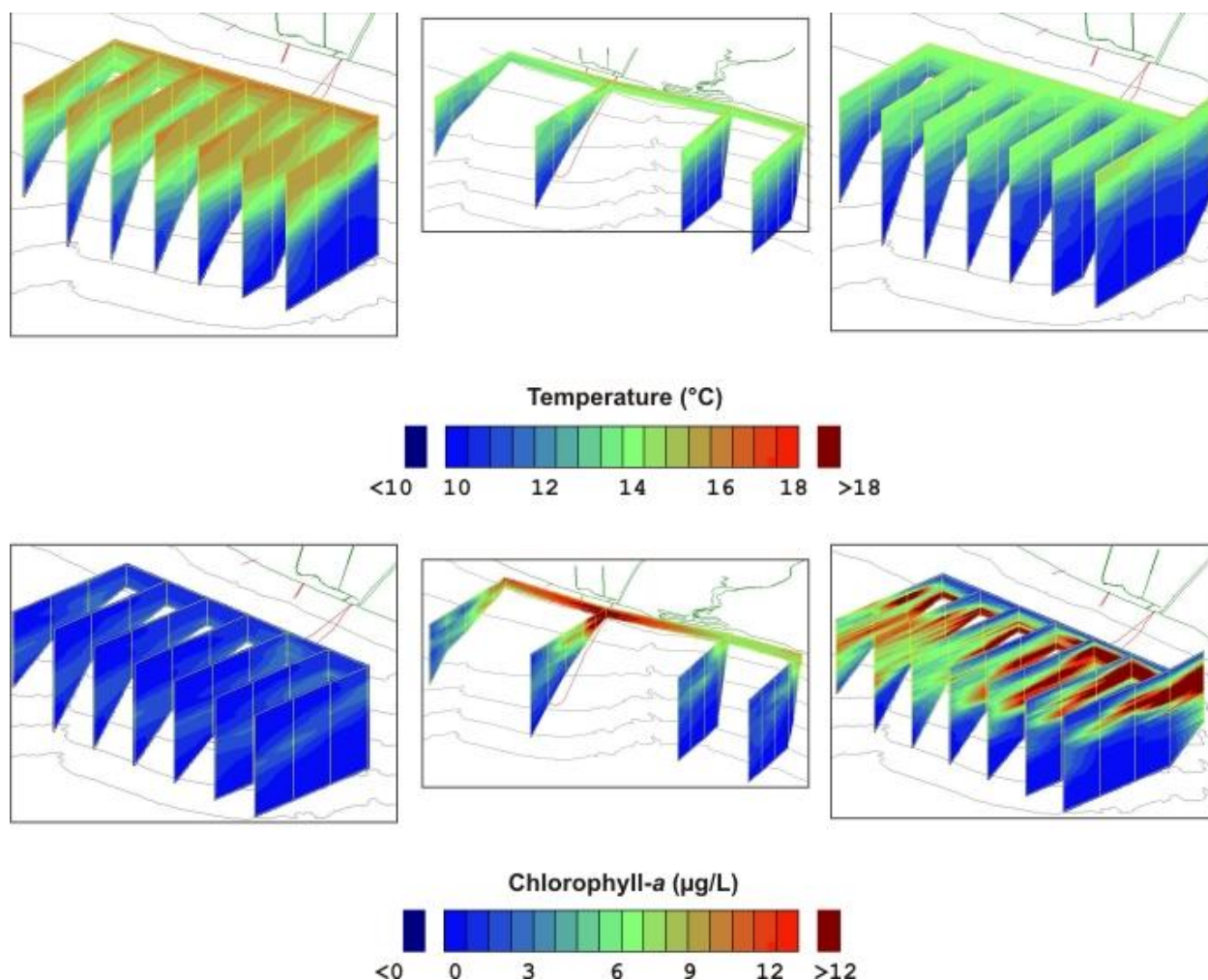


Figure IV-10 Temperature (top panel) and chlorophyll fluorescence (bottom panel) from ship surveys in April and May. Images on the left reflect data collected from the April 20, 2010 survey, middle images reflect data collected from the April 27, 2010 survey, and images on the right reflect data collected from the May 4, 2010 survey.

Nutrient ratios and concentrations are summarized in Table IV-6. Nutrient ratios indicated nitrogen limitation for DIN:PO₄ and DIN:SIO₄, and SIO₄ limitation before and after upwelling. Chlorophyll-*a* concentrations increased 2.7-fold with upwelling and continued to increase by 1.2-fold during the relaxation period. Nitrate, phosphate and silicate concentrations increased with upwelling, then decreased with the relaxation event, whereas ammonium and urea concentrations decreased throughout the observational period. Urea concentrations ranged from below the level of detection to 5.6 µM.

Domoic acid concentrations measured for all surveys in the San Pedro area ranged from below the level of detection (0.02 µg L⁻¹) to 1.5 µg L⁻¹ (except for 1 sample that measured 4.6 µg L⁻¹ collected on May 12,

2010 from station number 2504). These are extremely low concentrations as the maxima observed in other years (2003 to 2011) in this area range from 3 - 52 $\mu\text{g L}^{-1}$ (D. Caron, unpublished data).

Table IV-6 Average nutrient ratios, nutrient concentrations, and discrete chlorophyll-a concentrations summarized for the pre-upwelling (April 20, 2010), post-upwelling (April 27, 2010), and relaxation (May 4, 2010) events during the Orange County surveys. The Redfield ratios are listed in parenthesis.

	Chlorophyll	Nutrient Ratios			Nutrient Concentrations (μM)				
	Chl ($\mu\text{g L}^{-1}$)	DIN:PO ₄ (16:1)	DIN:SIO ₄ (16:15)	SIO ₄ :PO ₄ (15:1)	NO _x	NH ₄	Urea	PO ₄	SIO ₄
Pre-upwelling	2.5	7.3	0.8	11.6	3.1	1.0	0.8	0.4	5.2
Post-upwelling	6.8	9.7	0.7	13.8	5.0	0.7	0.3	0.5	7.4
Relaxation	8.4	6.7	0.7	9.9	2.1	0.5	*	0.3	2.6

*No urea samples were collected on the May 4, 2010 survey.

The two ESPs were deployed during April and observed the upwelling events as well as an increase in *Pseudo-nitzschia* (*P. multiseriis/pseudodelicatissima* probe signal; Figure IV-11). The offshore ESP, (7 km offshore), observed a short and mild upwelling event that began on April 21, 2010, but temperatures only fell below 12°C for 1 day. The detection of *P. multiseriis/pseudodelicatissima* corresponded with the initial upwelling signal on April 21, 2010 and steadily increased until the ESP stopped sampling on April 24, 2010. The nearshore ESP, (4 km from shore), showed a temperature drop from 15.5°C to below 12°C on April 20, 2010 and a relaxation event of warmer temperatures by April 23, 2010. *Pseudo-nitzschia* spp. was observed on April 25, 2010, a 3 day lag from the observed upwelling event, with an estimated 2,552 cells L^{-1} . *Pseudo-nitzschia* cells steadily increased until the ESPs were removed on April 28, 2010 with over 51,111 cells L^{-1} , a 20-fold increase in 3 days. Domoic acid was detected in the nearshore ESP with very low concentrations of 0.001 $\mu\text{g L}^{-1}$ on April 25, 2010 and April 26, 2010 and a 30-fold higher concentration of 0.03 $\mu\text{g L}^{-1}$ on April 27, 2010.

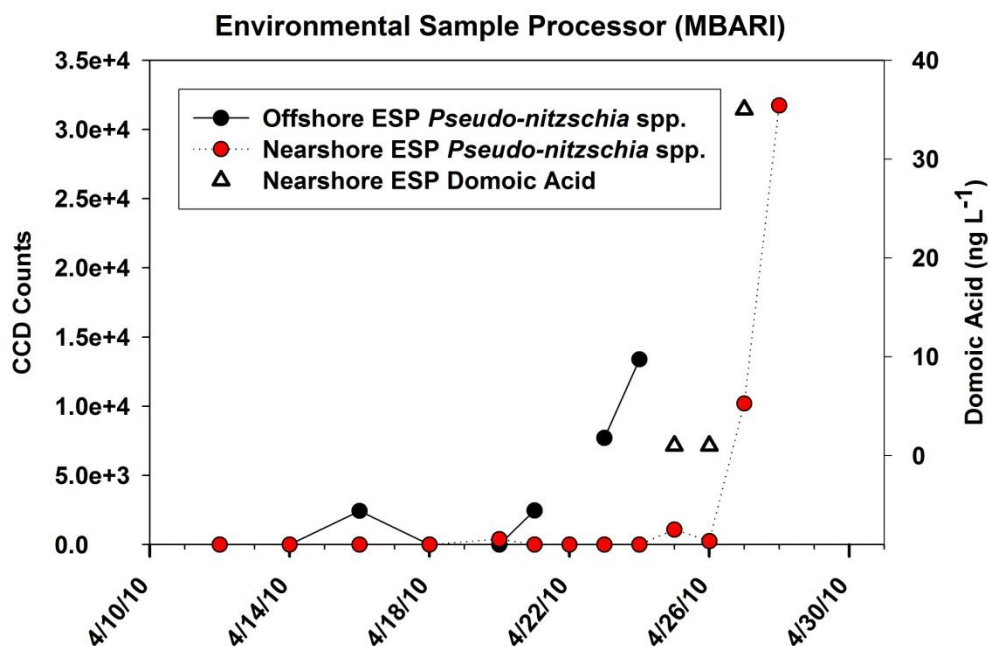


Figure IV-11 Offshore and nearshore Environmental Sample Processor (ESP) data collected in April 2010.

San Diego Area. The San Diego area observations are similar to the San Pedro subregion results in that there was an observed subsurface high chlorophyll feature followed by an upwelling event that transported algal populations into surface waters.

A mild drop in temperature was observed on March 11, 2010 at both the NDBC buoy (down to 14.8°C) and the Scripps Automated Pier sensor (down to 13.7°C). These observations are summarized in Figure IV-12.

The ship survey conducted on March 1 and 2, 2010, prior to the upwelling event, showed a stratified water column (warmest temperatures at the surface with colder temperatures at deeper depths) and a corresponding subsurface chlorophyll signature derived from the inshore surface signature (summarized in Figure IV-13). After the upwelling event, colder temperatures and a high chlorophyll signature at the surface were observed at the surface in the March 12, 2010 survey. These observations, summarized in Figure IV-13, are reflective of the corresponding mild upwelling event observed in the continuous data followed by the high chlorophyll signature at the surface.

The corresponding Scripps pier data from the same time-period (Figure IV-14) showed an increase in nitrate concentrations at the pier from 0.09 μM on March 8th to 2.0 μM on March 15th. The phytoplankton cell counts at Scripps Pier increased 5-fold simultaneously with nitrate concentrations (March 15th) and with 67% of the assemblage made up of dinoflagellates. Phytoplankton abundances continued to increase 1-2 weeks after the initial upwelling event (361,176 cells L^{-1} on March 18 and

453,031 cells L⁻¹ on March 22nd). The HAB species also increased simultaneously with nitrate concentrations as the dinoflagellates, *Lingulodinium polyedrum* and *Prorocentrum* increased (11.6-fold 105-fold respectively), while the diatom *Pseudo-nitzschia* was relatively unchanged, suggesting the subsurface algal population was mostly comprised of the harmful dinoflagellates, *Lingulodinium polyedrum* and *Prorocentrum* spp.

The April and May ship survey data is shown in Appendix D, and the Scripps Pier data documenting a red tide comprised of *Lingulodinium polyedrum* that began in mid-April and continued through mid-June is shown in Figure IV-14.

The nutrient ratios determined from the ship survey observations show nitrogen limitation and slight silicate limitation. Nutrient ratios and concentrations are summarized in Table IV-8. Urea concentrations ranged from below the level of detection to 6.9 µM. Domoic acid concentrations ranged from below the limit of detection to 1.0 µg L⁻¹, except one station (I37), where 2.95 1.0 µg L⁻¹ was detected on May 5, 2010.

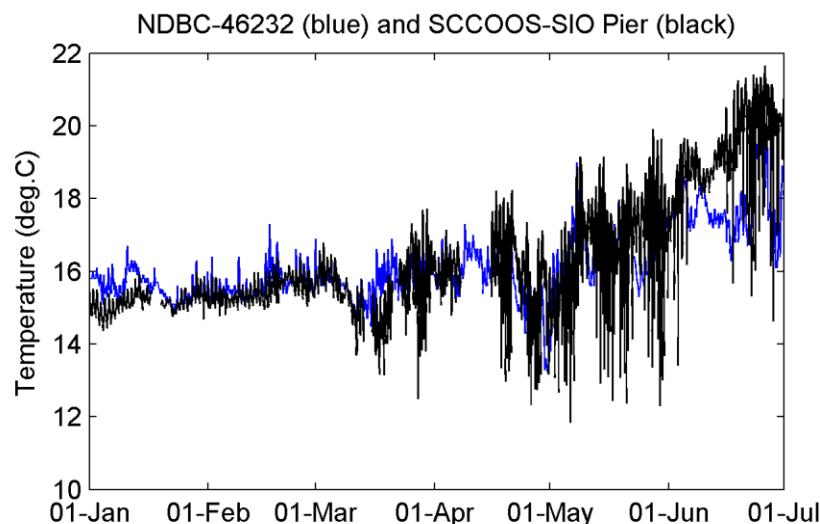


Figure IV-12 Temperature observations from the NDBC buoy and at the Scripps Institute of Oceanography (SIO) Pier.

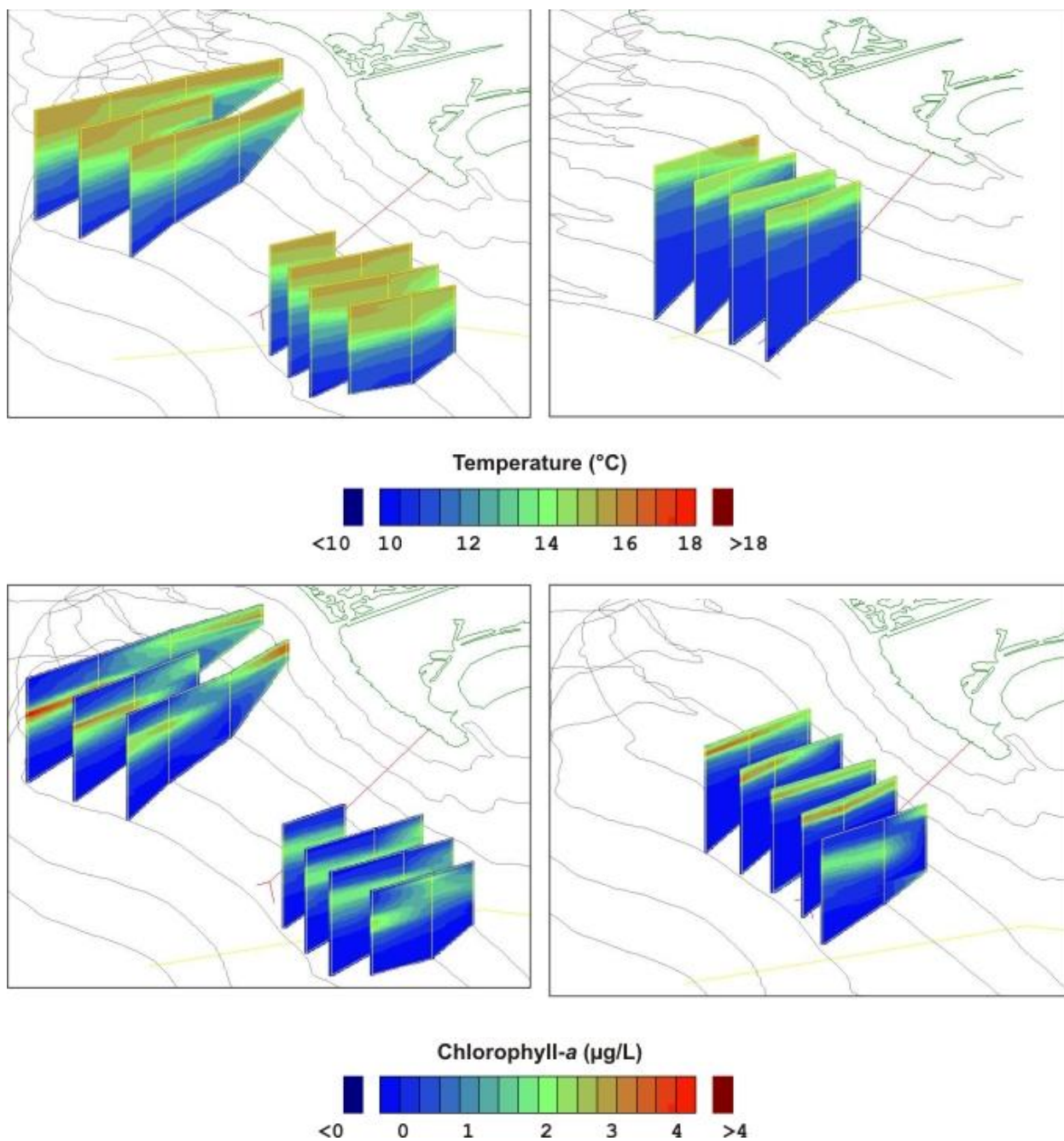


Figure IV-13 Ship-based observations for . temperature (0-18°C; top panel) and chlorophyll (scale range from 0-4 $\mu\text{g L}^{-1}$; bottom panel). Images on the left reflect observations from the March 1-2, 2010 survey, and images on the right reflect observations from the March 12, 2010 survey.

Table IV-7 Nutrient ratios and average concentrations summarized for the March surveys pre-upwelling (March 1 and 2, 2010) and post-upwelling (March 12, 2010). The Redfield Ratios are listed in parenthesis.

	Nutrient Ratios			Nutrient Concentrations (μM)				
	DIN:PO ₄ (16:1)	DIN:SiO ₄ (16:15)	SiO ₄ :PO ₄ (15:1)	NO _x	NH ₄	Urea	PO ₄	SiO ₄
Pre-upwelling	3.7	0.8	9.0	0.8	0.5	0.9	0.3	2.9
Post-upwelling	9.3	0.9	9.9	2.2	0.2	1.0	0.3	3.5

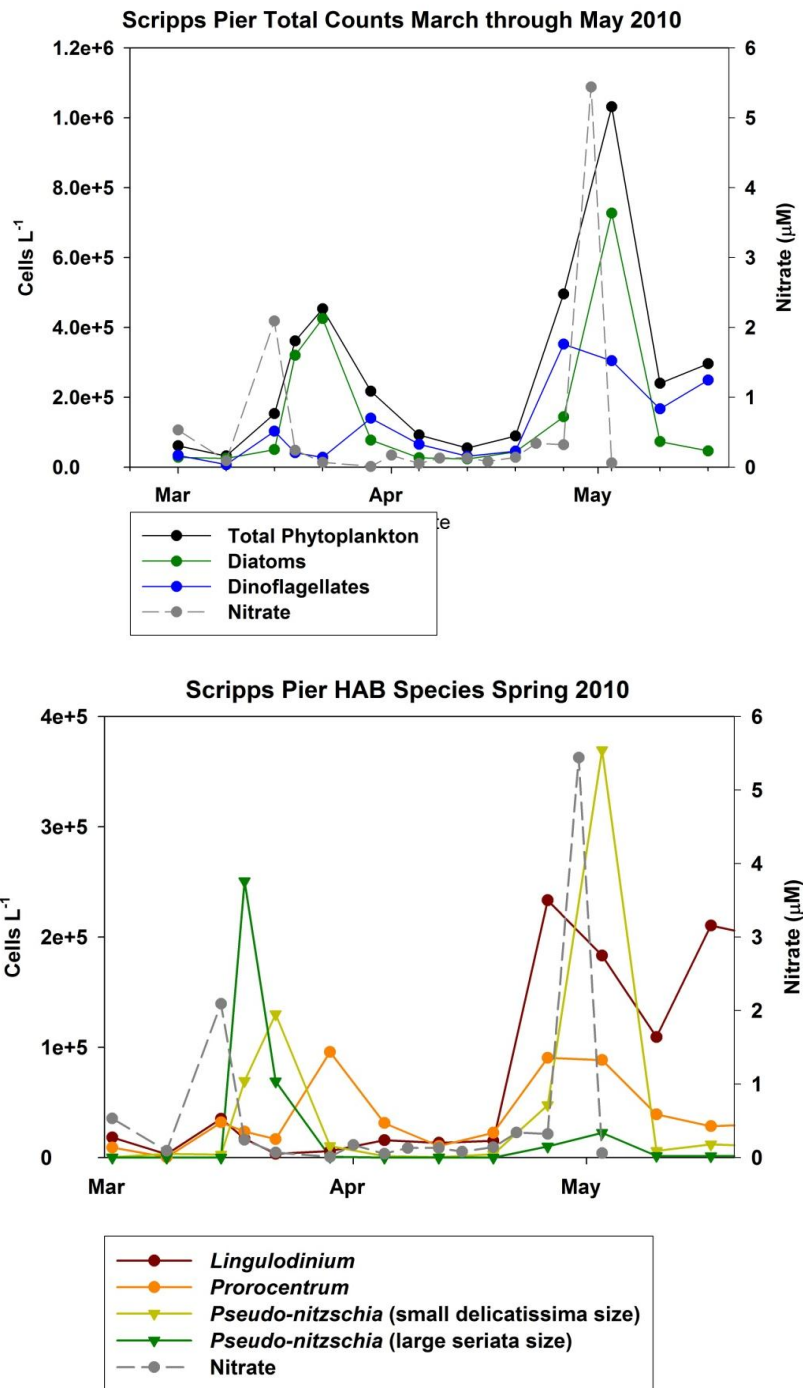


Figure IV-14 SCCOOS Scripps Institute of Oceanography (SIO) Pier data summarized for the spring of 2010. The top image shows respective assemblage cell counts and nitrate concentrations; the bottom panel shows HAB species cell counts and nitrate concentrations.

Santa Monica Bay. The ship surveys in Santa Monica Bay were not conducted following oceanographic triggers due to logistical issues and shared equipment. Therefore, these surveys did not capture as many oceanographic features as the ship surveys in other regions. Additionally, the event surveys were designed to be 1-day surveys that collected data from the main areas in SMB with anthropogenic inputs such as the effluent outfall pipe and the major rivers. Therefore, a smaller number of transects covering a large spatial area was deemed to be the appropriate design. In hindsight, the datasets produced by this study design were difficult to interpret as there were not many data points and there were large geographic distances between transects.

In March, there was a drop in temperature that began on March 9, 2010 and reached a low on March 11, 2010 (12.2°C at the Santa Monica Pier and 13.5°C from the NDBC buoy) as shown in Figure IV-15. The corresponding ship survey data showed higher chlorophyll fluorescence signatures from the March 15th survey when compared with surveys on March 5, 8, and 12, 2010 as shown in Figures IV-17 and IV-18.

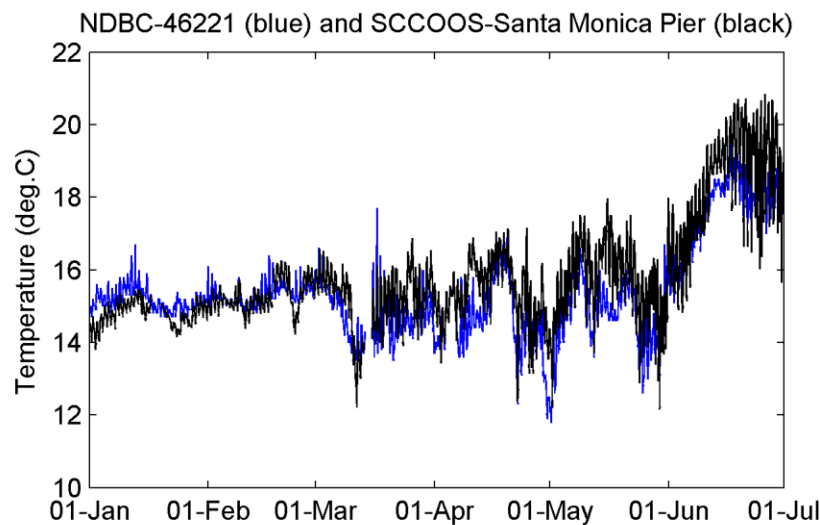


Figure IV-15 Temperature observations from the NDBC buoy and at the Santa Monica Pier.

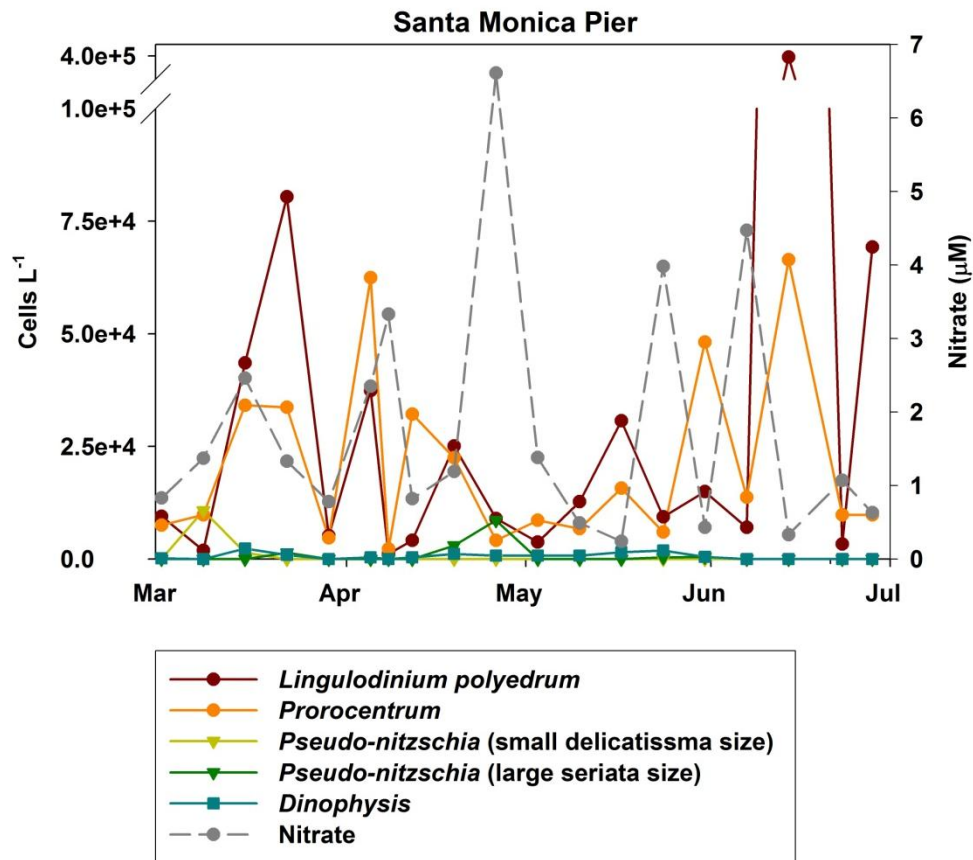


Figure IV-16 SCCOOS Santa Monica Bay Pier data summarized for the spring of 2010, including HAB species cell counts and nitrate concentrations.

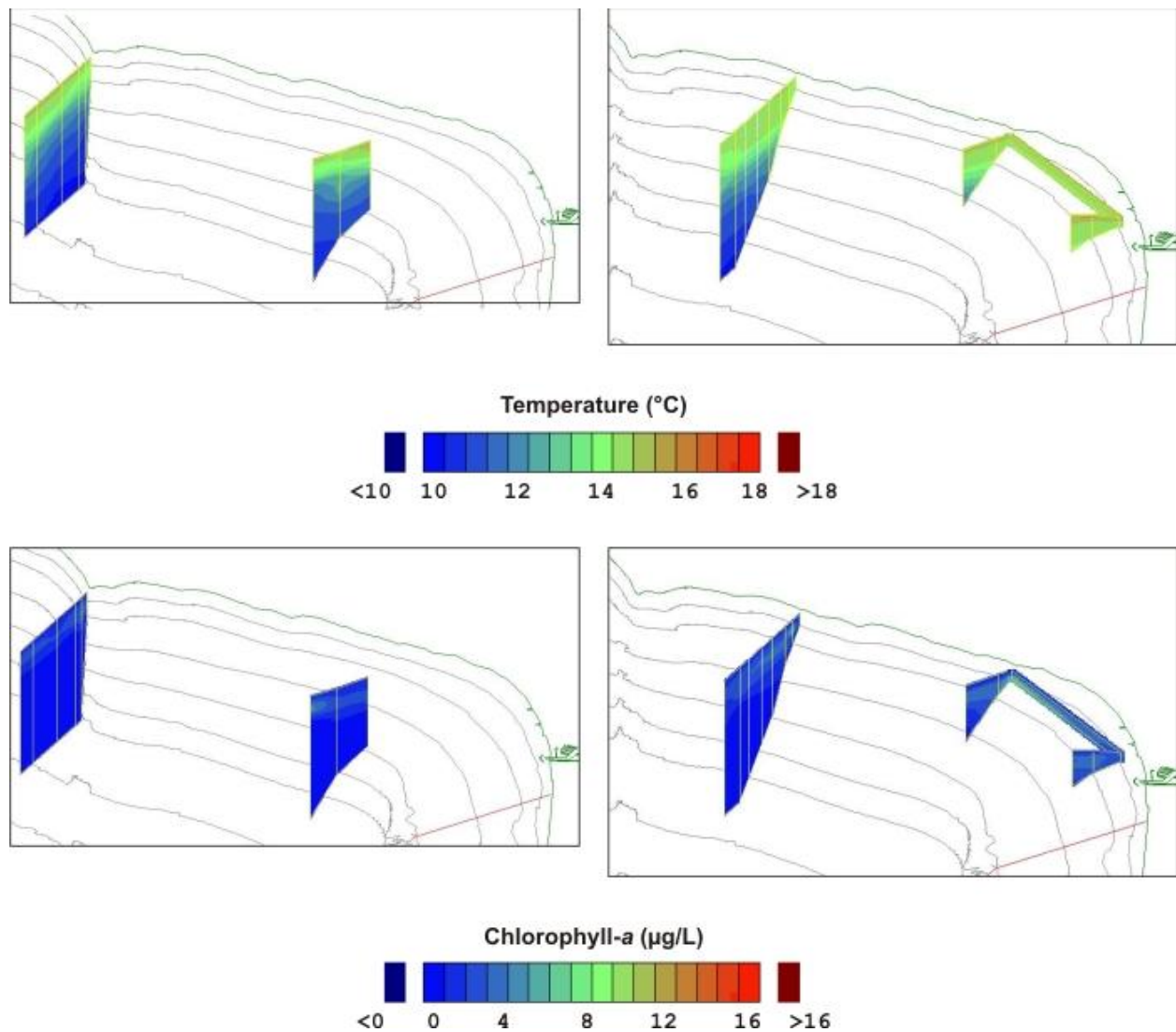


Figure IV-17 The temperature (top panel) and calibrated chlorophyll fluorescence (bottom panel) from the ship surveys in March before the observed upwelling event. Images on the left reflect observations from the March 5, 2010 survey, and images on the right reflect observations from the March 8, 2010 survey.

The Santa Monica Pier data (Figure IV-16) showed increasing nitrate concentrations for several consecutive weeks with the peak of 2.4 μM on March 15, 2010. The corresponding HAB species counts increased 3-fold from March 8th to the 15th, with the bulk of the assemblage consisting of the red tide forming dinoflagellates, *Lingulodinium polyedrum* (increased 23-fold) and *Prorocentrum* (increased 3-fold). There was no total phytoplankton, total diatoms or total dinoflagellate information obtained at this pier.

The nutrient ratios showed nitrogen and silicate limitation. The urea concentrations ranged from below the level of detection to 2.3 μM . The domoic acid concentrations were the lowest of all of the sub-regions ranging from below the limit of detection to 0.1 $\mu\text{g L}^{-1}$, which was consistent with the SMB pier observations.

In May, there was a decrease in temperature that began on April 30, 2010 and minimum temperatures were observed on May 1, 2010, 11.8°C at the NDBC buoy and 12.2°C at the Santa Monica Pier, as shown in Figure IV-16. The ship survey was conducted a week after the upwelling event and the water column had stratified and there was a distinct chlorophyll signature in the subsurface region (Appendix D).

Table IV-8 Nutrient ratios and concentrations summarized for the March surveys pre-upwelling (March 5 and 8, 2010) and post-upwelling (March 12 and 15, 2010). Optimum growth ratios are listed in parenthesis.

	Nutrient Ratios			Nutrient Concentrations (μM)				
	DIN:PO ₄ (16:1)	DIN:SiO ₄ (16:15)	SiO ₄ :PO ₄ (15:1)	NO _x	NH ₄	Urea	PO ₄	SiO ₄
Pre-upwelling	3.0	0.6	8.7	1.2	2.0	0.2	0.3	3.0
Post-upwelling	8.7	1.0	10.2	5.6	7.1	0.4	0.6	6.3

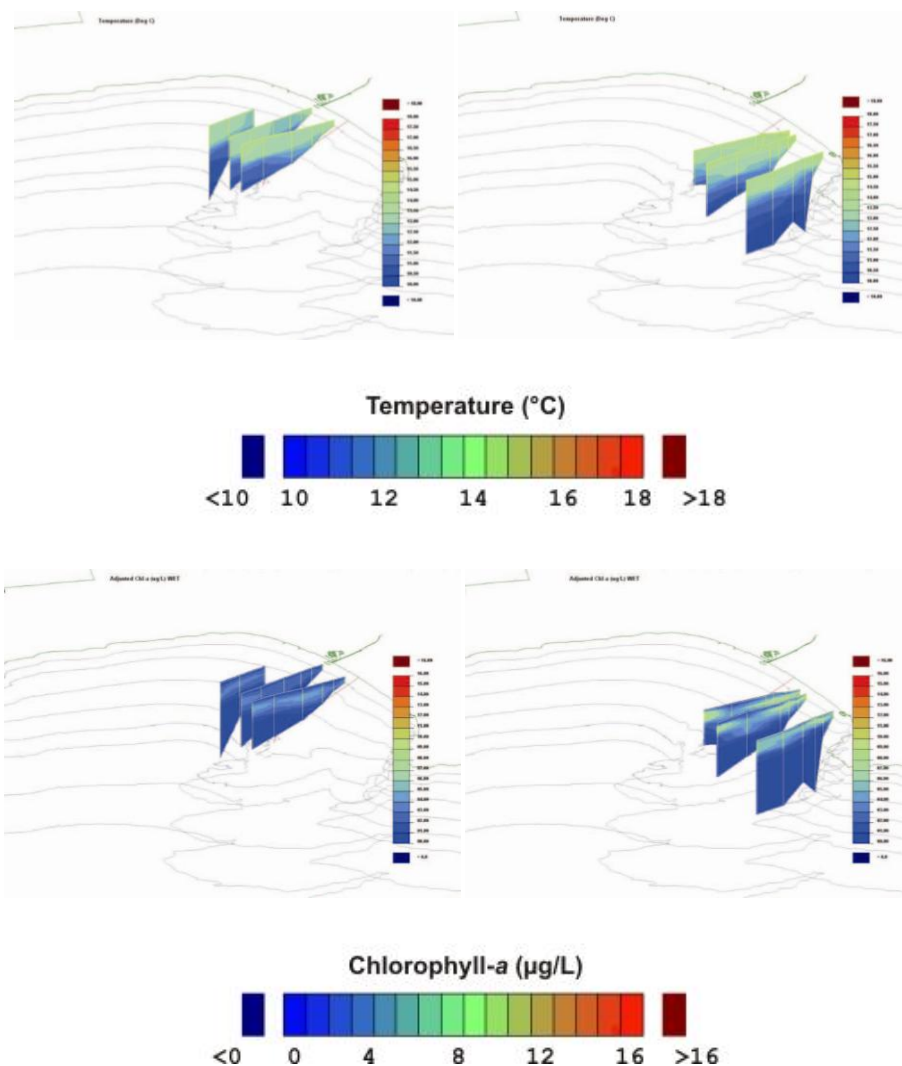


Figure IV-18 Temperature (top panel) and calibrated chlorophyll fluorescence (bottom panel) from the ship surveys in March after the observed upwelling event. Images on the left reflect observations from the March 12, 2010 survey, and images on the right reflect observations from the March 15, 2010 survey.

Ventura Results. The Ventura area had different patterns of oceanographic conditions than the other areas in this study. The temperature decreased in mid-March and reached the lowest value of 11.8°C on March 12, 2010 (Figure IV-19). The temperature and chlorophyll observations from the pre-upwelling ship surveys from March 1 through 3, 2010 showed a stratified water column and low chlorophyll signatures at the surface and at depth in the northern transects. The southern transects showed less chlorophyll compared to the northern transects. These results are summarized in Figure IV-20. There were two surveys after the observed upwelling event, one 10 days later on March 23 and 24, 2010, and the other 2 weeks later on April 7 and 9, 2010 (Appendix D). The general temperature and chlorophyll features were similar for these surveys in that there was a stratified water column and high chlorophyll

signature in the northern transects, close to the mouth of the Santa Clara River, and relatively less chlorophyll in the southern transects by Calleguas Creek.

Another upwelling event was observed beginning on April 30, 2010 with temperatures reaching a low on May 1, 2010 of 11.2°C (Figure IV-19). The temperature showed a mixed water column (i.e. similar temperatures throughout) and very high chlorophyll signatures, particularly in the northern transects, Figure IV-21. There was another temperature drop beginning on May 9th with the lowest temperatures observed on May 11th, at 11.5°C. The ship survey 2 days later (May 13th through 15th) showed a mixed water column in the northern transects but more stratification in the southern transects. The corresponding chlorophyll observations showed very high concentrations in the northern transects and low concentrations in the southern transects.

Nutrient ratios were predominantly silicate and nitrogen limited. The urea concentrations ranged from below the level of detection to 9.9 µM. Domoic acid concentrations were also extremely low in this area, from below the limit of detection to 1.5 µg L⁻¹.

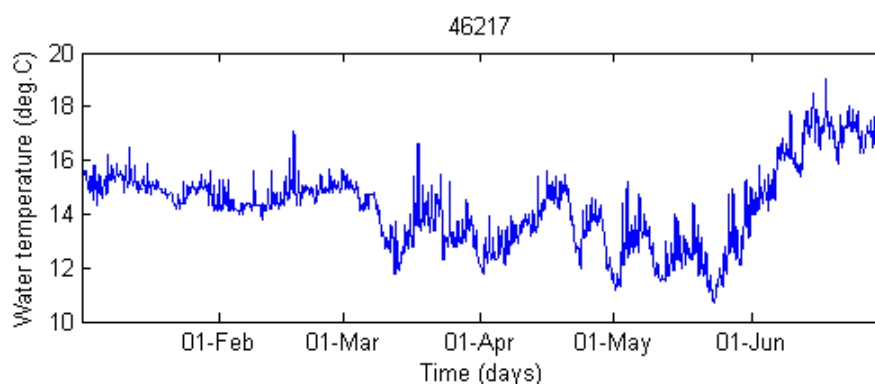


Figure IV-19 Temperature observations from the NDBC buoy in Ventura.

There was no SCCOOS pier station located in Ventura, however a comparison was made to the Stearn's Wharf measurements in Santa Barbara (Figure IV-22). There was no temperature data available during the study period from the automated shore system however, the observed nitrate pulses, usually an indication of an upwelling event, showed maximum concentrations on March 15, 2010 (8.4 µM) and April 15, 2010 (11.9 µM). Interestingly, there was a simultaneous increase in *Pseudo-nitzschia* abundance with nitrate on March 15, 2010, but no observed HAB abundance increases in April (Figure IV-22). While the March 15, 2010 nitrate pulse occurred at the same time as the low temperatures observed from the NDBC buoy in Ventura, there was no observed decrease in temperatures in Ventura in mid-April. Due to the complex physical circulation patterns in the northern SCB, the Stearn's Wharf location did not complement the Ventura region of ship surveys due to the large spatial distance between areas.

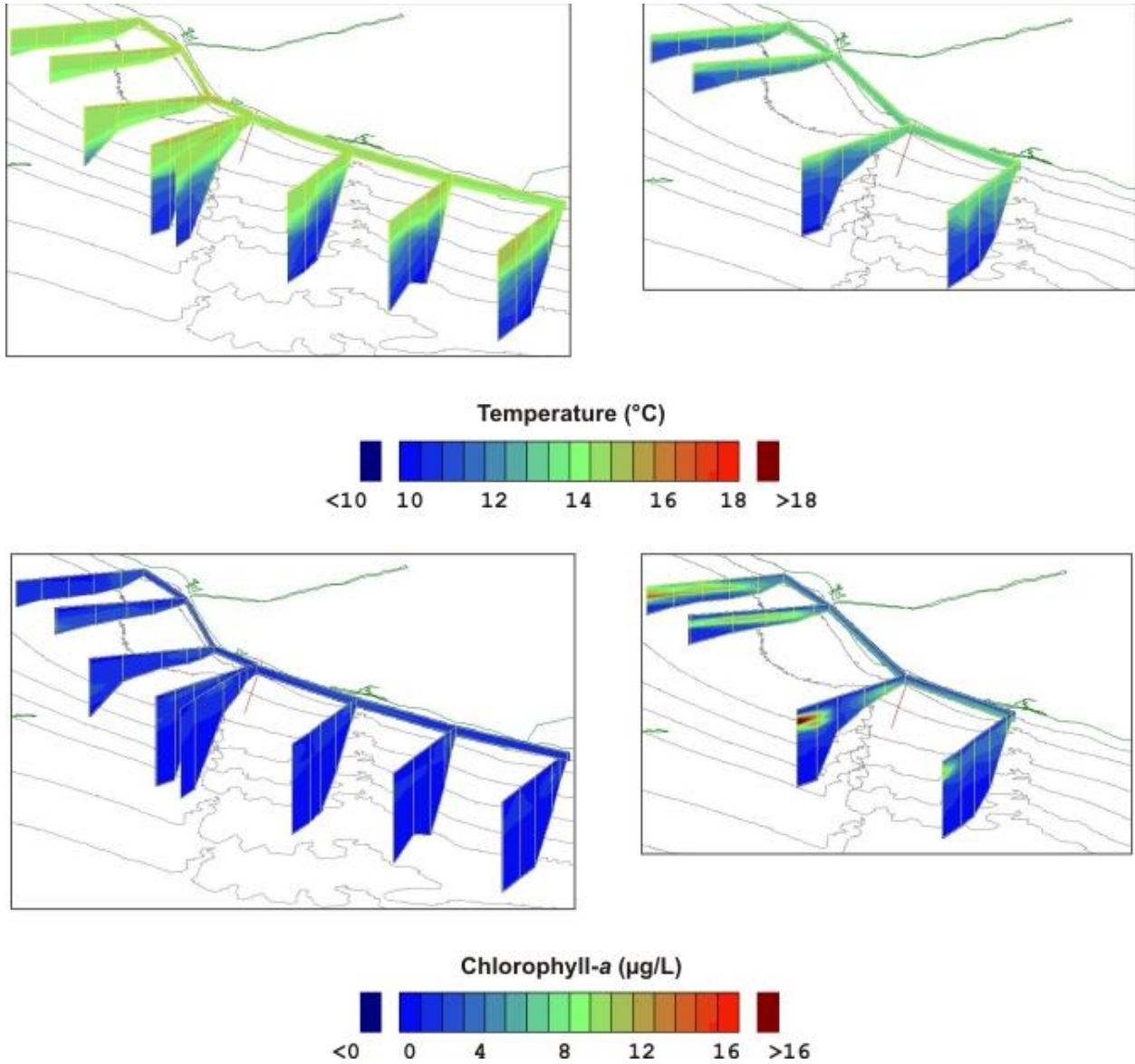


Figure IV-20 Temperature and chlorophyll fluorescence from the ship surveys in Ventura in March. The top panel summarizes temperatures and the bottom panel summarizes chlorophyll fluorescence observations. Images on the left reflect observations from the March 1-3, 2010 ship survey, and images on the right reflect the observations from the March 23-24, 2010 ship survey.

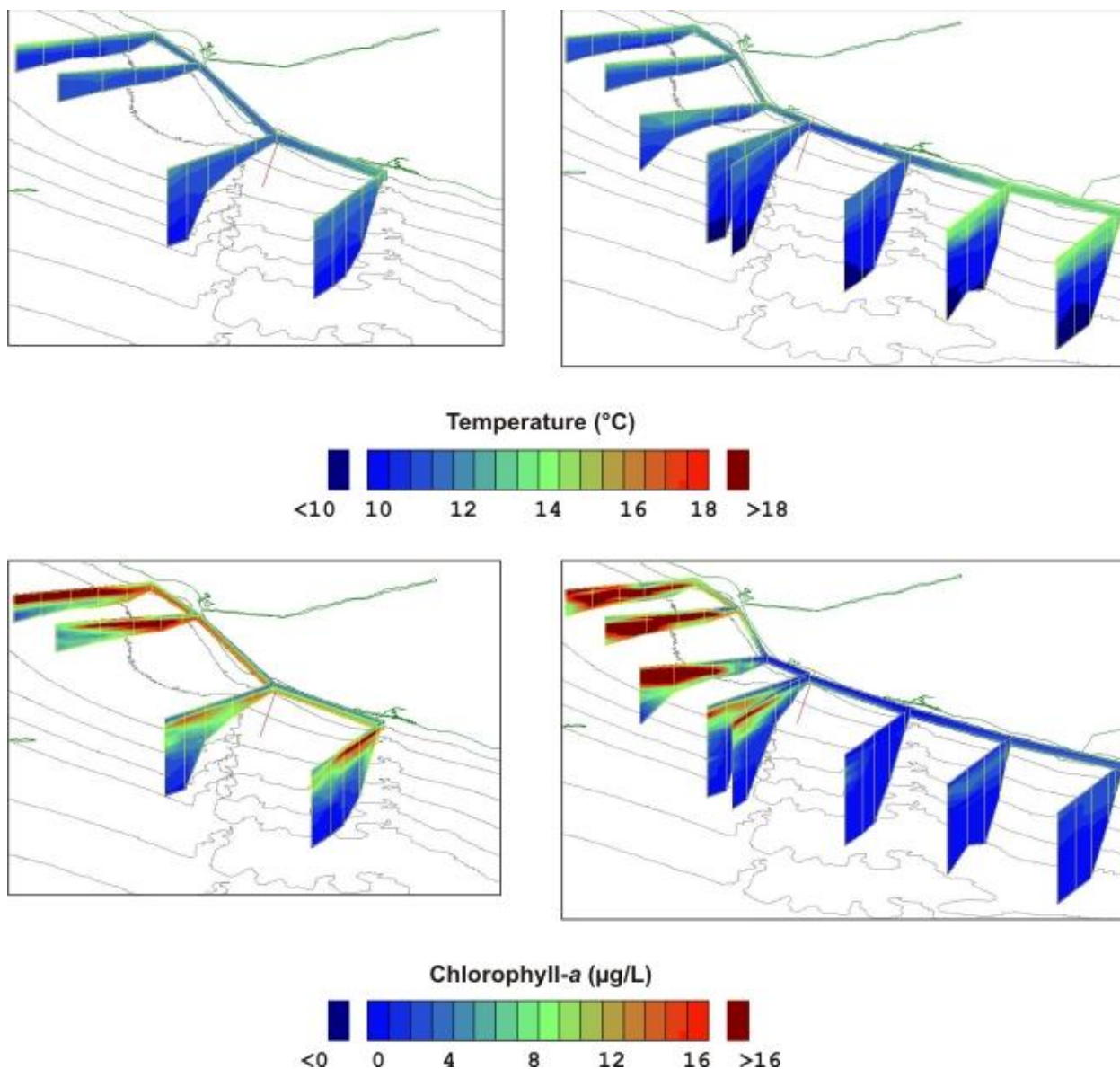


Figure IV-21 Temperature and chlorophyll fluorescence from the ship surveys in Ventura in May. The top panel summarizes temperatures and the bottom panel summarizes chlorophyll fluorescence observations. Images on the left reflect the ship survey observations from May 1 and 2, 2010, and images on the right reflect the observations from the May 13-15, 2010.

Table IV-9 The average nutrient ratios and concentrations summarized for the March surveys pre-upwelling (March 1, 2, 2010) and post-upwelling (March 23 and 24, 2010). Optimum growth ratios are listed in parenthesis.

	Nutrient Ratios			Nutrient Concentrations (μM)				
	DIN:PO ₄ (16:1)	DIN:SiO ₄ (16:15)	SiO ₄ :PO ₄ (15:1)	NO _x	NH ₄	Urea	PO ₄	SiO ₄
Pre-upwelling	5.9	1.2	7.5	1.3	0.8	1.1	0.3	2.5
Post-upwelling	9.4	1.3	13.3	3.3	0.7	1.3	0.3	4.8

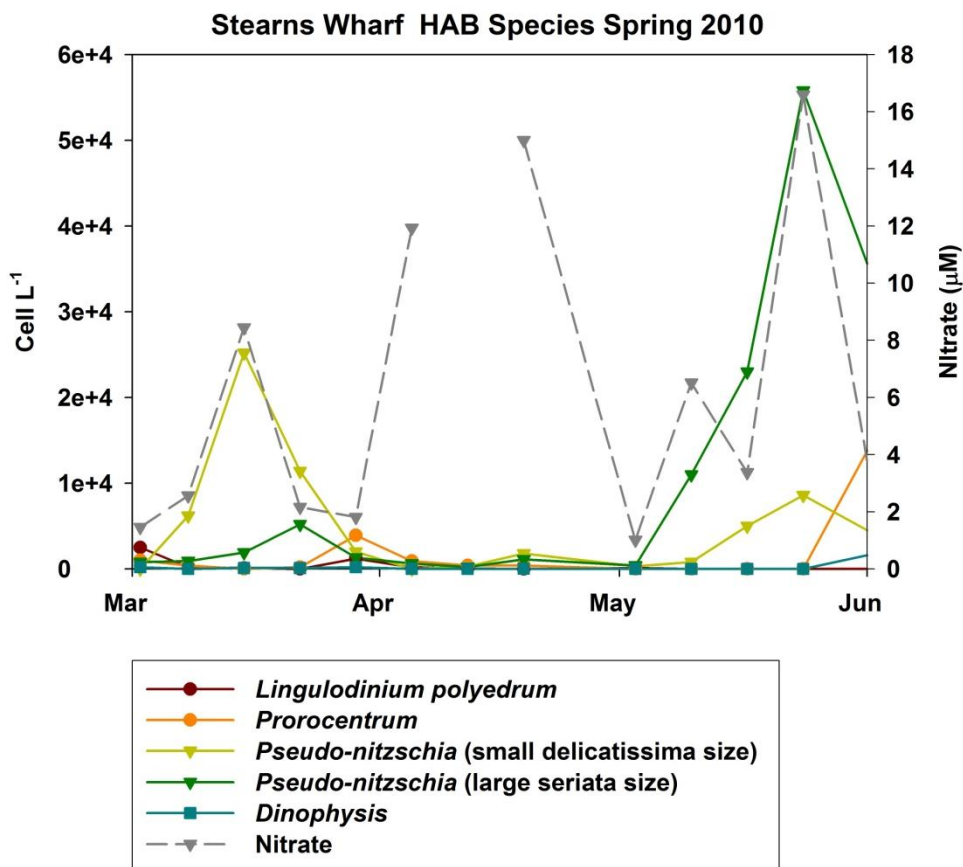


Figure IV-22 The SCCOOS Stern's Wharf Pier data, HAB species cell counts and nitrate concentrations, summarized for the spring of 2010.

North San Diego Area. There was only one survey conducted on March 25, 2010 in the North San Diego subregion. There was a highly stratified water column and low chlorophyll signature observed (see summarized figures in Appendix D).

Discussion

New View of Upwelling in Supporting Algal Bloom Development

Under certain conditions, physical transport mechanisms have been shown to transport both nutrients and phytoplankton into shallow surface waters close to shore. These mechanisms include wave driven transport, internal tides and the interaction of several processes (such as vertical shear in the alongshore currents, local wind and internal tides) (Nishimoto and Washburn 2002, Anderson et al. 2006, Noble et al. 2009, Lucas et al. 2011, McPhee-Shaw et al. 2011). In the present study, the intensive observations of the development, evolution, and dissipation of an algal bloom in San Pedro demonstrated for the first time that upwelling can also be a physical mechanism to transport subsurface algal blooms. These observational results also demonstrated that subsurface populations of algae and algal blooms are providing algal populations to the surface and acting as a seeding mechanism for surface blooms. Thereby, direct connectivity between subsurface and surface algal populations was demonstrated.

Prior to this study, upwelling was perceived to support algal bloom development by providing nutrients to surface waters for existing surface algal populations. This scenario was observed in March 2010 in San Pedro when upwelling was observed and algal cell concentrations increased 1-2 weeks after the upwelling event at the Newport Pier. However, the results from the present study have shown that upwelling can also be a physical mechanism that transports existing subsurface algal blooms into surface waters where the algae populations intensify due to higher light and nutrient conditions. This scenario was observed in San Pedro in April 2010 and San Diego in March 2010. In addition, study results show the development of a subsurface algal bloom that was not detected by satellite imagery, the evolution of that bloom being transported inshore into surface waters, and the intensification of the bloom in surface waters during a relaxation event. When algal cells are moved from low light conditions (at the subsurface depth) into higher light conditions (the well-lit surface waters), there is a rapid response of growth and productivity. If the subsurface population contains HAB species, then the total toxin concentration in the water can increase as a result of increased growth rate and cell abundance. The ESP results confirm that the subsurface algal bloom detected by the gliders and ship surveys did contain low concentrations of *Pseudo-nitzschia* spp., and that these populations moved past the fixed ESP locations once upwelling began, confirming that the subsurface populations were physically transported by upwelling.

Subsurface Algal Bloom or Deep Chlorophyll Maximum Feature

The subsurface high chlorophyll feature was detected throughout the sub-regions of this study. More recent glider missions in San Pedro have repeatedly detected the subsurface feature in the spring (B. Jones and B. Seegers, unpublished data). While the focus of this study was the spring algal bloom, the results raise additional questions as to the predominance of this feature in different seasons as well as

the spatial extent offshore. The field data for this study was collected as part of the NPDES monitoring permits, therefore, no multi-timepoint data was collected in areas of the SCB without anthropogenic discharges. Given that algal bloom hotspots have been identified in the SCB (Nezlin et al. 2011, Section 2), the possibility of elevated or enhanced primary productivity and algal biomass at these locations due to anthropogenic nutrient inputs remains uncertain, particularly in the subsurface depths.

While addressing all of these questions will require future research, there is existing SCCOOS data that can provide some insight. The SCCOOS program regularly deploys Spray Gliders at two locations in the SCB, (1) Line 80, Point Conception and (2) Line 90, Orange County (Figure IV-23) (<http://www.sccoos.org/data/spray/index.php>). Data was obtained from SCCOOS for the 2010 period that coincided with the Bight WQ study, mainly March, April, and the first few days of May. The chlorophyll concentration cannot be compared to the Bight WQ data due to raw data collected by the Spray Gliders from an uncalibrated fluorometer, however, the patterns of fluorescence can be evaluated in order to determine spatial extent of the subsurface feature.

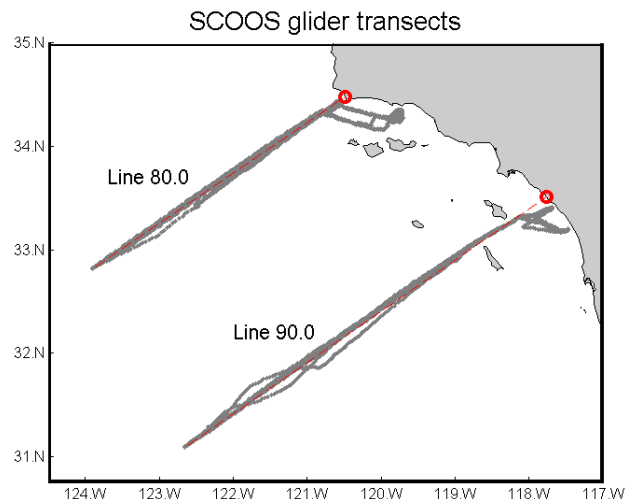


Figure IV-23 SCCOOS glider transects in the SCB.

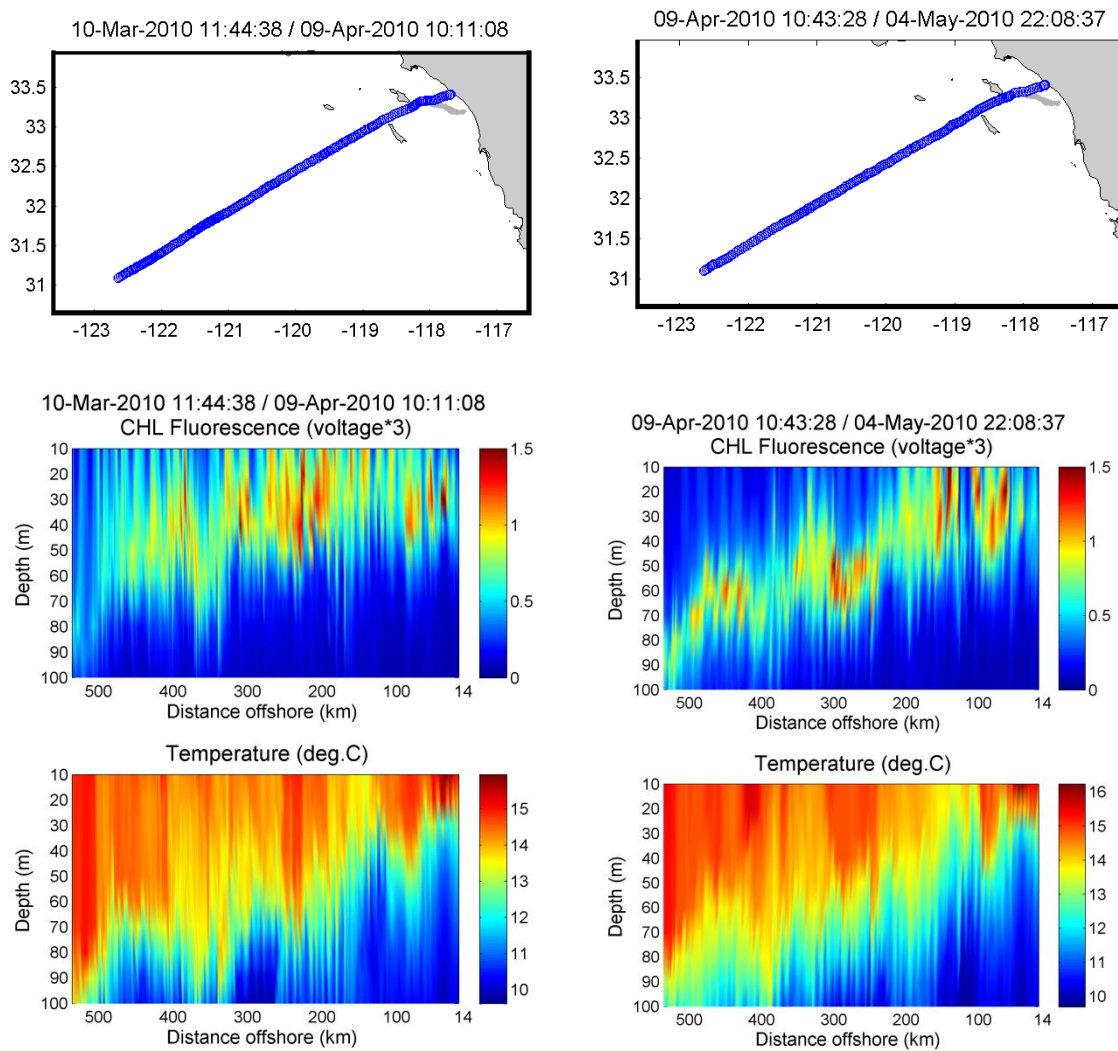


Figure IV-24 The SCCOOS Glider Data. The top panel shows the glider transect, the middle panels show the raw chlorophyll fluorescence (voltage*3) and the bottom panels show the temperature. The left column is the data collected from March 10, 2010 to April 9, 2010 and the right column is the data collected from April 10, 2010 to May 4, 2010. Note: The glider tracks are from 14 km to approximately 500 km offshore.

During the spring timeframe (i.e. March through early May), subsurface chlorophyll features are detected inshore and as far offshore as the gliders were deployed (transects started at 14km to approximately 500 km offshore). These subsurface chlorophyll features generally seem to coincide with the thermocline (Figure IV-24). While the SCCOOS dataset was useful to establishing the spatial extent of the subsurface feature, it cannot provide insight into the nutrient sources driving the subsurface feature (regardless of offshore or nearshore location). The presence of subsurface chlorophyll features in the far offshore region (i.e. >20 km) does not confirm nor contradict the finding from Section III (nutrient source comparison) that anthropogenic nutrients are important in SCB coastal waters. The conclusions from

Section III showed that the spatial scale is important and at smaller sub-regional spatial scales (<20 km offshore), which are more ecologically relevant for the development of algal blooms, anthropogenic nutrients are important and equivalent to natural sources (nitrogen only). Therefore, the SCCOOS dataset can be used to determine the spatial extent of the subsurface feature, however it cannot be used to evaluate whether anthropogenic nutrients are having an impact on algal biomass, community composition or overall primary production in the nearshore environment.

Regional Comparison of SCB

The regional comparison of temperature showed that upwelling events are temporally similar within most of the SCB. Ventura had a slightly different upwelling pattern and colder water temperatures due to the high upwelling in Point Conception and the physical circulation patterns in the northern SCB. There were two main bightwide upwelling events during the study period, one in mid-March and the second in early May. The remotely sensed surface chlorophyll patterns showed responses to both of those events in each sub-region; however the chlorophyll concentrations were higher in the northern SCB (Santa Barbara and Ventura). The satellite imagery can only detect surface chlorophyll signatures and are not reflective of chlorophyll patterns in the subsurface depths of the water column. However, the *in situ* chlorophyll fluorescence collected during the ship surveys provides measurements in the subsurface region but much less spatial and temporal coverage across sub-regions. Contrary to the remotely sensed results, the *in situ* results showed similar overall chlorophyll concentrations for each sub-region. However, in the shallower water depth analysis (0-15 m), Ventura had slightly higher chlorophyll concentrations in response to upwelling events, consistent with the remotely sensed results (Figure IV-4 and IV-6). The deeper water depths (15-30 m, 30-45 m and 45-100 m) had similar chlorophyll concentrations across sub-regions.

The Ventura area had different patterns of oceanographic conditions and *in situ* chlorophyll than the other areas in this study. There are complex ocean circulation patterns observed in this area, mainly due to the equatorward California Current that migrates onshore and penetrates into the SCB through the Santa Barbara Channel (see Section III for detailed description). Physical transport mechanisms have been shown to be important for both nutrient and algal transport into the surface and nearshore regions (Noble et al. 2009, Lucas et al. 2011, McPhee-Shaw et al. 2011). In addition to the physical circulation, several large rivers in the area, provide year round flow of large nutrient loads into the coastal waters (see Section III and Appendix E for details). These large dry weather nutrient loads have been shown to be the predominant nutrient source for short-term periods (Warrick et al. 2005, McPhee-Shaw et al. 2007). The observations at the SCCOOS pier station in Santa Barbara were not reflective of the oceanographic conditions and chlorophyll patterns observed in Ventura, mainly due to the complex circulation patterns described above and the large geographic distance between the sampling sites.

HAB Species, *Pseudo-nitzschia* and Domoic Acid

HAB species have been recorded in phytoplankton composition surveys in the SCB since 1902 (Torrey 1902, Allen 1922, Lange et al. 1994, Fryxell et al. 1997, Thomas 2001). Since the first recorded domoic acid (DA) poisoning event in California in 1991, *Pseudo-nitzschia* spp. has been observed as a common

and often dominant genus in the phytoplankton composition throughout southern California, most notably in Santa Barbara (Trainer et al. 2000; Anderson et al. 2006, 2009; Mengelt 2006), Los Angeles harbor and San Pedro Channel (Busse et al. 2006, Schnetzer et al. 2007, David Caron, unpublished data), Newport Beach (Villac, et al. 1993, Busse et al. 2006) and San Diego (Lange et al. 1994, Busse et al. 2006). Most recently, toxic blooms of *Pseudo-nitzschia* spp. in the San Pedro area have been particularly toxic, with some of the highest domoic acid concentrations recorded for the U.S. west coast (David Caron, unpublished data). Additionally, there have been significant mortality events of marine mammals and seabirds in recent years that generally occur before detection of DA in surface waters. The results from this field study in 2010, as well as the latest glider missions have provided an explanation of these mortality events in that the blooms are developing at depth (and intoxicating marine wildlife) and subsequently are transported into surface waters.

Pseudo-nitzschia spp. was observed throughout the study period in both surface and subsurface waters. However, the DA concentrations observed during this study were extremely low relative to other years. There have been many physiological and chemical factors identified in laboratory experiments that can induce, increase or decrease toxin production in HAB species. These factors include the following:

- (1) temperature (Ono et al. 2000);
- (2) light intensity (Ono et al. 2000);
- (3) salinity (Haque and Onoue 2002a, b);
- (4) trace metal availability, especially iron (Ladizinsky and Smith, 2000; Rue and Bruland, 2001; Maldonado et al. 2002; Wells et al. 2005; Sunda, 2006) but also copper (Maldonado et al. 2002) and selenium (Mitrovic et al. 2004, 2005);
- (5) macronutrient availability including silicate (Pan et al. 1996b, Fehling et al. 2004, Kudela et al. 2004), phosphate (Pan et al. 1996a, 1998; Fehling et al. 2004), nitrogen (Bates et al. 1991, Pan et al. 1998, Kudela et al. 2004a), urea (Howard et al. 2007) and combinations of nutrient limitation (Anderson et al. 1990, Flynn et al. 1994, John and Flynn 2000);
- (6) cellular elemental ratios of nutrients and physiological stress (Granéli and Flynn 2006, Schnetzer et al. 2007);
- (7) growth phase (Anderson et al. 1990, Bates et al. 1991, Flynn et al. 1994, Johansson et al. 1996, Maldonado et al. 2002, Mitrovic et al. 2004).

While most of these factors have been identified in laboratory experiments, the specific combination of environmental conditions that induce toxin production are poorly understood. While evaluating the factors promoting *Pseudo-nitzschia* toxin production was beyond the scope of this project, the results of this study provide a comprehensive dataset that will be used for an interannual comparison of toxin concentration and environmental variables. The 2010 was a low toxin production year which will

provide a informative contrast to other high toxin production years and will provide insight into environmental factors that affect toxin production in local *Pseudo-nitzschia* populations.

Urea was a measurable component of the nitrogen concentrations in all survey areas and concentrations ranged from below detection limit (0.08 μM) to 9.9 μM , with the highest concentration range in the Ventura sub-region. The results from Section III suggest that riverine runoff is the most likely source of urea in the SCB (it was <1% of the effluent loads). Based on these results, there is a potential for increased toxin production in certain *Pseudo-nitzschia* species populations and future studies should evaluate this aspect of HABs in the SCB.

In addition to the chemical factors, there are also physical factors that influence *Pseudo-nitzschia* blooms such as large-scale physical forcing processes. In recent years, toxic blooms of this genera have occurred during anomalously weak upwelling conditions and when macronutrients (e.g. nitrogen, phosphate, silicate) transition from excess concentrations to limiting concentrations. Additionally, there are *Pseudo-nitzschia* spp. 'hotspots' throughout California (Horner et al. 1997, Trainer et al. 2000, Hickey and Banas, 2003, Kudela et al. 2005, Schnetzer et al, 2007). Two of these hotspots, Monterey Bay and San Pedro, are the focus of a new NOAA funded ECOHAB (Ecology and Oceanography of Harmful Algal Blooms) project (<http://oceandatacenter.ucsc.edu/MBHAB/hotspots>). The main objective of this project is to determine the chemical and physical conditions leading to bloom initiation and the ecophysiological conditions that induce toxin production in *Pseudo-nitzschia* spp.

Lessons Learned and Implications for Monitoring Algal Blooms and HAB Events

The sampling design of this study was successful at achieving the goals of the study, mainly to capture the development, progression, and evolution of oceanographic features, such as upwelling events and algal blooms. The use of ship surveys that follow predefined oceanographic 'triggers' was a successful approach to capturing biological and physical oceanographic dynamics. The ship survey data that was collected weekly for four consecutive weeks provided a highly cohesive and comprehensive dataset that captured the oceanographic features and provided new insights into these physical and biological dynamics

Areas in which this temporal scale was unable to be achieved, or surveys that were not conducted following oceanographic triggers, did not capture oceanographic features. Additionally, ship surveys that sampled a smaller number of adjacent stations more frequently provided a robust dataset that enabled characterization of oceanographic dynamics. Surveys that sampled a higher number of stations over a larger geographic distance less frequently was not a preferable approach to capture and follow oceanographic patterns.

Future Studies and Recommendations

Future studies should focus on characterizing oceanographic dynamics by sampling on short time scales (weekly) and over short geographic distances in order to provide a highly resolved, comprehensive dataset. These short temporal and spatial scales for data collection are especially important in Ventura, as geographic connectivity is critical in order to characterize oceanographic dynamics. Future studies

should also include a pier-based site in Ventura since the Santa Barbara site is not reflective of conditions in Ventura.

The NPDES monitoring program has evolved significantly over the last 40 years due to changes in management issues, approaches to monitoring design, environmental assessment tools, and data interpretation (Setty et al. 2010). Although not previously considered, algal blooms, HAB events, and the potential for long-term enhanced primary production due to anthropogenic nutrient inputs in the nearshore waters are emerging management concerns. The current design of ambient discharge monitoring programs will not capture the temporal, spatial, and relational datasets needed to evaluate the indirect long-term impacts of anthropogenic nutrient inputs on primary production and algal community composition.

While the subsurface algal blooms and high chlorophyll concentrations observed in this study offer a new view of algal bloom development, they also raise several questions. The answers to these questions might be found through future studies that (1) identify the nutrient source(s) associated with and being utilized by these subsurface algal blooms, (2) determine how often and in what seasons they develop, (3) determine the pervasiveness of the blooms and (4) investigate how far offshore they are located. Drawing upon existing datasets and monitoring programs (such as the CalCOFI dataset, CBWQ group and SD NPDES monitoring), this study sets the stage for future studies.

References

- Allen, W.E., 1922. Observations on surface distribution of marine diatoms between San Diego and Seattle. *Ecology* 3(2): 140-145.
- Anderson, D.M., Kulis, D.M., Sullivan, J.J., Hall, S., Lee, C., 1990. Dynamics and physiology of saxitoxin production by the dinoflagellates *Alexandrium* spp. *Marine Biology* 104(3): 511-524.
- Anderson, D.M., Glibert, P.M., Burkholder, J.M., 2002. Harmful algal blooms and eutrophication: nutrient sources, composition, and consequences. *Estuaries* 25(4B): 704-726.
- Anderson, D.M., Burkholder, J.M., Cochlan, W.P., Glibert, P.M., Gobler, C.J., Heil, C.A., Kudela, R.M., Parsons, M.L., Rensel, J.E.J., Townsend, D.W., Trainer, V.L., Vargo, G.A., 2008. Harmful algal blooms and eutrophication: examining linkages from selected coastal regions of the United States. *Harmful Algae* 8: 39-53.
- Anderson, C.R., M.A. Brzezinski, L. Washburn, R. Kudela. 2006. Circulation and environmental conditions during a toxigenic *Pseudo-nitzschia australis* bloom in the Santa Barbara Channel, California. *Marine Ecology Progress Series* 327: 119-133.
- Anderson, C.R., Siegel, D.A., Kudela, R.M., Brzezinski, M.A. 2009. Empirical models of toxigenic *Pseudo-nitzschia* blooms: Potential use as a remote detection tool in the Santa Barbara Channel. *Harmful Algae* 8(3): 478-492.

Anderson, C.R., Kudela, R.M., Benitez-Nelson, C., Sekula-Wood, E., Burrell, C.T., Chao, Y., Langlois, G., Goodman, J., Siegel, D.A., 2011. Detecting toxic diatom blooms from ocean color and a regional ocean model. *Geophysical Research Letters*, 38:L040603.

Banase, K., and D.C. English, 1994. Seasonality of Coastal Zone Color Scanner phytoplankton pigment in the offshore oceans, *Journal of Geophysical Research-Oceans*, 99 (C4): 7323-7345, doi: 10.1029/93JC02155.

Bates, S.S., DeFreitas, A.S.W., Milley, J.E., Pocklington, R., Quilliam, M.A., Smith, J.C., Worms, J., 1991. Controls on domoic acid production by the diatom *Nitzschia pungens* f. *multiseries* in cultures: nutrients and irradiance. *Canadian Journal of Fisheries and Aquatic Sciences* 48(7): 1136-1144.

Bograd, S.J., I.D. Schroeder, N. Sarkar, X. Qiu, W.J. Sydeman, and F.B. Schwing (2009), Phenology of coastal upwelling in the California Current, *Geophysical Research Letters*, 36(1): L01602, doi: 10.1029/2008GL035933.

Brzezinski, M.A., 1985. The Si:C:N ratio of marine diatoms: interspecific variability and the effect of some environmental variables. *Journal of Phycology* 21: 347-357.

Busse, L.B., Venrick, E.L., Antrobus, R., Miller, P.E., Vigilant, V., Silver, M.W., Mengelt, C., Mydlarz, L., Prezelin, B.B., 2006. Domoic acid in phytoplankton and fish in San Diego, CA, USA. *Harmful Algae* 5(1): 91-101.

Campbell, J.W. (1995), The lognormal-distribution as a model for biooptical variability in the sea, *Journal of Geophysical Research-Oceans*, 100(C7): 13237-13254, doi: 10.1029/95JC00458.

Caron, D.A., M.E. Garneau, E. Seubert, M.D.A. Howard, L. Darjany, A. Schnetzer, I. Cetinic, G. Filteau, P. Lauri, B. Jones, and S. Trussell, 2010. Harmful algae and their potential impacts on desalination operations off southern California. *Journal of Water Research* 44: 385-416.

Esaias, W.E., M.R. Abbott, I. Barton, O.B. Brown, J.W. Campbell, K.L. Carder, D.K. Clark, R.H. Evans, F.E. Hoge, H.R. Gordon, W.M. Balch, R.M. Leteller, and P.J. Minnett, 1998. An overview of MODIS capabilities for ocean science observations, *IEEE Transactions on Geoscience and Remote Sensing* 36 (4): 1250-1265.

Fehling, J., Davidson, K., Bolch, C.J., Bates, S.S., 2004. Growth and domoic acid production by *Pseudo-nitzschia seriata* (Bacillariophyceae) under phosphate and silicate limitation. *Journal of Phycology* 40(4): 674-683.

Flynn, K., Franco, J.M., Fernandez, P., Reguera, B., Zapata, M., Wood, G., Flynn, K.J., 1994. Changes in toxin content, biomass and pigments of the dinoflagellate *Alexandrium minutum* during nitrogen refeeding and growth into nitrogen or phosphorus stress. *Marine Ecology Progress Series* 111: 99-109.

Fryxell, G.A., Villac, M.C., Shapiro, L.P., 1997. The occurrence of the toxic diatom genus *Pseudo-nitzschia* (Bacillariophyceae) on the West Coast of the USA, 1920 - 1996: a review. *Phycologia* 36(6): 419-437.

- Glibert, P.M., Anderson, D.M., Gentien, P., Granéli, E., and Sellner, K.G., 2005a. The global, complex phenomena of harmful algal blooms. *Oceanography* 18: 137-147.
- Glibert, P.M., Seitzinger, S., Heil, C.A., Burkholder, J.M., Parrow, M.W., Codispoti, L.A., and Kelly, V., 2005b. The role of eutrophication in the global proliferation of harmful algal blooms. *Oceanography* 18: 198-209.
- Granéli, E., Flynn, K., 2006. Chemical and physical factors influencing toxin content. Springer, Berlin. In: Granéli, E., Turner, J.T. (eds) *Ecology of Harmful Algae* pp. 229-241,
- Hallegraeff, G.M., 1993. A review of harmful algal blooms and their apparent global increase. *Phycologia* 32(2): 79-99.
- Hallegraeff, G.M., 2004. Harmful algal blooms: a global overview. In: Hallegraeff, G.M., Anderson, D.M., Cembella, A.D. (eds) *Manual on harmful marine microalgae. Monographs on oceanographic methodology*, UNESCO Publishing, Paris. 25-49
- Haque, S.M., Onoue, Y., 2002a. Effects of salinity on growth and toxin production of a noxious phytoflagellate, *Heterosigma akashiwo* (Raphidophyceae). *Botanica Marina* 45(4): 356-363.
- Haque, S.M., Onoue, Y., 2002b. Variation in toxin compositions of two harmful raphidophytes, *Chattonella antiqua* and *Chattonella marina*, at different salinities. *Environmental Toxicology* 17(2): 113-118.
- Hickey, B., and N. Banas, 2003. Oceanography of the U.S. Pacific Northwest coastal ocean and estuaries with application to coastal ecology, *Estuaries* 26: 1010-1031.
- Horner, R.A., Garrison, D.L., Plumley, F.G., 1997. Harmful algal blooms and red tide problems on the U.S. west coast. *Limnology and Oceanography* 42(2): 1076-1088.
- Howard, M.D.A., Cochlan, W.P., Ladizinsky, N., Kudela, R.M., 2007. Nitrogenous preference of toxigenic *Pseudo-nitzschia australis* (Bacillariophyceae) from field and laboratory experiments. *Harmful Algae* 6(2): 206-217.
- Johansson, N., Granéli, E., Yasumoto, T., Carlsson, P., Legrand, C., 1996. Toxin production by *Dinophysis acuminata* and *D. acuta* cells grown under nutrient sufficient and deficient conditions. In: Yasumoto, T., Oshima, Y., Fukuyo, Y. (eds) *Intergovernmental Oceanographic Commission of UNESCO, Paris. Harmful and Toxic Algal Blooms* 277-279
- John, E.H., Flynn, K.J., 2000. Growth dynamics and toxicity of *Alexandrium fundyense* (Dinophyceae): the effect of changing N:P supply ratios on internal toxin and nutrient levels. *European Journal of Phycology* 35(1): 11-23.
- Kudela, R.M., Roberts, A., Armstrong, M., 2004. Laboratory analyses of nutrient stress and toxin production in *Pseudo-nitzschia* spp. from Monterey Bay, California. Steidinger, K., Landsberg, J., Tomas, C., Vargo, G. (eds), pp. 136-138, Florida Environmental Research Institute and UNESCO, St. Petersburg.

- Kudela, R., G. Pitcher, T. Probyn, F. Figueiras, T. Moita, and V. Trainer, 2005. Harmful algal blooms in coastal upwelling systems, *Oceanography* 18: 184-197.
- Ladizinsky, N., Smith, G.J., 2000. Accumulation of domoic acid by the coastal diatom *Pseudo-nitzschia multiseries*: a possible copper complexation strategy. *Journal of Phycology* 36: 41.
- Lane, JQ, P Raimondi, and RM Kudela, 2009. The development of a logistic regression model for the prediction of toxigenic *Pseudo-nitzschia* blooms in Monterey Bay, California. *Marine Ecology Progress Series* 383: 37-51.
- Lange, C.B., Reid, F.M.H., Vernet, M., 1994. Temporal distribution of the potentially toxic diatom *Pseudo-nitzschia australis* at a coastal site in Southern California. *Marine Ecology Progress Series* 104(3): 309-312.
- Langlois, G., 2007. Marine biotoxin monitoring program annual report, California Department of Public Health for California Department of Fish and Game, Sacramento.
- Lucas, A.J., C.L. Dupont, V.Tai, J.L. Largier, B. Palenik, P.J. Franks, 2011. The green ribbon: Multiscale physical control of phytoplankton productivity and community structure over a narrow continental shelf. *Limnology and Oceanography* 56(2): 611-626.
- Maldonado, M.T., Hughes, M.P., Rue, E.L., Wells, M.L., 2002. The effect of Fe and Cu on growth and domoic acid production by *Pseudo-nitzschia multiseries* and *Pseudo-nitzschia australis*. *Limnology and Oceanography* 47(2): 515-526.
- Mengelt, C., 2006. Ultraviolet photoecology, dark survival, and seasonal abundance of *Pseudo-nitzschia australis* and *P. multiseries* in coastal waters of central California, dissertation., University of California, Santa Barbara.
- McPhee-Shaw, E.E., David A. Siegel, Libe Washburn, Mark A. Brzezinski, Janice L. Jones, Al Leydecker, and John Melack. 2007. Mechanisms for nutrient delivery to the inner shelf: Observations from the Santa Barbara Channel. *Limnology and Oceanography* 52(5): 1748–1766.
- McPhee-Shaw, E.E., K.J. Nielsen, J.L. Largier, B.A. Menge, 2011. Nearshore chlorophyll-a events and wave-driven transport. *Geophysical Research Letters* 38:L02604.
- Mitrovic, S.M., Fernández Amandi, M., MacKenzie, L., Furey, A., James, K.J., 2004. Effects of selenium, iron and cobalt addition to growth and yessotoxin production of the toxic marine dinoflagellate *Protoceratium reticulatum* in culture. *Journal of Experimental Marine Biology and Ecology* 313(2): 337-351.
- Mitrovic, S.M., Hamilton, B., MacKenzie, L., Furey, A., James, K.J., 2005. Persistence of yessotoxin under light and dark conditions. *Marine Environmental Research* 60(3): 397-401.
- Nezlin, N.P., Sutula, M.A., Stumpf, R.P., Sengupta, A., 2011. Phytoplankton blooms detected by SeaWiFS along the central and southern California Coast. SCCWRP Annual Report.

Noble, M., B. Jones, P. Hamilton, J. Xu, G. Robertson, L. Rosenfeld, J. Largier, 2009. Cross-shelf transport into nearshore waters due to shoaling internal tides in San Pedro Bay, CA. *Continental Shelf Research*, 29: 1768-1785.

Nishimoto, M.M., and L. Washburn, 2002, Patterns of coastal eddy circulation and abundance of pelagic juvenile fish in the Santa Barbara Channel, California, USA, *Marine Ecology Progress Series* 241: 183-199.

Ono, K., Khan, S., Onoue, Y., 2000. Effects of temperature and light intensity on the growth and toxicity of *Heterosigma akashiwo* (Raphidophyceae). *Aquaculture Research* 31(5): 427-433.

O'Reilly, J.E., S. Maritorena, B.G. Mitchell, D.A. Siegel, K.L. Carder, S.A. Garver, M. Kahru, and C. McClain (1998), Ocean color *chlorophyll*-algorithms for SeaWiFS, *Journal of Geophysical Research-Oceans* 103 (C11): 24937-24953, doi: 10.1029/98JC02160.

Pan, Y., Subba Rao, D.V., Mann, K.H., 1996a. Changes in domoic acid production and cellular chemical composition of the toxigenic diatom *Pseudo-nitzschia* multiseres under phosphate limitation. *Journal of Phycology* 32(3): 371-381.

Pan, Y., Subba Rao, D.V., Mann, K.H., Li, K.W., Harrison, W.G., 1996b. Effects of silicate limitation on production of domoic acid, a neurotoxin, by the diatom *Pseudo-nitzschia multiseres*. I. Batch culture studies. *Marine Ecology Progress Series* 131(1-3): 225-233.

Pan, Y., Bates, S.S., Cembella, A.D., 1998. Environmental stress and domoic acid production by *Pseudo-nitzschia*: a physiological perspective. *Natural Toxins* 6(3-4): 127-135.

Rue, E.L., Bruland, K.W., 2001. Domoic acid binds iron and copper: a possible role for the toxin produced by the marine diatom *Pseudo-nitzschia*. *Marine Chemistry* 76(1-2): 127-134.

Quay, J., 2011. New Tools and Insight for the Recognition of *Pseudo-nitzschia* blooms and Toxin Incidence. Doctor of Philosophy, Ocean Science, University of California, Santa Cruz.

Schnetzer, A., Miller, P.E., Schaffner, R.A., Stauffer, B.A., Jones, B.H., Weisberg, S.B., DiGiacomo, P.M., Berelson, W.M., Caron, D.A., 2007. Blooms of *Pseudo-nitzschia* and domoic acid in the San Pedro Channel and Los Angeles harbor areas of the Southern California Bight, 2003 - 2004. *Harmful Algae* 6(3): 372-387.

Smayda, T.J., 1990. Novel and nuisance phytoplankton blooms in the sea: evidence for a global epidemic. In: Granéli, E., Gundström, B., Edler, L., Anderson, D.M. (eds) Elsevier, New York. *Toxic marine phytoplankton* pp. 29-40.

Sunda, W., 2006. Trace metals and harmful algal blooms. In: Granéli, E., Turner, J.T. (eds) Springer, Berlin. *Ecology of harmful algae* pp. 203-214.

Thomas, W.H., Zavoico, T., Hewes, C., 2001. Historical phytoplankton species time-series data (1917 - 1939) from the North American Pacific Coast. Scripps Institution of Oceanography Ref. no. 01-12.
Torrey, H. B. (1902), An unusual occurrence of Dinoflagellata on the California coast, *American Naturalist* 36: 187-192.

Trainer, V.L., Adams, N.G., Bill, B.D., Stehr, C.M., Wekell, J.C., Moeller, P., Busman, M., Woodruff, D., 2000. Domoic acid production near California coastal upwelling zones, June 1998. *Limnology and Oceanography* 45(8): 1818-1833.

Villac, M.C., D.L. Roelke, F.P. Chavez, L.A. Cifuentes and G.A. Fryxell, 1993. *Pseudo-nitzschia australis* Frenguelli and related species from the west coast of the USA: occurrence and domoic acid production. *Journal of Shellfish Research* 12: 457-465.

Warrick, J., Washburn, L., Brzezinski, M., Siegel, D., 2005. Nutrient contributions to the Santa Barbara Channel, California, from the ephemeral Santa Clara River. *Estuarine, Coastal and Shelf Science* 62: 559–574.

Wells, M.L., Trick, C.G., Cochlan, W.P., Hughes, M.P., Trainer, V.L., 2005. Domoic acid: the synergy of iron, copper, and the toxicity of diatoms. *Limnology and Oceanography* 50(6): 1908-1917.

APPENDIX A - BIGHT '08 PARTICIPANTS

http://ftp.sccwrp.org/pub/download/DOCUMENTS/TechnicalReports/710_B08WQ_Appendix_A.pdf

APPENDIX B - QUALITY ASSURANCE AND QUALITY CONTROL PROCEDURES

http://ftp.sccwrp.org/pub/download/DOCUMENTS/TechnicalReports/710_B08WQ_Appendix_B.pdf

APPENDIX C - ADDITIONAL NUTRIENT SOURCE DATA SUMMARIZED

http://ftp.sccwrp.org/pub/download/DOCUMENTS/TechnicalReports/710_B08WQ_Appendix_C.pdf

APPENDIX D - SHIP SURVEY DATA SUMMARIZED

http://ftp.sccwrp.org/pub/download/DOCUMENTS/TechnicalReports/710_B08WQ_Appendix_D.pdf

APPENDIX E - RELATED MANUSCRIPTS

http://ftp.sccwrp.org/pub/download/DOCUMENTS/TechnicalReports/710_B08WQ_Appendix_E.pdf